DISSERTATION

LABORATORY STUDY OF ALLUVIAL RIVER MORPHOLOGY

Submitted by

Hamidur Rahman Khan

In partial fulfillment of the requirements

for the Degree of Doctor of Philosophy

Colorado State University

Fort Collins, Colorado

March, 1971

COLORADO STATE UNIVERSITY

March 1971

WE HEREBY RECOMMEND THAT THE DISSERTATION PREPARED UNDER OUR SUPERVISION BY A.K.M. HAMIDUR RAHMAN KHAN

ENTITLED LABORATORY STUDY OF ALLUVIAL RIVER MORPHOLOGY

BE ACCEPTED AS FULFILLING THIS PART OF THE REQUIREMENTS FOR THE DEGREE OF DOCTOR OF PHILOSOPHY

Committee on Graduate Work

Adviser

Adviser

Head of Department

ABSTRACT OF DISSERTATION

LABORATORY STUDY OF ALLUVIAL RIVER MORPHOLOGY

A concrete recirculating flume 100 feet long, 24 feet wide, and about 3 feet deep was used to study the different alluvial river channel patterns. The flume was filled with sand and a series of tests were made in which discharge was varied from 0.1 to 0.3 cfs and slope was varied from 0.001 to 0.020.

Four channel patterns, straight, meandering thalweg, meandering, and braided were observed in the laboratory. Straight channels developed at very flat slopes (slopes flatter than 0.0047 or 0.0026 depending on whether the flow entered the channel straight or at an angle to the axis of the flume) with very low bedload concentrations (less than 740 ppm). Meandering thalweg channels developed for slopes between 0.0023 and 0.013 and for bedload concentrations of 740 and 2180 ppm. The sinuosity was very low in these channels. Braided channels occurred at very steep slopes (slopes equal to or greater than 0.016) with high concentrations of bedload (equal to or greater than 3110 ppm). No meandering channel developed in noncohesive material. Meandering channel developed with 3% concentration of clay in the flow.

Velocities were very low in straight channels (less than 0.84 fps). Meandering thalweg channels developed for velocities between 0.84 and 1.53 fps, and braided channels developed for velocities higher than 1.53 fps. Because of such variation of velocity with channel pattern, Froude number of flow, shear, and stream power was very high in a braided channel, very low in a straight channel, and intermediate in a meandering thalweg channel. Because of its low velocity, the flow in a straight channel was incapable of causing any significant erosion and as a result it maintained its original straight alignment. Meandering thalweg and braided channels developed only when the flow conditions were such that there were pronounced erosion of the channel banks.

For any given bed material, thalweg meander geometry and channel geometry depend on discharge and slope or discharge and bedload concentration. Thalweg sinuosity in a meandering channel depends on discharge, slope, and bedload concentration. Width-depth ratio of channels was found to increase with bedload concentration.

Laboratory experiments showed that a change in the sediment type from bedload to suspended load transforms a wide, shallow, less sinuous meandering thalweg channel into a narrow, deep, and more sinuous meandering channel. The smoothness of bed and banks, caused by the deposition of clay among the coarser materials, reduced the resistance to flow and increased the average velocity. The increased velocity caused scour of the bed. Some of the clay also deposited on the alternate bars. Continued building up of bars and scour of bed along the thalweg caused exposure of bars above water surface and the flow took place in a narrow, deep, and sinuous meandering channel.

Hamidur Rahman Khan
Civil Engineering Department
Colorado State University
Fort Collins, Colorado 80521
March, 1971

ACKNOWLEDGMENTS

The writer wishes to express his appreciation to his advisors, Dr. Daryl B. Simons and Dr. Stanley A. Schumm, for their guidance, encouragement, and indulgence during the course of his graduate program and research. The research project was supported by National Science Foundation Grant (No. GA4450) to Dr. Stanley A. Schumm. The writer was supported by this grant from the Spring of 1969 to the Fall of 1970. Dr. Daryl B. Simons supported the writer with a graduate research assistantship for the remainder of the period of his study.

The writer wishes to thank other members of his research committee: Dr. E. V. Richardson, and Dr. J. Gessler, who reviewed the thesis and made many valuable comments, criticisms, and suggestions which greatly improved the report.

The writer also extends thanks to Mr. Laurence Garretson who made the prints from photographs and to Mary Grace Smith, and Julie Dunning for taking great care in typing the rough draft and final copy of the thesis respectively.

Finally, the author wishes to compliment his wife, Shahana, for helping in laboratory work on many weekends and holidays, and for her patience and understanding during the period of his doctoral study program.

TABLE OF CONTENTS

Chapter		Page
	ABSTRACT OF DISSERTATION	iii
	ACKNOWLEDGEMENTS	v
	LIST OF TABLES	viii
	LIST OF FIGURES	ix
	LIST OF SYMBOLS	xiv
I	INTRODUCTION	1
	General	1
	Variables Affecting Alluvial Rivers	2
	Classification of Stream Forms	4
	Channel Patterns	5
	Straight channel	5
	Meandering channel	5
	Braided river	10
	Slope-Discharge Relations	11
	Objectives	12
II	EXPERIMENTAL METHOD AND DATA COLLECTION	14
	Equipment	14
	Discharge	15
	Sand Feeding at Entrance	16
	Bed Material	16
	Suspended Sediment	17
	Experimental Procedure	17
	Description of Tests	19
III	RIVER CHANNEL PATTERNS	20
	Straight Channel	20
	Meandering Thalweg Channel	21
	Development of alternate bars	22
	Pools and crossings	23
	Transverse circulation at bends in open channel flow	25
	Tahlweg meander geometry	26
	Meandering Channels	29
	Braided Channels	30
	Sinuosity	33
IV	EFFECT OF BEDLOAD DISCHARGE ON CHANNEL PATTERNS	39
	Introduction	39

TABLE OF CONTENTS (Continued)

Chapter		Page
	Complexity of Sediment and Streamflow Relationships. .	39
	Velocity and Bedload Discharge	42
	Shear and Stream Power	48
V	EFFECT OF SUSPENDED SEDIMENT ON CHANNEL MORPHOLOGY . .	53
	Effect of Suspended Sediment Concentration on Velocity	54
	Wdith, Depth, and Hydraulic Radius	58
	Sinuosity.	60
	Photographs.	61
VI	EFFECT OF DISCHARGE, SLOPE, AND BEDLOAD CONCENTRATION ON CHANNEL GEOMETRY.	62
	Straight Channels.	62
	Depth	62
	Width	62
	Width-depth ratio	63
	Area.	63
	Meandering Thalweg Channels.	64
	Depth	64
	Area.	66
	Velocity.	66
	Hydraulic radius.	67
	Width-depth ratio	67
VII	GEOMETRY OF POOLS AND BENDWAYS	68
	Theoretical Considerations	68
	Determination of K_o (Rzhanitsyn's morphometric parameter) values	73
	Length of pools in bends.	74
	Longitudinal profile of the channel bottom in bend	75
VIII	EXAMPLES	78
	Straight Channel	78
	Meandering and Braided Channels.	79
	Sinuosity and Valley Slope	81
IX	CONCLUSIONS.	82
	REFERENCES	88
	APPENDIX A - Figures	96
	APPENDIX B - Data.	172

LIST OF TABLES

Table		Page
1	Classification of Alluvial Clannels	6
2	Illinois River from Kampsville, Illinois to Mouth . . .	79
3	Data for Straight Channels (straight entrance), S = 0.0015, Q = 0.10, 0.15, and 0.20 cfs	173
4	Data for Straight Channels (straight entrance), S = 0.0028, Q = 0.10, 0.15, and 0.20 cfs	174
5	Data for Straight Channels (straight entrance), S = 0.0038, Q = 0.10, 0.15, and 0.20 cfs	175
6	Data for Straight Channels (straight entrance), S = 0.0040, Q = 0.10, 0.15, and 0.20 cfs	176
7	Data for Straight Channels (entrance at an angle), S = 0.0010, 0.0017, and 0.0020, Q = 0.15 cfs	177
8	Data for Meandering Thalweg Channels (entrance at an angle), S = 0.0043, Q = 0.10, 0.15, 0.21, 0.25, and 0.30 cfs.	178
9	Data for Meandering Thalweg Channels (entrance at an angle), S = 0.0059, Q = 0.10, 0.15, 0.21, 0.25, and 0.30 cfs.	180
10	Data for Meandering Thalweg Channels (entrance at an angle), S = 0.0085, Q = 0.10, 0.15, 0.21, and 0.25 cfs.	182
11	Data for Meandering Thalweg Channels (entrance at an angle), S = 0.0026, 0.0064, 0.0075, 0.010, and 0.013, Q = 0.15 cfs.	184
12	Data for a Channel Having a Combination of Meandering Thalweg and Braided Patterns (entrance at an angle), S = 0.015, Q = 0.15 cfs.	186
13	Data for Braided Channels (entrance at an angle), S = 0.016, 0.018, and 0.020, Q = 0.15 cfs.	187
14	Data for Suspended Sediment Tests (meandering channels), S = 0.0026, 0.0064, 0.0075, and 0.0085, Q = 0.15 cfs	188

LIST OF FIGURES

Figure		Page
1	Slope-discharge relations for meandering streams in sand (after Lane, 1957).	97
2	Slope-discharge relations for braided streams (after Lane, 1957).	98
3	Experimental set up	99
4	Size distribution of bed material	100
5	Different channel patterns.	101
	Photographs of different channel patterns	103
6	Photographs showing the gradual development of alternate bars.	104
7	Flow in the bend of a meandering thalweg channel. . . .	106
8	Secondary currents in pipes (after Goldstein, 1965) . .	107
9	Secondary currents at bends of open channels (after Simons, 1970).	107
10	Variation of thalweg meander dimensions with discharge and slope	108
11	Relationship among (a) thalweg meander wave length, discharge, and slope, and (b) thalweg meander wave length, discharge, and bedload concentration.	109
12	Relationship among (a) thalweg meander width, discharge, and bedload concentration, and (b) thalweg meander width, discharge, and slope	110
13	Relationship between thalweg meander wave length and channel width	111
14	Relationship between thalweg meander wave length and radius of bend.	112
15	Variation of radius of bend with discharge.	113
16	Variation of maximum depths in pools with radius of bends	114
17	Sinuosity versus slope for a constant slope of 0.15 cfs.	115

LIST OF FIGURES (Continued)

Figure		Page
18	Variation of thalweg sinuosity with discharge and slope	116
19	Variation of thalweg sinuosity with discharge and bedload concentration	117
20	Variation of sinuosity with mean velocity	118
21	Variation of sinuosity with Froude number	119
22	Variation of sinuosity with stream power	120
23	Variation of bedload discharge with mean velocity and channel pattern	121
24	Variation of bedload discharge with shear and channel pattern	122
25	Variation of bedload discharge with stream power and channel pattern	123
26	Variation of bedload discharge with discharge and slope	124
27	Variation of bedload concentration with discharge and slope	125
28	Variation of velocity with slope and channel pattern for a constant discharge of 0.15 cfs	126
29	(a) Variation of area and wetted perimeter with slope and channel pattern for a constant discharge of 0.15 cfs	127
	(b) Variation of hydraulic radius, and Chezy C with slope and channel pattern for a constant discharge of 0.15 cfs	128
30	Variation of shear with slope and channel pattern for a constant discharge of 0.15 cfs	129
31	Variation of bedload discharge with slope and channel pattern for a constant discharge of 0.15 cfs	130
32	Effect of suspended sediment concentration on mean velocity	131
33	Effect of suspended sediment concentration on mean velocity	132

Figure		Page
34	Effect of suspended sediment concentration on cross sectional area	133
35	Effect of suspended sediment concentration on cross sectional area	134
36	Effect of suspended sediment concentration on channel width	135
37	Effect of suspended sediment concentration on maximum depths in pools	136
38	Effect of suspended sediment concentration on maximum depths in crossings	137
39	Effect of suspended sediment concentration on $\frac{W}{D_{max}}$ in pools	138
40	Effect of suspended sediment concentration on $\frac{W}{D_{max}}$ in crossings	139
41	Effect of suspended sediment concentration on hydraulic radius	140
42	Relation of width-depth ratio to weighted mean percent silt-clay (after Schumm, 1960)	141
43	Length of scour holes in bends of meandering channels	142
44	Sinuosity versus slope	143
45	Relation of sinuosity to silt-clay in perimeter of channel (after Schumm, 1963b)	144
46	Effect of high concentration of suspended sediment on channel morphology	145
47	Maximum depths versus $Q/S^{2/3}$ in straight channels	146
48	Relationship among maximum depth, discharge, and bedload concentration in straight channels	147
49	Relationship among channel width, discharge, and slope in straight channels	148

LIST OF FIGURES (Continued)

Figure		Page
50	Relationship among channel width, discharge. and bedload concentration in straight channels.	149
51	Relationship between $\frac{W}{D_{max}}$ and bedload concentration in straight channels.	150
52	Variation of cross sectional area with discharge and slope in straight channels.	151
53	Variation of cross sectional area with discharge and bedload concentration in straight channels.	152
54	Relationship among maximum depths in pools and crossings discharge, and slope for meandering thalweg channels.	153
55	Relationship among maximum depths in pools and crossings, discharge, and bedload concentration in meandering thalweg channels.	154
56	Relationship among areas in pools and crossings, discharge, and slope in meandering thalweg channels . .	155
57	Relations among areas in (a) pools, and (b) crossings, discharge, and bedload concentration for meandering thalweg channels	156
58	Variation of velocity in pools with discharge and slope in meandering thalweg channels.	157
59	Variation of velocity in crossings with discharge and slope in meandering thalweg channels.	158
60	Relations among velocity in pools and crossings, hydraulic radius, and slope in meandering thalweg channels.	159
61	Relations among hydraulic radius in pools and crossings, discharge and slope for meandering thalweg channels.	160
62	Relationship between $\frac{W}{D_{max}}$ and bedload concentration in meandering thalweg channels.	161

LIST OF FIGURES (Continued)

Figure		Page
63	Transverse inclination of water surface at bends of open channels	162
64	Relation of coefficient of η to the stability coefficient and to Lokhtins number (after Rzhanitsyn, 1960)	163
65	Length of pool versus discharge in meandering thalweg channels.	164
66	Length of pools versus maximum depths in pools in meandering thalweg channels.	165
67	Nondimensional longitudinal profile of channel bed at bends.	166
68	Relative depth of pool versus relative length of pool depression (after Rzhanitsyn, 1960)	167
69	Plan and profile of a meandering reach of the Popo Agie River near Hudson, Wyoming (after Leopold and Wolman, 1957)	168
70	Plan and profile of Corronwood Creek near Daniel, Wyoming. In this reach the river changes its pattern from meander to braid (after Leopold and Wolman, 1957)	169
71	Plan and profile of laboratory stream showing combination of meandering thalweg and braided channel patterns.	170
72	Longitudinal river profile and valley profile, Calamus River, Nebraska (after Brice, 1964)	171

LIST OF SYMBOLS

Symbol	Definition	Units
A	Area of cross section	ft^2
A_1	Dimensionless constant used by Bagnold (1956).	--
B_1	Dimensionless constant used by Bagnold (1956).	--
C	Chezy $C = \frac{V}{D^{1/2}S^{1/2}}$	$ft^{1/2}/sec$
C_s	Bedload concentration	ppm
D	Mean depth of flow	ft
D_{max}	Maximum depth of flow	ft
d	Particle size expressed as a diameter or the geometric mean diameter of a size range.	ft
d_m	Effective diameter of the bed-material mixture (the particle size of uniform sediment) and equal to Σdi_b for bed sediment of a range of sizes.	ft
d_{50}	Particle size for which 50 percent of the bed material by weight is finer. Subscripts 65 and 90 have comparable meanings. Hence d_{50} is the median particle size.	ft
F	Width-depth ratio	--
g	Acceleration due to gravity	ft/sec^2
i_b	Fraction by weight of bed sediment in a size range.	--
K_o	Rzhanitsyn's morphometric parameter $= \frac{Lrg}{WC^2D}$	--
K_r	A measure of resistance to flow and equal to the mean velocity V divided by the quantity $(R^{2/3}S^{1/2})$.	$ft^{1/3}/sec$
K'_r	A comparable measure of the flow resistance due only to the resistance of the stationary grains, and for metric units it can be computed from $26/(D_{90})^{1/6}$ in.	$ft^{1/3}/sec$

LIST OF SYMBOLS (Continued)

Symbol	Definition	Units
k	The turbulence constant (von Karman universal constant) which is about 0.40 for clear-water flow and certain types of boundary roughness but may vary widely for sediment-laden flow and dune roughness	--
L	Length of bend	ft
L_p	Length of pool	ft
M	Percent silt-clay in the perimeter of channel	--
M_ℓ	Meander wave length	ft
M_w	Meander width	ft
n	Manning's coefficient	sec/ft$^{1/3}$
P	Wetted perimeter of the channel	ft
Q	Discharge	ft^3/sec
Q_s	Bedload discharge	gm/min
q_B	Bedload discharge per foot of width in terms of weight of sediment per unit time.	lbs/sec ft
q_B'	Bedload discharge per unit width in terms of underwater weight of sediment per unit time.	lbs/sec ft
$Q_{\tau c}$	Probability that in a given flow the local shear stress acting on an individual grain is smaller than the critical shear stress of that grain. $= \frac{1}{\sigma\sqrt{2\pi}} \int_{-\infty}^{\frac{\tau}{\bar{\tau}} - 1} \exp\left(-\frac{X^2}{2\sigma^2}\right) dx$	--
R	Hydraulic radius $= \frac{A}{P}$	ft
r	Radius of bend	ft
S	Slope of the channel	--

LIST OF SYMBOLS (Continued)

Symbol	Definition	Units
u	Velocity at a distance y from bed	ft/sec
u_{max}	Velocity at the surface	ft/sec
u'	Turbulent velocity fluctuations in the x direction	ft/sec
V	Mean velocity = Q/A	ft/sec
v'	Turbulent velocity fluctuations in the y direction	ft/sec
W	Width of channel	ft
x	Distance along the channel	ft
y	Distance above the channel	ft
Δz	Superelevation	ft
ε_m	Turbulent momentum transfer coefficient	ft^2/sec
γ	Specific weight of water	lbs/ft^3
γ_s	Specific weight of the sediment particles	lbs/ft^3
ρ	Mass density of water	$lbs\ sec^2/ft^4$
ρ_s	Mass density of sediment	$lbs\ sec^2/ft^4$
σ'	Gradation of bed material	--
σ	Standard deviation of the shear stress fluctuations.	--
τ	Local shear stress	lbs/ft^2
$\overline{\tau}$	Mean bed shear stress	lbs/ft^2
τ_c	Critical shear stress of the individual grain under consideration	lbs/ft^2
θ_F	A dimensionless measure of the apparent tangential stress due to action of external forces on the fluid and equal to $[\rho_f/(\rho_s - \rho_f)](RS/D)$.	--

Symbol	Definition	Units
θ_t	That value of θ_F (determined by extrapolation) at which sediment particles begin to move on a rippled sand bed.	--
η	Ratio of actual length to computed length of bend	--

Chapter I

INTRODUCTION

General

The bed and banks of an alluvial river are composed of sedimentary material that has been transported and deposited by the river itself. Alluvial rivers have played and at present play a major role, not only in the shaping of the earth's surface, but also influencing man's life on earth. From earliest times alluvial rivers have been arteries for travel and trade, and along their banks civilization arose. Their broad fertile floodplains were the sites of early agricultural efforts and are the sites of modern cities.

However, alluvial rivers also cause tremendous problems to man. An occasional flooding of the lowlands refertilizes the soil and may be beneficial under pristine conditions, but such floodings frequently bring disastrous loss of crops, destruction of engineering works, and loss of life. As a result attempts are made to control the rivers so that flood damages are reduced and dependable navigation channels are maintained. However, before a river can be controlled it should be studied in sufficient detail, so that its response to the controls can be anticipated.

Rivers flowing in alluvial materials, under a given set of climatic, hydrologic, geologic, and geomorphic conditions, exhibit a similarity of pattern and shape that implies cause and effect relations. It is, of course, very important to understand the behavior of rivers under diverse conditions and to identify the complex and interdependent variables which are responsible for the geomorphic and hydraulic character of a stream. However, the nature of a change of river character may be clearly apparent to the trained observer but the reasons therefor often are obscure or, if suspected cannot be proved. This is because there are many interdependent variables influencing a river and rarely can one be isolated and its effects studied. For example, Lane (1957) stated that "There is nearly infinite variety in stream forms, if considered in detail. No stream is exactly like any other stream and no part of any stream is exactly like any other part of the same stream". This is because stream channel forms are the result of a great many factors, and the same combination of these factors is never exactly repeated. However, stream channels, forms and shapes are the results of physical laws and if the conditions controlling the shape of any part of a stream were exactly reproduced, the same form of a stream would result.

Variables Affecting Alluvial Rivers

A great many factors affect stream channel forms. Some affect the the form directly, and others affect it because of their influence on the directly affecting variables

According to Lane (1957), the most important variables affecting alluvial streams are: (1) stream discharge, (2) slope, (3) sediment load, (4) resistance of banks and bed to movement by flowing water, (5) vegetation, (6) temperature, (7) geology, and (8) works of man. Undoubtedly, other factors are involved, but Lane believed these eight to be major. They are not all independent, however, as many depend to a greater or less extent on the others. The interrelation between slope, sediment load, and resistance of the banks and bed to movement is particularly close and complex.

Simons (1970) stated that "variables affecting alluvial channel forms are numerous and inter-related. Their nature is such that, unlike rigid boundary hydraulic problems, it is not possible to isolate and study the role of an individual variable". For example, if one attempts to evaluate the effect of increasing channel depth on the average velocity, additional related variables respond to the changing depth. Similarly, not only will the velocity respond to the change in depth but also the form of bed roughness, the position and shape of alternate, middle, and point bars, the shape of cross section, the magnitude of sediment discharge, and so on. Consequently, the mechanics of flow in alluvial channels and the response of channel geometry is not as well understood and explained as many other areas of fluid mechanics and hydraulics.

Simons (1970) gave the list of the most important variables which influence the geometry of river channels. That list includes the following variables:

$$\phi[V, D, S, \rho, \mu, g, d, \sigma, \rho_s, S_p, S_R, S_C, f_s, C_T] = 0 \qquad (1)$$

in which

V = velocity,

D = depth,

S = slope of energy grade line,

ρ = density of water-sediment mixture,

μ = apparent viscosity of water-sediment mixture,

g = gravitational constant,

d = representative fall diameter of the bed material

σ = gradation of bed material

ρ_s = density of sediment,

S_p = shape factor of the particles,

S_R = shape factor of the reach of the stream,

S_C = shape factor of the cross section of the stream,

f_s = seepage force in the bed of the stream, and

C_T = concentration of bed-material discharge.

The majority of these variables were discussed in the analysis of forms of bed roughness by Simons and Richardson (1962).

Using V, D, and ρ as the repeating variables and applying the Pi-theorem

$$\phi_1 \left[S, \frac{VD\rho}{\mu}, \frac{V}{\sqrt{gD}}, \frac{d}{D}, \sigma, \frac{\rho_s}{\rho}, S_p, S_R, S_C, \frac{f_s}{\rho V^2}, C_T \right] = 0. \qquad (2)$$

Equation 2 gives the list of the nondimensional parameters which are important in the study of alluvial river characteristics.

Classification of Stream Forms

In spite of the many variables that appear to determine river morphology, Schumm (1963a) proposed to base the classification of river channels on only the type of sediment load carried by the river. He stated that of the two independent variables, discharge and sediment load, the discharge determines mainly the size of the channel and is not as critical as the type of sediment load which determines channel shape, and sinuosity, (Figures 42 and 45). He then proposed a river classification based on this concept. The three classes are: bedload channel, mixed-load channel and suspended load channel. He stated that the type of material transported or the mode of its transport as bed load or suspended load appeared to be a major factor determining the character of a stream channel. A final subdivision of channels is based on channel stability as influenced by quantity of sediment load (Table 1).

Channel Patterns

Channel pattern is also used as a basis for classification of rivers. By channel pattern is meant the configuration of a river as viewed on a map or from the air. Channel patterns are either straight, meandering, or braided.

Straight Channel - A straight channel is one that does not display a sinuous course. However, very few streams are completely straight for any appreciable distance. Furthermore, a stream may have relatively straight banks but its thalweg may be sinuous. Thus there is no simple distinction between a straight channel and a meandering channel.

The ratio of channel length to downvalley distance is often used as a basis for distinguishing between meandering and straight channels. This ratio, called sinuosity, varies in rivers from a value of unity to a value of about 3 or more. Leopold, Wolman, and Miller (1964) arbitrarily used a sinuosity of 1.50 as the division between meandering and straight channels. Nevertheless a river with a sinuosity of 1.25 or greater would be considered to be meandering by most observers.

Meandering Channel - In this study a meandering stream is defined as one whose channel alignment consists of easily recognized bends. A meander consists of two consecutive bends, in one of which if the water is flowing in a clockwise direction in the other it will flow in a counter-clockwise direction. The phenomenon of meandering in rivers is one of great interest because there is no obvious reason why a stream should not follow a direct route down its valley. This interest is manifested

Table 1. Classification of Alluvial Channels*

Mode of Sediment Transport and type of Channel	Channel Sediment (M) Percent Silt-clay	Bedload (Percentage of Total Load)	Channel Stability		
			Stable (Graded Stream)	Depositing (Excess Load)	Eroding (Deficiency of Load)
Suspended Load	20	3	Stable suspended-load channel. Width-depth ratio less than 10; sinuosity usually greater than 2.0; gradient relatively gentle.	Depositing suspended load channel. Major deposition on banks cause narrowing of channel; initial stream-bed deposition minor.	Eroding suspended-load channel. Streambed erosion predominant; initial channel widening minor.
Mixed Load	5-20	3-11	Stable mixed-load channel. Width-depth ratio greater than 10 less than 40; sinuosity usually less than 2.0 greater than 1.3; gradient moderate.	Depositing mixed-load channel. Initial major deposition on banks followed by streambed deposition.	Eroding mixed-load channel. Initial streambed erosion followed by channel widening.
Bedload	5	11	Stable bedload channel. Width-depth ratio greater than 40; sinuosity, usually less than 1.3; gradient relatively steep.	Depositing bedload channel. Streambed deposition and island formation.	Eroding bedload channel. Little streambed erosion; channel widening predominant.

*After Schumm (1963a).

by many scientific papers in which meandering channels have been described with various degrees of sophistication, and a variety of explanations of the cause of meandering have been offered.

Papers presenting arguments to explain why meanders occur are discussed in the next few pages. They can be grouped into four main sets, depending on the nature of the argument used and they are discussed in the following sequence:

1. Secondary currents
2. Dynamic instability concept
3. Statistical arguments
4. Miscellaneous.

Secondary currents always occur in bends of pipes and open channels where they are explained by the difference of the centrifugal forces acting on flow lines of different velocities. The existence of secondary currents in bends and the way these affect the movement of bed material make it clear that they have a significant effect on the growth and migration of a meander. Prus-Chacinski (1956) showed that secondary currents cause meanders to form if a slight asymmetry of the flow makes the streamlines curve. However, the secondary currents may themselves be the result of the meander. Therefore, for secondary currents to be important in the formation of meanders it must be demonstrated that secondary currents can occur in a straight channel. It is also necessary to show that the secondary current can be reversed periodically along the channel.

Although the papers of Einstein and Li (1958) and Delleur and McManus (1959) do not provide a solution, they do show that secondary currents are possible and indeed probable in straight channels.

Considerable support for the idea that secondary currents cause meanders is given by Shen (1961) and Einstein and Shen (1964). In experiments in flumes 1 foot, 3 feet, and 10 feet wide, two kinds of meandering patterns were observed. They concluded that the first type of alternating diagonal bar pattern resulted from surface waves on the water. The second type of pattern had alternating scour holes and occurred predominantly when the water was flowing between banks which were rougher than the bed. Shen (1961) argued that the pool and bar configuration in this case was caused by secondary currents. He also showed how the secondary currents can be reversed periodically along the length of the channel.

More formal mathematical studies have been based on the concept of dynamic instability. In these, the aim is to determine how the amplitude of a disturbance to the bed changes with time. Several such studies have dealt with the formation of bed features; those of Exener, Anderson, Kondratev, Lyapin and Kennedy have been summarized by Raudkivi (1967). The suggestion that meanders arise from instability of the bed was made by White (1940), although he did not attempt a mathematical treatment of the problem. His suggestion was based on observations in small laboratory channels with loose boundaries. When sand was fed in the channel at its inlet, long mounds formed on the bed of the channel and, as they moved downstream, they migrated to one side or the other of the channel. As a mound approached a bank, the asymmetry of the flow caused erosion of the opposite bank, and the additional bedload augmented the next mound downstream. This occurred in straight channels, and no disturbance was required at the upstream end. White's observations show that the bank caving, which Friedkin (1945) said is essential for the development of meanders, can be caused by instability of the bed. Others who contributed in this field are Reynolds (1965), Hansen (1967) and Callender (1969).

In recent works by Leopold and Langbein (1962) and Scheidegger and Langbein (1966) an attempt has been made to treat landscape processes generally as if they were stochastic in nature, that is, as if they occurred in random fashion. The underlying assumption is that a river channel adopts a form which is most probable. The most probable path between two points, A and B, is understood to be one which would be followed most frequently if the journey is repeated a large number of times. With regard to meandering, Langbein and Leopold (1966) assumed that there are a multitude of random effects that influence the flow of a river thereby causing its deviation from a straight course. Consequently, a river has a finite probability to deviate from its previous direction in progressing a certain small distance downstream. The actual meander path corresponds to the most probable river path that one would obtain between two points A and B, if the direction of flow at the point A is fixed and the probability of a change in direction per unit river length is given by the Gaussian Probability distribution. This formulation of the problem is identical to that of a class of random walk problems that have been studied by von Schelling (1951, 1964) in a different context. Solutions by von Schelling show patterns that are characteristically seen in river meanders. These works show that the simple statistical assumption introduced above explain the existence of meanders.

A series of experiments which were intended to throw light upon the problem of meandering tendencies of alluvial streams, were performed by Tiffany and Nelson (1939) and Friedkin (1945).

Tiffany and Nelson (1939) concluded that meandering is essentially the result of erosional and depositional processes. The materials eroded from the banks are deposited to form bars, and these bars, by constricting the channel, pushed the flow against the opposite banks which caused more erosion of banks.

Friedkin's (1945) observations regarding the formation of meanders support the observations made by Tiffany and Nelson, that is, the sole cause of meandering appeared to be bank erosion.

Tanner (1960) experimented with minute meandering streams suspended by surface tension on the underside of a sloping sheet of glass and concluded that meandering cannot be ascribed to granular bedload. Bagnold (1960) found that minimum head loss in pipe bends has been consistently reported at a ratio of bend radius to pipe diameter between 2 and 3. Noting that Leopold and others (1960) had reported a similar minimum for open channels with rigid boundaries at the same ratio, Bagnold (1960a) concluded that meander form would be such so that head loss is minimum.

Braided River - River braiding is characterized by channel division around alluvial islands. Braiding was studied by Leopold and Wolman (1957) in a laboratory flume, and they concluded that braiding is one of the many patterns which can maintain quasi-equilibrium among discharge, sediment load, and transporting ability. They also stated that braiding does not necessarily indicate an excess of total load.

As a result of the studies discussed in his 1957 report and his studies on the design of stable channels in irrigation canals, Lane (1957) concluded that there are two primary causes of braiding streams. Either one of these two causes alone may be responsible for the braided pattern, or they may both be acting to cause it. These causes are: (1) overloading, i.e., the stream may be supplied with more sediment that it can carry and part of it may be deposited, and (2) steep slopes causing a wide, shallow channel, in which bars and islands readily form.

Slope-Discharge Relations

Efforts have been made to distinguish between meandering and braided streams on the basis of slope-discharge relations. For example, Lane (1957) made a plot showing the relationship between slope and discharge for sand bed meandering stream (Figure 1). By drawing a line in Figure 1 through the points (1, 2) representing the model of the Mississippi River and averaging those representing the sections (3, 4) of the lower Mississippi River, he obtained a line described by the equation

$$S = \frac{0.0017}{Q^{\frac{1}{4}}}. \tag{3}$$

Observing that this form of equation fits a large amount of data from meandering sand streams, Lane expressed the equation in the following form

$$S = \frac{K}{Q^{\frac{1}{4}}} \tag{4}$$

where $K = 0.0017$ for all meandering streams in sand under equilibrium conditions.

By using only data from sand streams having steep slopes he made a quantitative comparison of the slope-discharge relations for braided streams. The slope-discharge relations for braided streams can be approximately represented by a line having an equation [Figure 2]

$$S = \frac{0.01}{Q^{1/4}} \qquad \text{i.e.,} \quad K = 0.01. \tag{5}$$

This represents a slope of about six times as steep as that for meandering sand streams.

Objectives

Cost aside, it is very difficult to make a sufficient number of accurate surveys of a rapidly changing river to determine what is occurring. In a great river it is difficult to see the movement of sand along the bottom and to observe how bars are formed. It is also very difficult to determine where materials caved from banks go, and where the materials deposited on bars originate and how braiding occurs. Thus, it is even more difficult to establish cause and effect relations. However, one way in which these problems may be approached and even solved efficiently and economically, is through model studies. By using small streams flowing in selected erodible materials, it is possible to study the development of different channel patterns, the mechanics of bed material transport, bar formation, and other fluvial characteristics which improve our understanding of the complicated phenomena of alluvial rivers. In the laboratory, variables can be controlled and isolated permitting evaluation of their influence on alluvial river morphology.

In all previous experimental studies of model meander development (Friedkin, 1945; Tiffany and Nelson, 1939; Nagabushanaiah, 1967;

Velikanov, 1950; Andreev and Yaroslavtseu, 1953), sand-size sediment has been used to form the bed and banks of the model channel. During longer spans of time, sediment load characteristics may change in response to climate change, and it has been concluded for some alluvial rivers that the formation of meanders accompanies a decrease in bedload (Schumm, 1963b). River meanders, therefore, appear to have more than just a hydraulic control, and it is anticipated that a sinuous channel will develop in the laboratory when suitable adjustments are made in the type of sediment load moving through the channel.

The objectives of this research are to:

a. investigate the cause of different channel patterns as well as to document the morphologic character of different channel types,

b. establish the effect of discharge, sediment load, and slope on channel morphology.

Chapter II

EXPERIMENTAL METHOD AND DATA COLLECTION

Equipment

A concrete recirculating flume 100 feet long, 24 feet wide, and about 3 feet deep was used in this study (Figure 3). The flume has double walls along its length; the inner wall of each pair being permeable. The flume was filled with sand, and the water table in the sand was regulated by controlling the water level between the double walls.

A steel bridge spans the width of the flume and is mounted on rails on the inner walls. The bridge is moved by an electric motor drive. It is equipped with a cantilevered boom for illuminating and photographing the model channels and point gages for measuring elevations of the sand surface. Ten 300-watt light bulbs and a cinetron provided light for photographs. Metric scales were installed along the length of the flume, and along the sides of the bridge; these were used to establish a coordinate system, and channel morphology was measured in relation to them.

Water was introduced into the upper end of the flume through entrance baffles, which after flowing through the model channel, entered the tail box and was recirculated by means of an axial flow pump. Water discharge was measured by a 2-inch venturi meter. A float valve was installed in the tail box, which regulated flow from a 3/4-inch line, and this arrangement prevented the water level in the tail box from falling below a specified level. A 2-inch pipe was also installed for the purpose of draining water from the tail box. This pipe could be raised or lowered and it was used to prevent the water level in the tail box from rising above the desired level. The combination of the float valve and the 2-inch pipe was necessary for maintaining a constant water level in the tail box during each experiment. The control of the tail box water level was essential for the following reasons:

1. to provide a specific depth of flow where water enters the tail box;
2. to eliminate back water effects in the lower part of the laboratory channel, and
3. to maintain a constant water level, which permits the pump to operate at a constant head, thereby maintaining a constant discharge.

A 2½-inch pump was used for recirculating the water in the flume. The total flow was divided into two parts just below the pump and a small fraction of the total flow was diverted back to the tail box in order:

1. to reduce pressure on the manometer which was connected to the venturi meter, and
2. to create sufficient turbulence in the tail box to maintain fine materials like silt and clay in suspension.

A smaller pump was also installed to pump water into the side channels and tail box from the sump located under the floor of the laboratory.

Discharge

The minimum flows used were 0.10 cfs and the maximum flows were 0.30 cfs. Five tests were made with water which contained a high concentration of suspended sediment. A constant discharge of 0.15 cfs was used for these tests. In all other tests, clear water was used.

Sand Feeding at Entrance

Sand was introduced at the entrance of the channel to compensate for the sediment trapped in the tail box. Although the water was recirculated, most of the coarse load remained in the tail box, and relatively clear water was returned to the channel. Clear water caused scour at the upstream part of the channel and the addition of sand to the system prevented this scour.

The rate at which sand was fed at the entrance was determined by trial and error tests. The proper rate was that which maintained the initial longitudinal slope of the bed in the upstream portion of the model river. When less than the required rate was introduced the channel deepened, and its slope became flatter. When more than the required rate was introduced the channel aggraded, and its slope became steeper. Using constant longitudinal slope as the criterion, sand was fed to the stream at the entrance at practically the same rate at which sand was leaving the channel at the downstream end. The determination of the appropriate rate of sand feed emphasized that for each discharge and slope only one rate of sand feed maintained the desired slope. The higher the discharge or the greater the slope, the higher was the required rate of sand feeding.

Bed Material

The bed and banks of the channels were composed of sand, the size distribution of which is shown on Figure 4. Although the median grain size was about 0.70 mm, the size of the material varied over a wide range and sorting was poor. The gradation, σ, of a material is defined as

$$\sigma' = \frac{1}{2} \left(\frac{d_{84}}{d_{50}} + \frac{d_{50}}{d_{16}} \right) .$$

The gradation for the sand was 2.22. This sand was also fed into the channel as described previously. This range of bed material size distinguishes these experiments from others in which more or less uniform bed material size was used.

Suspended Sediment

Five tests were made with water containing a high concentration of suspended sediment. In all the tests of this type, a constant concentration of 3 percent (30,000 ppm) by dry weight was maintained. The clay (kaolinite) was added to the water in the tail box, turbulence in the tail box appeared sufficient to keep it in suspension, but nevertheless, the water in the tail box was frequently agitated by hand to ensure suspension of the clay. Some clay was deposited in the channel and therefore it was necessary to add clay to maintain a constant concentration of fine sediment. The water was sampled frequently and the concentration was measured by using a hydrometer. The hydrometer was calibrated by using water with known concentrations of suspended materials.

Experimental Procedure

Before each test, the sand in the flume was compacted and leveled. In order to consolidate the sand, the flume was flooded with water and after a short period the water was drained to a lower level.

A channel was then excavated along the center line of the flume. The initial channel was about 1 foot wide and about 3 inches deep. In each test the bed of the channel was graded to the desired slope. To establish a specific slope, wooden stakes were placed along the length of the channel at intervals of 6 feet. The elevations of these stakes were fixed by leveling, and the channel was graded to the desired slope using the stakes as guides.

Prior to introduction of running water into the channel, the ground-water table was raised by pumping water into the side channels and filling the tail box.

Water was introduced into the channel by starting the recirculating pump, and discharge was gradually increased to the desired level.

Sand was added at the entrance from the vibrating sand feeder at a rate to compensate for the coarse material which trapped in the tail box.

Water was allowed to flow through the initial channel until the channel adjustments were complete and the channel became stable. During each test elevations of water surface and bed were measured at various points along the thalweg by using the point gage. The difference between these two elevations gave the depth of flow.

At the end of each experiment the following data were collected:

a. location of the left and right banks;

b. location of the thalweg;

c. location of pools and crossings;

d. longitudinal profile along the thalweg; and

e. cross sections of channels at various sections.

In addition, the rate of sand feed and discharge was noted. Morphologic and hydraulic characteristics of the channel and values of velocity, shear, stream power, Froude number, etc. were calculated by using these data.

Description of Tests

The experiments were divided into 3 major groups depending on the entrance conditions and sediment load. In one series of experiments, a straight entrance was used. Meander patterns developed in the laboratory channel with a straight entrance, but an uniform meander pattern along the length of the channel could not be obtained because of the short length of the flume. For this reason the second set of tests were made with an initial bend at the inlet in order to obtain a more or less uniform meander pattern along the length of the channel. Friedkin (1945) showed that the development of a series of uniform bends from an initiating bend was possible and capable of duplication. Development of an uniform meander pattern was essential for the study of hydraulic characteristics and geometry of meandering channels and for comparison with straight and braided channels. In this series of tests, a short entrance channel was molded at an angle of 40 degrees to the longitudinal axis of the flume. The entrance in both cases was made of stable materials such as gravel and small rocks. The most satisfactory type of entrance was relatively long (about 4 feet) so that the decrease in velocity from the inlet box to the channel proper occurred slowly. For example, rapid acceleration of flow in the entrance often caused excessive scour just below the entrance, and when the channel scoured below the lip of the entrance, the drop caused further local turbulence and scour.

In the third series of experiments, a high concentration (30,000 ppm) of kaolinite was maintained in the flow. The entrance condition in this final series of experiments was similar to that of the second series of experiments. The purpose was to study the effect of change of sediment characteristics of a meandering channel.

Chapter III

RIVER CHANNEL PATTERNS

In order to study the characteristics of different alluvial river channel patterns, a series of tests were made in which discharge was kept constant and the slope was varied from 0.001 (very flat) to 0.02 (very steep). Each test was performed at a different slope.

Several channel patterns were observed in the laboratory. Plan view, cross sections and photographs of different channel types are shown in Figure 5. Characteristics of various channel patterns are described in the next few pages and basic data are presented in the appendix.

Straight Channel

In the laboratory, straight channels occurred at very flat slopes. With the straight entrance, straight channels persisted for slopes equal to or flatter than 0.004. With an initial bend, the straight channel was maintained for slopes flatter than 0.0026.

A straight channel had a deep and narrow cross section and the banks were straight. The cross sections of the channels were almost uniform throughout the length of the channel. Two or three bends formed in the channel in those tests (flatter than 0.0026) with an initial bend. The initial bend, of course, directed water against the bank and caused erosion and alternate bars were formed due to the migration and deposition of bed materials. However, the size of the bends decreased sharply in the downstream direction and the channel became straight in the lower part of the flume. Such a channel was considered to be a straight channel (see Figure 5).

Meandering Thalweg Channel

Meandering thalweg channels occurred at slopes slightly steeper than those for straight channels. The banks were more or less straight but series of alternate bars developed, which produced a sinuous thalweg.

The meandering thalweg developed for slopes equal to or greater than 0.0047 and 0.0026 depending on whether the water enters the channel straight or at an angle. That is, the meandering tendency occurred at a flatter slope with initial bend. At slopes greater than 0.0026, the initial bend caused the development of series of more or less uniform bends and bars throughout the length of the channel. Each bend developed as a result of impingement of flow and erosion of banks with deposition of sand on the inside of the bend. At these slopes flow conditions were such that erosion of the banks occurred throughout the length of the channel. It was this bank erosion that supplied material for the formation of alternate bars.

Ippen and Drinker (1962) performed a series of tests to study the distribution of boundary shear stresses in curved trapezoidal channels. Their work provides an explanation for the fact that meandering develops at a flatter slope with an initial bend. They showed that bends of channels were subject to shear stresses, which increased in intensity, as well as in areal extent, with conditions of increasing radius of bend, and that the maximum shear stress in a bend exceeded in intensity the mean shear for uniform motion in straight reach by over 100 percent. The maximum ratio for these two shear stresses was 2.4. The locations of the local higher shear stresses were associated with the path of the flow filament of the highest velocity and with the zones of local accelerated motion. For a bend having a smaller radius of curvature, the increased stresses appeared along the outer bank, in the downstream portion of the curve.

The high local shear stress near the concave banks of bends caused significant erosion which supplied bed load for the formation of alternate bars. The bars pushed the flow towards the outer bank and restricted the flow in a narrow channel which caused further erosion of the banks.

Development of alternate bars - Photographs in Figure 6 show the different stages in the development of a meandering thalweg in a straight channel. The first photograph of that Figure shows the initial channel of a laboratory stream which was straight except for an initiating bend. The bed and banks of this small scale river were composed of erodible material, the longitudinal slope was uniform, and a constant rate of flow of 0.15 cubic foot per second was passed through the channel. Successive photographs show the gradual development of meandering thalweg from this initial channel. Observations shortly after the test were started indicate that a sinuous flow existed in the channel even before the development of bars and pools. The fact that the bars and pools formed almost simultaneously throughout the length of the channel (although with a progressive dampening effect as their distance from the entrance increased) also supports this contention. The development of the meandering of the thalweg occurred in the following manner. The maximum impingement of the current, with resulting scour, occurred against the concave bank in the lower part of the initial bend. The sand scoured from this bank was moved along the bed to form a bar on the same side of the stream and just below the point of scour. As the bar increased in size and was built out into the stream, a corresponding increase in the size of the pool on the opposite side of the stream occurred, thus starting a bend in the reverse direction. An area of dead water was created on the sheltered (downstream) side of the bar due to the protection of the bar itself; the result was that this area did not fill with sand. Inasmuch as similar phenomena occurred almost simultaneously throughout the length of the channel, several bends were developed simultaneously.

As the tests progressed and before the channel became stable the continuation of the above action caused a continuous increase in the size of the bends, which was accompanied by a progressive downstream movement of the bends. In every bend scour occurred on the concave bank, usually in the downstream portion of the bend. The sand eroded from this bank was carried downstream and most of it was deposited on the alternate bar on the same side of the stream from which it was eroded. Some of the sand, however, was carried still further downstream, to be deposited either in the crossing or on the next alternate bar downstream.

Soon after the start of a test, there were several clearly outlined bends. As the test progressed, the bends enlarged and progressed downstream. At the end of a test there were usually fewer bends remaining within the flume and the channel became stable.

Pools and crossing - The cross sections of the small-scale meandering thalweg channels were deep along the concave banks of bends and shallow in the tangents between bends so that the thalweg profile consisted of a series of deeps separated by shoals. The deeper portion of the channel is called a pool or bendway, and the shallower portion between the pools is known as a crossing.

As shown in Figure 7, bendway section is deep with a steep bank profile on the concave side of the channel. The depth decreases sharply toward the convex side of the bend as the channel bottom grades into the alternate bar. At the crossing or point of inflection of the bend, cross sectional shape is not completely symmetrical; rather it is slightly deeper near the bank which was concave in the bend immediately upstream.

The typical cross sections in pools and crossings are due to secondary currents and convergence of flow in the bends of the channels.

A brief description of the secondary current is given below. It will be discussed in detail in the next section.

As the water moves in a winding pattern in a bend, it develops a strong centrifugal force which causes a superelevation of the water level on the outside of the bend. Pressure from the excess weight of water piled up in this way caused a helical flow at the bend, giving a strong downward movement on the outside with consequent erosion. This is, in its turn, compensated for by an outward flow at the surface. The final effect is a circulatory flow pattern like that shown in Figure 7. This secondary flow pattern in the bends of rivers tends to scour sediment from the outside bank and to deposit it on the inside bank, forming a typical bendway cross section as shown in Figure 7.

Ippen and Drinker (1962) conducted a series of tests to study the flow of water in the bends of rivers. They observed that a zone of separation formed at the inside of bends. A similar observation was made during this study [Figure 7]. Such a zone of separation reduced the effective area of the flow cross section, resulting in acceleration of the constricted flow and a deflection of the flow away from the inner bank. It means that the flow into the bend converges towards the outer bank and in flowing out of the bend it diverges and so on. Where the flow converges it excavates a deep into the bed of the river. Some sediment is carried downstream by the flow and some of the materials are moved towards the inner bank by the secondary currents. The diverging flow downstream of the bend cannot carry all of this sediment and deposits some, leading to the shallow banks at inflection points.

Transverse circulation at bends in open channel flow - When the hydraulic engineer speaks of an open channel flow he visualizes boundaries confining a flow which is predominantly one-directional. However such flows have been observed to possess a rotation or circulation around an axis parallel to the main flow velocity, transforming it into a helical or multihelical flow. These superimposed relations are usually called secondary motion. Best known is the occurence of secondary currents in bends of pipes and open channels, where they are explained by the difference of the centrifugal effects in flow lines of various flow velocities.

For example, if fluid is flowing along a curved pipe of any cross section there must be a pressure gradient across the pipe to balance the centrifugal force. The pressure must be greatest at the outer wall, and least at the innerwall. The fluid near the top and bottom walls is moving more slowly, however, than the fluid in the central portions, and requires a smaller pressure gradient to balance its centrifugal force. In consequence, a secondary flow is set up in which the fluid near the top and the bottom moves inwards and the fluid in the middle moves outwards [Figure 8]. The pressure at the outer wall is greater at the middle of the pipe then at the top or the bottom, whilst at the inner wall it is less. The secondary flow is superposed on the main stream, so that the resultant flow is helical in the top and the bottom of the pipe.

Helical flow occurs in open channels, and in rivers at bends. As a result, the region of maximum velocity is displaced from the center of the pipe or of the free surface of the channel or river towards the outer wall.

To prove the existence of transverse current in a bend of open channel flow, let us separate a fluid element with length dx and depth h as in Figure 9, and let us consider the forces acting on it in the radial direction. Two forces will act on the element under consideration; the centrifugal force, whose variation over the vertical will correspond to the variations of the square of tangential velocities, and an opposing force, due to the existence of a transverse slope; this force is obviously constant throughout the depth and can be expressed by the quantity γdz. A graphical summation of these two curves (Figure 9) indicates the absence of equilibrium in the fluid in the plane of the stream cross section. The curve obtained from the summation of the transverse velocity components indicates the presence of a flow directed toward the concave bank in the upper part of the vertical, and of a reverse flow in its lower part. Since there should be no residual flow discharge in the transverse direction, the areas of these curves of opposite direction must be equal. Transverse currents superimposed on the longitudinal flow, form a screwlike type of circulation which can be observed in river bends.

Thalweg Meander Geometry - The purpose of this section is to determine the relationship between free thalweg meander dimensions, discharge, and slope for the range of data covered under the present study. A free meander is defined as one developed in alluvium and free to erode laterally, unrestrained by valley walls, and with wave forms not materially distorted by inhomogenities in the alluvium.

Figure 10 shows the relationship between thalweg meander wave length, slope, and discharge and thalweg meander width, slope and discharge. Thalweg meander wave length and thalweg meander width increases with discharge for a given slope. At any given discharge there is an increase in the meander dimensions with increasing slope. The increase in meander dimensions are due to higher erosion capabilities associated with greater discharges and steeper slopes. An increase in discharge at a constant slope implies greater depth, higher velocity and shear. Whereas an increase in slope at constant discharge means a smaller depth of flow and higher velocity and shear. Moreover a greater discharge needs a larger radius of curvature to change the direction of flow because of its higher inertia of motion. Similarly a flow having a higher velocity tends to form a larger bend. A larger bend means larger meander wave lengths and meander widths.

Figure 11 shows the relationship between thalweg meander wave length, slope and discharge. Mathematically this relationship is

$$M_\ell = 107\ Q^{0.25}\ S^{0.25} \tag{6}$$

where M_ℓ is the thalweg meander wave length.

Figure 11 also shows that thalweg meander wave length is proportional to 1/4 power of bedload concentration. A greater bedload concentration is the result of a higher velocity. A greater velocity is associated with higher discharges and steeper slopes which in turn developes larger bends. The relationship between thalweg meander wave length, discharge and bedload concentration is

$$M_{\ell} = 5.36\, Q^{0.25}\, C_s^{\;0.25}. \tag{7}$$

Figure 12 shows the relationship between thalweg meander width, slope, and discharge and is given by the following equation:

$$M_w = 41\, Q^{0.26}\, S^{0.26}. \tag{8}$$

A similar relationship between thalweg meander width, discharge, and bedload concentration is (Figure 12)

$$M_w = 1.45\, Q^{0.28}\, C_s^{\;0.28}. \tag{9}$$

Figure 13 shows the relationship between thalweg meander wave length and channel width and it is represented by the following equation:

$$M_{\ell} = 8.0\, W^{0.66} \tag{10}$$

in which W is the channel width.

The above equation shows that thalweg meander wave length increases with channel width. Physical explanations for such a relationship are as follows. A greater width is associated with a larger discharge and a larger discharge produces greater meander dimensions. A similar observation was made by Jefferson (1902) regarding the relationship between meander wave length and channel width. He argued that streams are composed of many threads of water side by side, and the wider the stream the more threads of currents, and the consequent greater difficulty in making sharp bends.

Figure 14 gives the variation of thalweg meander wave length with radius of bends. The present data fits the Leopold and Wolman's lationship between meander wave length and radius of bends. This relationship can be expressed by the following equation:

$$M_\ell = 4.7\ r^{0.98} \tag{11}$$

where r is the radius of bend.

Figure 15 gives the relationship between radius of bend and discharge. Radius of curvature increases with discharge. The reason for this relationship is that a greater discharge needs a larger bend to change the direction of flow.

Figure 16 shows that the maximum depth in a pool increases with the radius of curvature of bend. A greater discharge forms a bend with larger radius of curvature and also it needs a greater depth in the pools. Hence, maximum depths in pools increase with radius of curvature of bends as shown in Figure 16.

Meandering Channels

Meandering thalweg channels developed in non-cohesive materials. This type of channel is wide and shallow in cross section. Wide and shallow channels always form in non-cohesive materials because banks of shallow channels are subjected to smaller shear stresses.

Meandering channels developed with high concentration of clay in the flow. Meandering channels had narrow and deep cross sections. Clay deposited among the coarser materials in the bank and acted as binding agent which enabled the banks to withstand greater shear stress. As a result a narrow and deep channel formed.

Detailed discussions about the mode of development and characteristics of meandering channels is given on Chapter V.

Braided Channels

A braided channel is one which flows into two or more interlacing channels separated by alluvial islands. River braiding took place at steep slopes and with high concentrations of bedload. Braided conditions occurred in the laboratory for slopes equal to or greater than 0.016. This study indicated that braided channels were steeper, wider, shallower, and had a higher concentration of bedload than meandering or straight channels. All braided channels observed in the laboratory had several common characteristics in addition to that of multiple channels. These are as follows:

1. straight banks;
2. steep longitudinal slopes;
3. wide and shallow cross section; and
4. high concentration of bed load.

It can be explained why an extremely meandering alignment, in which the stream at the two ends of a bend come close together, is less likely to occur in steep streams than in ones of flatter gradient. When a stream is steep the differences of elevations of the water surface at the two ends of the bend is much greater for a given length of bend than when the gradient is small. Moreover higher velocity is associated with steeper slopes. Because of the higher velocity and greater differences of elevations of the water surface at the two ends of the bend (i.e., steeper slope), the flow cuts through the alternate bars and follows a straight path. As a result the sinuous thalweg disappears and the banks become relatively straight. The adverse bed profile from a pool to a crossing also facilitates the above mentioned phenomenon.

A stream with non-cohesive banks tends to develop a wide, shallow cross section. If a large steady flow of water is turned into a small, steep channel, the channel will be made wider by scour of the banks until the shear on the banks is reduced to a magnitude equal to that which the material composing them can resist. Since for a given slope of the stream the shear is proportional to the depth of flow, a wide, steep stream produces less shear on the sides than a deep one of equal slope, and the banks of the wide, shallow, steep streams can, therefore, resist scour better than deep ones of the same slope. Consequently, when a natural stream with steep slope is formed in erodible material, it tends to adopt this wide, shallow shape. If the shape at any section of a stream is such that the shear value on the banks is too high, bank scour occurs and the channel widens until the shear is reduced to a value which does not produce too severe bank scour.

A given value of shear in a stream will scour the banks more severely than the bed because the force of gravity acting on the material on the banks assists the scouring by the moving water, but in a stream cross section the maximum value of the bank shear is less than the bed shear and the effect of gravity is thus offset. The more easily eroded the bank material is, the wider will be the channel formed. This is probably the origin of Friedkin's view that braided channels result when the banks are extremely easily eroded.

Braided channels were observed to carry mostly coarse materials as bedload. Coarse bed materials were moving on or near the bed of the stream. The large concentration of bed material in braided channels was due to high shear stress caused by steep slopes. Stream beds tend to have coarse material on the bed because such streams produce high turbulence in the flowing water and most of the fine materials are kept in suspension and they move down the stream without being deposited on the bed.

A braided pattern developed after the formation of alluvial bars in the channel which caused the water discharge to flow in two or more anastomosing channels around alluvial islands. Observations during experiments showed that these bars formed as a result of deposition of coarse particles at some portions of the channel. The stream could not transport those coarse particles under the local conditions existing in that particular reach. Some finer materials were trapped among the coarse particles and as a result the initial bars increased in size. Development of the bars forced the flow against the banks causing further erosion. Similar observations regarding the formation and development of braided channels were made by Leopold and Wolman (1957) and Lane (1957). Leopold and Wolman (1957) stated that the growth of an island begins as the deposition of a central bar which results from sorting and deposition of the coarser fractions of the load which locally cannot be transported. According to Lane (1957), "The multiple channels can be formed by deposition of a small part of the heavy load being carried in certain places forming bars which often cause small islands at low flows, and thus multiple channels. In times of low flow the bars themselves form the multiple channels, although they are usually rapidly changing. On some of these bars vegetation grows, which causes still more deposition, and islands form which persist for some time even with high water flows. These depositions are the result of local overloading at the points where they are formed, but the river as a whole may be transporting downstream as much sediment as is being brought to it, the bars and islands at some places being formed and enlarged by a rate of deposition equal to the rate of scouring with which bars and islands at other points are being removed."

Meandering thalweg channels developed in the laboratory for slopes between 0.0026 and 0.0013 when water entered at angles. Braided channels developed for slopes equal to and steeper than 0.016. The flow developed a combination of meandering and braided patterns at a slope of 0.015.

With a slope of 0.015, meandering thalweg developed in the upstream portion of the channel though the banks were almost straight in that reach. Braiding of the channel developed in the downstream part of the channel. Longitudinal profiles of the channel showed that the slope in the braided reach was steeper than the reach where the thalweg followed a meandering path. Though the average slope of the channel was 0.0015, the braided reach had a slope steeper than 0.0015 and braiding developed in this reach.

Sinuosity

Figure 17 shows the variation of thalweg sinuosity with slope for a constant discharge of 0.15 cfs. The sinuosity is equal to unity (straight channel) for slopes equal to or less than 0.0020. Sinuosity increased between slopes of 0.0020 and 0.013. Between these two slopes, sinuosity of the thalweg increased rapidly at flatter slopes and the rate of increase decreased progressively as the slope increased. Beyond the slope of 0.013, sinuosity decreased due to the development of braiding in the channel. The channel pattern was a combination of meandering and braided for a slope of 0.015. In this type of channel, some part of the channel had a meandering thalweg and the rest of the channel was braided. The braided reach of the channel was straight and hence the sinuosity was unity for the braided reach. Sinuosity of the channel was unity for slopes equal to or greater than 0.016. For this range of slope, braiding developed in the entire length of the channel.

The sinuosity is equal to unity for slopes equal to or flatter than 0.0020 and for slopes equal to and steeper than 0.016. Although the sinuosity was unity (i.e., straight channel) for those ranges of slopes but the channel characteristics were completely different in each case. At flat slopes, the river had one channel, and it was relatively deep and narrow. Velocity of flow and bedload transport was low. Shear stress was low because of the low velocity of flow and as a result there were no significant bank erosions. Banks were very stable.

Sinuosity was also unity at steep slopes but the channel was braided in this case.

Braided channel developed at higher velocities. At higher velocities the flow cut through the bars and the channel became very wide and shallow and alluvial islands readily formed in such a channel. Because of the higher inertia of motion associated with a faster moving mass of water, the flow had a tendency to follow a straight path and as a result it cut through the bars. Alluvial islands developed in a braided channel due to the deposition of some of the coarser materials which the flow could not transport. Finer materials were trapped among the coarser particles and the bars increased in size. Finally the flow took place in a number of interlaced channels separated by these islands. The velocity and bedload transport was very high in a braided channel. The depths were very shallow. Between the slopes of 0.002 and 0.013, sinuosity of the thalweg increased with slope. This is due to the higher velocities and erosive capabilities associated with flow at steeper slopes. Moreover a faster moving mass of water needs a larger bend to change the direction of flow.

Figure 18 shows variation of sinuosity with slope and discharge. At a given slope, sinuosity increases with discharge. Rate of increase of sinuosity with discharge decreases progressively as discharge increases. Figure 18 also shows that for a given dischrage, sinuosity increases with slope up to certain limits.

Figure 19 shows the relationship between thalweg sinuosity, bedload concentration, and discharge. For a constant discharge of 0.15 cfs, thalweg sinuosity varies with bedload concentration in the following manner:

a. Thalweg sinuosity is unity (i.e., straight channel) for bedload concentrations equal to or less than 573 ppm (very low bedload concentrations).

b. Thalweg sinuosity increases with bedload concentration for bedload concentrations between 573 and 2180 ppm. For this range of bedload concentration, sinuosity increases rapidly at smaller concentrations and the rate of increase of sinuosity decreases as the bedload concentration increases.

c. Thalweg sinuosity decreases for bedload concentrations beyond 2180 ppm. This reduction in the value of sinuosity is due to development of braiding in the channel. The river channel pattern is a combination of meandering thalweg and braided for bedload concentrations between 2180 and 3200 ppm.

d. Sinuosity is unity for bedload concentrations greater than

3200 ppm. Braided rivers occur for bedload concentrations greater than 3200 ppm.

Figure 19 also shows that thalweg sinuosity of a meandering thalweg channel increases with bedload concentration for a constant discharge. For a constant bedload concentration, thalweg sinuosity increases with discharge.

It is seen from Figures 17 and 19 that for a given discharge, the relationship between thalweg sinuosity and slope, and thalweg sinuosity and bedload concentration are similar. The reason for such a similarity in relationships is that bedload discharge increases with slope for a constant discharge.

Figures 20, 21 and 22 show the variation of thalweg sinuosity with velocity, Froude number and stream power respectively. Figure 20 shows that:

a. straight channels occur at very low velocities;

b. thalweg develops a meandering path at slightly higher velocities and the sinuosity of the thalweg increases with velocity until a velocity of 1.55 fps;

c. channel braids at velocities higher than 1.55 fps and as a result sinuosity decreases;

d. sinuosity of the channel becomes unity for velocities equal to and greater than 1.92 fps.

Straight channels develop at very low velocities when the flow does not have adequate erosive capacity to cause significant erosion of banks. Meandering thalweg develops at slightly higher velocities when the flow is capable of causing erosion of the banks. Braided channels develop at very high velocities and the flow in such a channel is also capable of pronounced bank erosion. In a meandering thalweg channel, some of the eroded materials are deposited to form alternate bars which makes the thalweg to follow a sinuous path. At very high velocities flow cuts through the alternate bars and the channel becomes straight, wide, shallow, and braided. Greater inertia of motion associated with higher velocity makes the flow to follow a straight course and as a result it cuts through the alternate bars.

Figures 21 and 22 show the variation of sinuosity with Froude number and stream power respectively. These relationships are similar to the relationship between thalweg sinuosity and mean velocity as shown in Figure 20. This is because Froude number is proportional to square of mean velocity and stream power varies as the third power of mean velocity. Figure 21 shows that:

a. straight channels occur at low values of Froude numbers;

b. meandering thalweg channels occur at intermediate values of Froude numbers;

c. channel develops braiding at high values of Froude numbers.

Froude number is defined as the ratio of inertia forces to gravity forces. Figure 21 shows that inertia forces are small in comparison to gravity forces in a straight channel. A river develops braiding when the inertia forces are great in comparison to gravity forces. Both of these forces are comparable in a meandering thalweg channel.

Figure 22 shows that:

a. stream power is very low for straight channels;

b. braided channel is associated with very high stream power;

c. meandering thalweg channels develop for intermediate values of stream powers. For a value of stream power between 0.020 and 0.09 pounds per ft-sec, sinuosity increases with stream power.

Stream power is defined as the rate at which a stream loses energy per unit area of the boundary. Rate of energy loss per unit area of the boundary is highest in a braided channel, lowest in a straight channel and intermediate in a meandering thalweg channel.

Chapter IV

EFFECT OF BEDLOAD DISCHARGE ON CHANNEL PATTERNS

Introduction

When water flows very slowly over a bed of sand, none of the sand grains move. If velocity near the bed is slowly increased, a critical velocity will be reached at which some sand grains occasionally move along the bed. Obviously, this critical velocity is somewhat indefinite because initial movement of the grains depends on the arrangement of the grains, gradation of the grains, and on local variations of velocity.

If the velocity near the bed is greater than critical, sand grains move intermittently by rolling, sliding, or skipping along the bed. The movement is within a very thin bed layer, a few grain diameters thick. The grains which thus move in the bed layer and which are supported mainly by contact with the streambed compose the bedload.

Complexity of Sediment and Streamflow Relationships

The relationships of sediment discharge to characteristics of sediment, and streamflow are complex because of the large number of variables involved, the problems of expressing some variables simply, and the complicated relationships among the variables. Colby (1964b) stated that "At a cross section of a stream, the sediment discharge may be considered to depend: on depth, width, velocity, energy gradient, temperature, and turbulence of the flowing water; on size, density, shape, and cohesiveness of particles in the banks and bed at the cross section and in upstream channels; and on the geology, meteorology, topography, soils, subsoils, and vegetal cover of the drainage area."

Moreover, simple and satisfactory mathematical expressions for such factors as turbulence, size and shape of the sediment particles in the streambed, topography of the drainage basin, and rate, amount, and distribution of precipitation are very difficult, if not impossible, to obtain.

The concentration of the moving sediment is generally nonuniform both laterally and vertically in the cross section, and each sediment size (more precisely, sediment of each fall velocity) will have a vertical and lateral distribution that differs from the distribution of sediment of any other size. Similarly, the depth, velocity, turbulence, shear, and other characteristics of flow vary, sometimes widely across a stream. Thus a single value such as an average depth, a mean velocity, or a median particle size may be a somewhat unsatisfactory measure of depth, velocity, or particle size for a cross section.

An adequate knowledge of these difficulties indicates that (a) sediment discharge cannot, in general, be precisely related to the characteristics of flow and sediment, and (b) some assumptions are necessary to reduce the problem of sediment transportation to manageable proportions.

As the preceding sections indicate, many factors have complex and interrelated effects on bed-material discharge. Important measures are those factors or variables that can be related to compute reasonably accurate bed-material discharges as conveniently and simply as possible from data that are generally available or that can be obtained readily. Accuracy of a dominant measure indicates the general quality of agreement between bedload discharge and the dominant measure if the effects of usually measured secondary factors are evaluated correctly.

Research workers have used several dominant measures in a variety of ways. However, most of these dominant measures are closely related to shear, average velocity, or stream power.

Probably the simplest measure of the force that moves sediment in a stream is the mean velocity. Studies by Gilbert (1914), Colby (1957), and Rottner (1959) have shown an approximate relationship between the discharge of bed material and roughly the third power of the mean velocity, except at low velocities when there is not much sediment movement.

Shear or tractive force is an obvious measure of the force that may cause sediment to move and it has been widely used as a parameter of sediment discharge. The shear, or tractive force, exerted on a unit bed area is commonly defined as the weight of the water above the unit bed area times the slope of the channel. The volume of water (area x depth) above a unit bed area will be numerically equal to the depth of the water D, and the weight will therefore be given by γD (dimensions FL^{-2}). The shear per unit bed area is therefore γDS, in pounds per square foot. This expression gives the intensity of shear corresponding to a depth D.

In order to develop an expression for computing average shear per unit area of channel boundary, the following procedure is used. In a uniform flow the tractive force is apparently equal to the effective component of the gravity force acting on the body of water, parallel to the channel bottom and equal to γALS, where A is the wetted area, L is the length of the channel. Thus, the average value of the tractive force per unit wetted area, τ_o, is equal to $\gamma ALS/PL = \gamma RS$, where P is the wetted perimeter and R is the hydraulic radius and is equal to A/P; that is

$$\tau_o = \gamma RS. \qquad (12)$$

By using Chezy equation it is possible to show that shear is proportional to V^2.

Stream Power, as the term was used by Cook (1935) and Bagnold (1960b) is the rate at which a stream loses energy per unit area of the boundary. The power for a whole channel can be defined as the product of the weight of fluid (in pounds) flowing per second and the energy per unit weight of fluid (in foot pounds per pound). This product can be written as γQx energy. The dimensions are FLT^{-1}. When the flow is uniform the energy loss per foot of channel length is given by the slope S, so that the stream power per unit length of channel becomes γQS (dimensions FT^{-1}).

The stream power per unit bed area

$$= \frac{\gamma QS}{W} \tag{13}$$

$$= \frac{\gamma VWDS}{W}$$

$$= \gamma DSV$$

$$= \tau V \tag{14}$$

where

W = channel width, and

Q = VWD (wide channel).

This equation shows that stream power is proportional to V^3.

Velocity and Bedload Discharge

Figure 23 shows the variation of bedload discharge with mean velocity of flow. Bedload increases with velocity, and the rate of increase of bedload decreases at higher velocities when channel braiding takes place. The reasons for the change in the slope of the curve will be explained later. The good correlation between velocity and bedload discharge can be explained by considering some of the standard procedures used for the bedload computation.

A reasonably simple and evidently fairly accurate formula for bedload discharge was developed by Meyer-Peter and Müller (1948). For channels having neglibible bank friction, the formula may be written as (Colby 1964b)

$$\gamma_f\left(\frac{K_r}{K'_r}\right)^{3/2} RS = A(\gamma_s-\gamma_f)\ d_m + B\ \left(\frac{\gamma_f}{g}\right)^{1/3}\ q_B'^{\,2/3} \qquad (15)$$

in which

γ_f and γ_s are the specific weights, respectively, of the fluid and the sediment particles;

K_r is a measure of resistance to flow and equals the mean velocity V divided by $(R^{2/3}S^{1/2})$;

K'_r is a comparable measure of the flow resistance due only to the resistance of the stationary grains and for metric units can be compiled from $26/(D_{90})^{\frac{1}{6}}$. D_{90} is the particle size, in meters, for which 90 percent of bed sediment by weight is finer;

R is the hydraulic radius;

S is the energy gradient;

A and B are dimensionless constants that may be used as 0.047 and 0.25, respectively;

d_m is the particle size of uniform sediment and equals Σdi_b for bed sediment of a range of sizes; i_b is the fraction by weight of sediment of a size d in the streambed;

g is the gravity constant; and

q_B' is the bedload discharge per unit width by weight under water. Equation (9) for bedload discharge, in foot-pound-second units, when γ_s is equal to 165 pounds per cubic foot, can be written as

$$\left(\frac{K_r}{K_r'}\right)^{3/2} RS = 0.077\ d_m + 0.0050\ (q_B')^{2/3} \tag{16}$$

For convenience, the bedload discharge per foot of width can be expressed in terms of the dry weight per foot of width (q_B) through the relationship

$$(q_B')^{2/3} = \left[\frac{(165 - 62.4)}{165}\right]^{2/3} q_B^{2/3} \tag{17}$$

and equation (16) becomes

$$\left(\frac{K_r}{K_r'}\right)^{3/2} RS = 0.077\ d_m + 0.0036\ q_B^{2/3}\ . \tag{18}$$

According to Equation (18), no bedload moves until the left-hand side exceeds $0.077\ d_m$. For high velocities and small particle sizes $0.077\ d_m$ becomes relatively small. If it is disregarded and (K_r/K_r') is constant, the computed bedload discharge varies as $(RS)^{3/2}$ or as the third power of the mean velocity if the Chezy C is constant.

A similar relationship between mean velocity and bedload discharge can be obtained by using the Bagnold's formula for the computation of bedload. For bed sediment of uniform size, his equation (Bagnold, 1956, Eq. 42C) is

$$q_B = A_1 B_1 K_1 d^{3/2} \sqrt{\cos\beta}\ (\theta_F - \theta_t)\theta_F^{\frac{1}{2}} \tag{19}$$

in which

A_1 is a dimensionless constant that has value of about 9;

B_1 is a dimensionless constant that varies slowly with particle size;

$$K_1 = \rho_s \, g^{3/2} \left[\frac{\rho_s - \rho_f}{\rho_f}\right]^{1/2} \tag{20}$$

θ_F is a dimensionless measure of the apparent tangential stress due to action of external forces on the fluid and equals $\left[\frac{\rho_f}{(\rho_s - \rho_f)}\right] \frac{RS}{D}$,

θ_t is that value of θ_F (determined by extrapolation) at which sediment particles begin to move on a rippled sand bed, and

β is declination of bed surface below the horizontal, and $\cos\beta$ generally can be considered to equal unity and be disregarded.

For a particular grain size, for constant densities, and for moderately high velocities for which θ_t becomes relatively insignificant, the bedload discharge according to Equation (19) is about proportional to $(RS)^{3/2}$. For these stated conditions, the bedload discharge is also about proportional to the third power of the mean velocity if the Chezy C is constant.

Figure 23 shows that the rate of increase of bedload with velocity decreases as the channel pattern changes from meandering to braiding. The following explanations are proposed for this change in the rate of increase of bedload with velocity.

a. Bed material consisted of particles whose sizes ranged from silt and clay to about 3 mm. The median size was about 0.7 mm. Mostly the smaller-sized particles were carried at smaller velocities (meandering channels). Bedload in a braided channel was observed to be coarser than that in a meandering channel. This was due to higher velocities associated with braided channels. With much coarser particles as bedload, the rate of increase of bedload discharge with mean velocity should decrease in a braided channel.

If an alluvial bed consisting of nonuniform coarse material is exposed to shear stress, erosion of the finer fractions of the material is more likely to occur sooner than that of the coarser fractions. As pointed out by Lane and Carlson(1953), no definite grain size can be found indicating the border between movable and nonmovable grains. During the course of exposing the bed, a coarse top layer gradually develops as a result of selective erosion. Eventually, the underlying material will be completely covered by a stable armor coat preventing any further degradation.

Gessler (1970) showed that such a process of self stabilization is very closely related to the problem of incipient motion of the individual grains. Assuming that the shear stress fluctuations are normally distributed, he gave the following expression for the probability that in a given flow the local shear stress acting on an individual grain is smaller than the critical shear stress of that grain

$$q_{\tau c}\left(\frac{\tau}{\tau_c} < 1\right) = \frac{1}{\sigma\sqrt{2\pi}} \int_{-\infty}^{\frac{\tau}{\bar{\tau}} - 1} \exp\left(-\frac{x^2}{2\sigma^2}\right) dx \qquad (21)$$

in which

τ = local shear stress

τ_c = critical shear stress of the individual grain under consideration

σ = standard deviation of the shear stress fluctuations

$\bar{\tau}$ = mean bed shear stress; and x = dummy variable.

The critical shear stress was obtained from a graph of dimensionless critical shear stress, Shields' parameter, versus grain Reynolds number. The grain will be moved if $\tau > \tau_c$. For coarse material, the standard deviation was determined experimentally to be $\sigma = 0.57\ \bar{\tau}$, a value which is equivalent to the root mean square of the velocity fluctuation of $u'/u_* \approx 2.4$ at a distance from the rough wall equal to the height of the controlling roughness element.

Gessler (1970) plotted the probability of grains to stay as part of armor coat versus $\tau_c/\bar{\tau}$. A small grain with a low value for $\tau_c/\bar{\tau}$ is certainly more likely to be removed than a large grain with a high value for $\tau_c/\bar{\tau}$. Despite a considerable scatter in the above mentioned relationship which is common to most of the studies in the field of sediment transport, there is without question, a very definite trend. Gessler's work supports the observation that bedload is coarser in braided channels than in meandering channels. The calculations based on Gessler's relationship between probability of grains staying as part of armor coat and $\tau_c/\bar{\tau}$ showed that more than 90 percent of the materials in the bed were moved as bedload in braided channels.

b. In the present set of tests, the bedforms in a braided channel were observed to be plain bed with moving bed and antidunes whereas in a meandering channel, the bedforms were ripples. It was observed by Colby (1964) that the rate of increase of bedload discharge with velocity decreases as the bedforms changes from ripples and dunes to plain beds or antidunes.

c. Bars in a braided channel caused increased resistance to the movement of bedload discharge. As a result of this additional resistance, the rate of increase of bedload with velocity can drop significantly.

Shear and Stream Power

Figures 24 and 25 show the relationship between bedload discharge and shear and bedload discharge and stream power respectively. Rate of increase of bedload with shear decreases as the channel pattern changes from meandering to braided. A similar relationship between bedload discharge and stream power is shown in Figure 25. By using Chezy equation it can be shown that shear is proportional to square of mean velocity for constant C, and stream power is proportional to the third power of velocity. This explains the similar trends in the relationships between Q_s and V, Q_s and τ_o, and Q_s and Stream Power.

Figure 26 shows the variation of bedload discharge with slope and discharge. For any given slope, bedload discharge increases with water discharge. For any given discharge, bedload increases with slope. It will be shown later that the velocity increases with discharge for any slope and also velocity increases with slope for any given discharge. Such an increase in velocity accounts for the increase of bedload with discharge for constant slope and with slope for constant discharge.

Figure 27 shows that the bedload concentration increases slightly with discharge for any given slope but it increases significantly with slope at a given discharge. At a given slope, velocity increases with discharge and as a result bedload discharge also increases with discharge. Bedload concentration does not increase appreciably because of increase of water discharge. However, for a given discharge, velocity increases with slope and hence the bedload discharge also increases with slope. In this case bedload concentration increases significantly with increasing slope because water discharge is constant.

Figure 28 shows the variation of mean velocity with slope and channel patterns at a constant discharge. Velocity increases very slowly with slope in a straight channel. The rate of increase of velocity with slope is higher in a meandering thalweg channel and is highest in a braided channel.

Figure 29 can be used to explain the change in the slope of the curve in Figure 28. Figure 29 shows the variation of cross sectional area A, wetted perimeter P, hydraulic radius R, and Chezy C with slope and channel pattern. Chezy C was slightly higher for a braided channel. The bedforms in a braided channel were mostly plain beds and antidunes whereas the bedforms in straight and meandering thalweg channels were ripples.

Bedforms were extensively studied by Simons and Richardson (1963, 1966). They showed that the ripple bed offers a greater resistance to flow than plane bed or antidune bed. A brief description of some of the bed forms are given below (after Simons and Richardson, 1963, 1966).

Ripples are small triangle-shaped elements having gentle upstream slopes and steep downstream slopes. Resistance to flow is large, and the resulting discharge coefficient $(C/\sqrt{g})$ ranges from 7 to 12. As depth increases, resistance to flow due to roughness decreases. Thus, there is a relative roughness effect produced by the ripple bed. Resistance to flow is independent of sand size when the bed configuration is one of ripples. The bed material discharge is small.

A plane bed is a bed without elevations or depressions larger than the largest grains of the bed material. The resistance to flow for flow over a plane bed results largely from grain roughness and $C/\sqrt{g}$ is large, ranging from 14 to 23. Grain roughness is not of the usual type, however, because grains roll, hop, and slide along the bed. For flow over a plane bed with sediment movement, the resistance to flow is slightly less than that for flow over a static plane bed, which is essentially an artificial rigid boundary condition that exists after screeding when stream power is insufficient to cause significant transport of the bed material. The magnitude of the stream power at which the dunes or transition roughness changes to the plane bed depends mainly on the fall velocity of the bed material. Dunes of fine sand (low fall velocity) are washed out at lower values of stream power than are dunes of coarser sand.

Antidunes form as a series or train of inphase symmetrical sand and water waves. Antidunes do not exist as a continuous train of wave that never change shape, rather, they form as trains of waves that gradually build up from plane bed and a plane water surface. The waves may grow in height until they become unstable and break like the sea surf, or they may gradually subside. The former have been called breaking antidunes, or antidunes; and the latter, standing waves. As the antidunes form and increase in height, they may move upstream, downstream, or remain stationery. Resistance to flow due to antidunes depends on how often the antidunes form, the area of the reach that they occupy, and the violence and frequency of their breaking. If the antidunes do not break, resistance to flow is about the same as for a plane bed, and $C/\sqrt{g}$ ranges from 14 to 23.

According to Chezy equation

$$V = C\sqrt{RS} \tag{22}$$

where C is the Chezy coefficient;

R is the hydraulic radius, and

S is the slope of the energy line.

Figure 29 shows that hydraulic radius decreases with increasing slope. The rate of decrease of hydraulic radius with slope is smallest for a braided channel. This explains why the rate of increase of velocity with slope is greatest for a braided channel. The reasons for the slowest rate of decrease of hydraulic radius with slope for a braided channel are as follows. It has already been shown that a braided channel develops a wide, shallow cross section. With an increasing slope, width of a braided channel was observed to increase, but the wetted perimeter decreased slightly because of an increase in the intensity of braiding. In a meandering thalweg channel cross sectional area decreases, and the wetted perimeter increases with an increase in slope. The increase in the wetted perimenter is due to the increase in the width of the channel. As a result hydraulic radius of a meandering thalweg channel decreases faster with increasing slope than in a braided channel.

Wetted perimeter, in a straight channel, increases rapidly with increase in slope and as a result the hydraulic radius decreases very fast with increasing slope. This rapid increase in the wetted parimeter with an increase in slope is due to rapid widening of channel at flat slopes.

Figure 30 shows that the relationship between average shear and slope is similar to the relationship between average velocity and slope. This is due to the fact that shear is proportional to square of velocity.

Figure 31 shows the variation of bedload discharge with slope and channel pattern for a constant discharge of 0.15 cfs. This relationship is also similar to the velocity-slope relationship as shown in Figure 28. It has already been shown that total bedload discharge is proportional to velocity. This explains the similarity between velocity-slope and bedload discharge-slope relationships for a constant discharge.

Figure 31 shows that for a constant discharge the rate of increase of bedload discharge with slope is highest for a braided channel, intermediate for a meandering thalweg channel, and lowest for a straight channel. This means that in a braided channel, a slight increase in slope causes a significant increase in bedload carrying capacity of stream. Conversely, a large increase of the bedload discharge at a constant discharge will increase the slope of braided stream slightly. As explained above for velocity, this appears to be due to the increase of slope, the change of roughness and the reduction in the rate of decrease of depth.

Chapter V

EFFECT OF SUSPENDED SEDIMENT ON CHANNEL MORPHOLOGY

Friedkin (1945) showed that the rate at which sand enters a meandering river from caving banks, that is, the rate of bank erosion, is important not only in determining the rate of meandering, but also in determining the depth and width of the cross section. Easily erodible banks result in wide and shallow cross sections, and resistant banks result in deep and narrow cross sections.

Meandering thalweg channels developed in non-cohesive materials. This type of channels are wide and shallow in cross sections and the sinuosity of banks are very low. The thalweg meandered because of the development of a series of alternate bars along the length of the channel. No true meandering channel could be developed in non-cohesive material during this experimental study program.

Schumm (1960) showed the importance of cohesive materials like silt and clay in the perimeter of a channel. By analyzing the field data, he showed that the perimeter of a narrow, deep, and sinuous channel contains high percent of silt and clay.

A series of tests were made to determine the effect of high concentration of suspended sediment (clay) on the channel characteristics and to study the effect of the different types of sediment load on the channel patterns. The main purpose was to develop meandering channels. Results of the tests with high concentrations of suspended sediment in the flow will be discussed in this chapter.

Effect of Suspended Sediment Concentration on Velocity

Clay (Kaolinite) was used as suspended sediment and a constant suspended sediment concentration of 3 percent (30,000 ppm) was introduced and maintained in the flow. Initially a meandering thalweg channel was formed by passing a constant water discharge of 0.15 cfs. This flow had little or no suspended sediment. The bedload was fed at the entrance to compensate for the coarse sediment trapped in the tail box. After the development of meandering thalweg, clay was mixed with water and the resulting mixture was allowed to flow through the channel. Bedload feeding was continued at the entrance but at a reduced rate. The bedload rate was regulated so that there was no aggradation or degradation of the bed near the inlet. Measurements of the cross sectional areas, longitudinal profiles, and water levels of the channel were taken before and after the change of sediment characteristics in the flow in order to find the changes resulting from such an operation.

High concentration of suspended sediment in the flow caused some significant changes in the channel cross section and geometry.

Figures 32 and 33 show that the average velocities in pools and crossings increased significantly after the increase of suspended sediment concentration. The increase in velocities are in the range of 10 to 15 percent. This increase in velocity can be explained from both theoretical and practical point of views. Theoretical reasonings are based on the theories of suspended sediment transportation and the mechanics of turbulent flow of fluids.

For a two-dimensional turbulent flow in the x-direction with a velocity $u(y)$, in which y is normal to x, the shear parallel to x on a plane normal to y is expressed by

$$\tau = \rho\overline{u'v'} \ . \qquad (23)$$

Here ρ is the mass density of the fluid, and u' and v' are the turbulent velocity fluctuations in the x and y directions, respectively, and the bar denotes mean value.

Boussinesq introduced an expression for the shear of the form,

$$\tau = \rho\varepsilon_m \frac{du}{dy} \qquad (24)$$

in which the quantity $\rho\varepsilon_m$ (often called the eddy viscosity) is analogous to the coefficient of viscosity in the expression for viscous shear; and u is the mean velocity in the x-direction. The quantity ε_m has the dimensions of a kinematic viscosity ν, but unlike its counterpart it is a function of flow conditions, and therefore, varies from point to point. The quantity ε_m is a coefficient expressing the exchange of momentum between neighboring filaments of fluids. This quantity is called the turbulent momentum transfer coefficient. Obviously it has the dimensions, length x velocity.

The expression for the shear is given by

$$\tau = \tau_o \frac{D-y}{D} \qquad (25)$$

in which τ_o is the shear at the bottom, or,

$$\tau_o = \gamma DS \ .$$

An expression for the velocity gradient is given by the von Karman universal defect law.

$$\frac{u - u_{max}}{\sqrt{\frac{\tau_o}{\rho}}} = \frac{1}{k} \log_e \frac{y}{D} \tag{26}$$

where

u_{max} is the velocity at the surface, and

k is the von Karman universal constant.

The derivative of the velocity then becomes,

$$\frac{du}{dy} = \frac{1}{k} \sqrt{\frac{\tau_o}{\rho}} \frac{1}{y} . \tag{27}$$

From Equations (26) and (27)

$$\varepsilon_m = ky \frac{\tau}{\rho\sqrt{\tau_o/\rho}} . \tag{28}$$

Equation (28) shows that momentum transfer coefficient is directly proportional to k. A decrease in k, decreases ε_m, and if the shear (depth and slope) is kept constant the velocity gradient will have to increase to compensate for the reduced ε_m and a higher velocity gradient means an increased average velocity. So in order to show that the velocity of flow increases with an increased suspended sediment concentration we need to show that the value of k decreases as the suspended sediment concentration is increased.

Vanoni (1946) carried out experiments in a flume with a fixed artificially roughened bed and varying suspended sediment load. The results showed that the von Karman constant k is substantially reduced by the suspended sediment.

Einstein and Chien (1954) also reasoned that the work done in keeping sediment grains in suspension must come from the vertical components of turbulent fluctuations and must result in damping turbulence. By plotting data as k versus the ratio of the power to suspend sediment to the power to overcome hydraulic resistance to the flow a definite trend was observed which showed marked decrease in the value of k with increasing suspended sediment concentration.

According to this concept of variation of the von Karman constant with concentration of suspended sediment, flows with suspensions of neutrally buoyant particles should remain unaffected because no energy is required to suspend these particles. Yet Elata and Ippen (1961) showed experimentally that the von Karman constant of flow with suspensions of neutrally buoyant particles decreases with increasing concentration and that turbulent intensity increases.

Mikio Hino (1963) approached the problem from the equations of motion of turbulent flow. He used a lengthy and thorough mathematical procedure. His results showed that the von Karman constant will always decrease and that the turbulent intensity will increase with increasing concentration of buoyant particles and decrease with increased density of particles.

The above review of the research on the field of turbulent transport of suspended sediment shows that the value of von Karman k decreases with an increase in suspended sediment load. Laboratory observations under the present study showed that the bed and banks of the channel were very smooth due to the deposition of finer sediments among the coarser material in the bed and banks. This smoothness of bed and banks reduced the resistance to flow and increased the average velocity.

It will be shown later that with sufficient amount of silt and clay in the flow, the channel develops a narrow and deep cross section. For the same cross sectional area, the hydraulic radius for a narrow, deep channel is greater than the hydraulic radius for a wide, shallow channel. High concentration of clay in the flow causes a decrease in the channel roughness and an increase in the hydraulic radius of the channel, which means a higher mean velocity.

Figures 34 and 35 show the cross sectional areas in pools and crossings before and after increasing the suspended sediment concentration. Due to the higher velocity, cross sectional areas are smaller with a higher suspended sediment concentration in the flow.

Width, Depth, and Hydraulic Radius

Figure 36 shows the channel widths before and after the increase of suspended sediment concentration. It shows that a suspended sediment channel is smaller in width than a corresponding bedload channel. In both the cases width increased with slope.

Figure 37 shows that the maximum depth in a pool increases after the increase in the suspended sediment load. Figure 38 shows a similar trend for crossings. A suspended load concentration of 3 percent in the flow transformed a meandering thalweg channel into a meandering channel and a brief description of such change will explain the relationships shown in the above Figures.

The flow depths over the bars of a meandering thalweg channel were very shallow. However, some of the fine sediments deposited on the bars when there was a high concentration of suspended sediment in the flow. Such deposition built up the bars. It has already been explained that the velocity of flow increases after the increase of suspended sediment concentration. Due to the building up of the bars, the flow was restricted in a narrow channel in which water was flowing faster due to its high suspended sediment content. The increased velocity caused scour of the bed. Flow was then concentrated in the thalweg which was much deeper than the corresponding predominantly bedload channel. This higher velocity also caused erosion of the concave banks, and as a result, the sinuosity of the channel increased slightly after the increase of suspended sediment concentration. Continued building up of bars and scour of bed along the thalweg caused exposure of the bars above the water surface. The flow then took place in a narrow, deep and more sinuous meandering channel.

Figure 39 shows the $\frac{W}{D_{max}}$ values in pools before and after the increase of suspended sediment concentration. Figure 40 gives a similar relationship for crossings. In both the cases $\frac{W}{D_{max}}$ values are smaller for suspended load channel. This is due to the development of a deep and narrow channel after the increase of suspended sediment concentration.

Physical reasoning also shows that a narrow, deep channel develops with a high concentration of clay in the flow. Sufficient quantity of clay in the banks acts as a binding agent for the coarser particles and enable the banks to withstand a higher shear stress. Narrow and deep channels develop only when the banks can withstand a higher shear stress.

Figure 41 shows that the hydraulic radius for a suspended sediment channel is larger than that for a bedload channel. A larger hydraulic radius is due to the narrow and deep channel associated with higher clay concentration.

Schumm (1960) demonstrated the importance of the percentage of silt and clay in the perimeter of a stream channel to channel shape. He showed that as the percentage of silt and clay increases the width-depth ratio decreases according to the following equation (Figure 42):

$$F = \frac{255}{M^{1.08}} \quad (29)$$

He suggested that the percentage of silt and clay represents the resistance to erosion or general behavior of sediment in a stream channel containing only small amounts of gravel. A study of this aspect of the physical properties of sediment is needed before it will be possible to suggest other than that the silt-clay acts as a binding agent in which the larger sediment grains are fixed. Undoubtedly, the type of clay present and the ratio fo silt and clay are also important.

It has already been explained that a narrow and deep channel developed after the increase of concentration of clay in the flow. The increase of depth was due to scour of bed. The scour of bed caused the development of a series of deep holes in pools. Figure 43 gives the dimension of those scour holes. Lengths of the scour holes were observed to increase with slope.

Sinuosity

Figure 44 shows the sinuosities before and after the increase of suspended sediment in the flow. Sinuosity increases with the increase of clay concentration in the flow. This increase of sinuosity was due to the erosion of the concave banks after the increase of clay concentration. Increase of suspended sediment concentration caused higher velocity which eroded the concave banks slightly.

Schumm also showed that the sinuosity of a river is increased as the percentage of silt and clay in the perimeter of river is increased

(Figure 45). He gave the following relationship between sinuosity (P) and percent silt-clay (M)

$$P = 0.94\ M^{0.25} \tag{30}$$

Photographs

Photographs in Figure 46 show the changes in the channel characteristics resulting from a change in the nature of sediment in the flow. The first photograph shows the meandering thalweg channel with little or no suspended sediment. It carried mostly bedload. Second photograph shows the meandering channel which resulted after a suspended sediment concentration of 3 percent was maintained in the flow for about 15 hours. This channel is narrow and the bars are exposed over the water surface. The channel is also more sinuous than the channel in the first photograph. The next photograph shows close view of a bar in a meandering channel. The bars built up due to the deposition of clay on it. The last photograph shows scour holes in the pools of meandering channels.

Chapter VI

EFFECT OF DISCHARGE, SLOPE, AND BEDLOAD CONCENTRATION ON CHANNEL GEOMETRY

Hydraulic characteristics of straight channels and meandering thalweg channels will be discussed in this chapter.

Straight Channels

Depth - Data for depths show that for a given slope, depth increases with discharge. Depth increases with increasing slope for a given discharge. Figure 47 shows the relationship among D_{max}, Q, and S. Mathematically the relationship among D_{max}, Q, and S is given by

$$D_{max} = 0.0356 \frac{Q^{0.42}}{S^{0.28}} \quad . \tag{31}$$

Figure 48 gives a similar relationship among D_{max}, Q, and C_S.

$$D_{max} = 8.6 \frac{Q^{0.33}}{C_S^{0.66}} \tag{32}$$

where C_S is the bedload concentration.

Width - Width of a channel increases with discharge for any given slope. Width also increases with slope for any given discharge. Both of these trends are due to increased shear stresses caused by steeper slopes and higher discharges.

Shear stress is proportional to depth of flow and longitudinal slope of the channel and is given by the equation

$$\tau = \gamma DS.$$

For a given discharge, an increase in slope causes a decrease in depth. Equation (31) shows that depth of flow is proportional to $S^{-0.28}$. So the net effect of increasing slope is an increase in shear stress. At a given slope, an increase in discharge is accompanied by a greater depth which in turn causes higher shear stress. Figure 49 shows the relationship among W, Q, and S and is given by the following equation:

$$W = 17.5\ Q^{0.16}\ S^{0.32}\ . \tag{33}$$

Figure 50 gives the relationship among W, Q, and C_S and is given by the following equation:

$$W = 0.21\ Q^{0.22}\ C_S^{\ 0.44}. \tag{34}$$

<u>Width-depth ratio</u> - Figure 51 shows the variation of width-depth ratio for a straight channel with bedload discharge. $\frac{W}{D_{max}}$ increases very rapidly with an increase in bedload discharge. Bed material discharge increased with slope at a constant discharge. It also increases with discharge at a constant slope. Discussions in the last two sections showed that the width of a straight channel increases with discharge and slope, whereas the depth of flow is proportional to some power of discharge and is versely proportional to some power of slope. As a result width-depth ratio increases rapidly with bedload discharge. The relationship between $\frac{W}{D_{max}}$ and C_S is given by the following equation:

$$\frac{W}{D_{max}} = 0.052\ C_S^{\ 1.05} \tag{35}$$

<u>Area</u> - Area increases with discharge. The relationship among A, Q, and S is given in Figure 52. This relationship can be expressed by the following equation:

$$A = 0.29\ \frac{Q^{0.85}}{S^{0.14}} \tag{36}$$

The relationship among A, Q, and C_S is given in Figure 53:

$$A = 2.9 \frac{Q^{0.90}}{C_s^{0.15}} . \tag{37}$$

Meandering Thalweg Channels

Geometric characteristics of meandering thalweg channels will be discussed in the next few pages.

Depth - Depth for a particular slope and discharge was obtained by averaging the depths for all pools and crossings for that test. Each depth on the next few figures represents an average of six or seven depths. The data shows that for a particular slope and discharge the depth in a pool is always greater than that in a crossing. On the average the maximum depth in a crossing is about 50 to 70 percent of the maximum depth in a pool or bendway. The depth in both cases increases with discharge for a given slope. The crossings are comparatively shallow and as a result they are the most troublesome stretches from the standpoint of navigation depths.

The typical cross sections for pools and crossings obtained in the laboratory can be used to explain the very popularly known fact that when compared with crossings, the slope of the energy line in the pools are flatter during low stages and steeper during high stages.

If we look at the typical cross section for pools and crossings, it is evident that a substantial area is available in pools for flow at low river stages. Moreover the wetted perimeter is much smaller for pools than crossings at low stages and hence water can flow without much resistance in pools than in crossings at low flow. As the stage rises, the area in the pools does not increase as rapidly as in the crossings, but the wetted perimeter in the pools increases many times due to the submergence of the bars. The area available for flow in crossings increases rapidly due to increase of stage because of the relatively level bottom. As a result, though the slope of the energy line over the crossings is comparatively steep during low stages, it becomes gentler as the stage rises, but the opposite happens in the pools.

For a particular discharge, the maximum depth decreases with increasing slope. It can be explained by the fact that velocity is expected to increase with slope and a higher velocity needs smaller area and hence a shallower depth.

Figure 54 shows the plotting of D_{max} versus $Q/S^{3/2}$ for pools and crossings. The relationship among D_{max}, Q, and S for pools and crossings are given by the following equation:

$$D_{max} = 0.024 \frac{Q^{0.25}}{S^{0.375}} \qquad \text{(Pool)} \tag{38}$$

$$D_{max} = 0.015 \frac{Q^{0.25}}{S^{0.375}} \qquad \text{(Crossing)} \ . \tag{39}$$

Figure 55 shows the relationship among D_{max}, Q, and C_S for pools and crossings. These relationships are represented by the following equations:

$$D_{max} = 2.66 \frac{Q^{0.316}}{C_S^{\ 0.474}} \qquad \text{(Pool)} \tag{40}$$

$$D_{max} = 1.61 \frac{Q^{0.316}}{C_S^{\ 0.474}} \qquad \text{(Crossing)} \ . \tag{41}$$

The above equations show that a smaller D_{max} is associated with a higher bedload concentration for a given discharge. This is due to the fact that D_{max} decreases with increasing slope at a given discharge whereas a higher slope causes greater shear stress which in turn is responsible for higher bedload concentration.

Area - The data for areas shows that for a given discharge and slope the pool area is always smaller than the crossing area. It will be shown later that these differences are due to higher velocities in pools. For a given slope, the area of both pools and crossings increase with discharge.

Figure 56 shows the relationship among A, Q, and S for pools and is represented by the following equation:

$$A = 0.086 \frac{Q^{0.80}}{S^{0.40}} . \tag{42}$$

The relationship among A, Q, and S for crossings is also shown in the same figure and is represented by the following equation:

$$A = 0.098 \frac{Q^{0.80}}{S^{0.40}} . \tag{43}$$

The relationship among A, Q, and C_S for pools and crossings are shown in Figure 57. For pool, the relationship is

$$A = 2.44 \frac{Q^{0.80}}{C_S^{0.20}} \tag{44}$$

and for crossing

$$A = 2.77 \frac{Q^{0.80}}{C_S^{0.20}} . \tag{45}$$

Velocity - Figures 58 and 59 show the variation of average velocity against discharge for various slopes in pools and crossings respectively. Average velocity in a pool is slightly higher than that in a crossing. The flow in a bend converges towards the outer bend and is flowing out of the bend it diverges. The separation zone that originates at the inside of the bend reduces the effective area of the section. Velocity in a pool is higher because of the convergence of this flow.

Figures 58 and 59 show that the velocity increases with discharge for a given slope. At a given discharge, velocity increases with increasing slope.

Figure 60 shows the relationship among V, R, and S. A single curve fits the data for both pools and crossings. The equation of the line in this figure is:

$$V = 38(R^2 S)^{0.38} \quad . \tag{46}$$

Hydraulic Radius - The relationship among R, S, and Q for pool (Figure 61) is

$$R = 0.0037 \frac{Q^{0.25}}{S^{0.50}} \tag{47}$$

and for crossing

$$R = 0.0046 \frac{Q^{0.25}}{S^{0.50}} \quad . \tag{48}$$

Width-depth ratio - The variation width-depth ratio with bedload discharge for meandering thalweg channels are shown in Figure 62. $\frac{W}{D_{max}}$ increases with an increase in bedload discharge. The relationship between $\frac{W}{D_{max}}$ and C_S is given by the following equation

$$\frac{W}{D_{max}} = 0.116 \quad C_S^{0.82} \quad . \tag{49}$$

Chapter VII

GEOMETRY OF POOLS AND BENDWAYS

Theoretical Considerations

In general, meandering rivers assume a natural allignment consisting of bends and crossings. The channel is deep along the concave banks of the bends and shallow in tangents or crossings between the bends. The profile of the thalweg consists of successive deeps or pools in the bends, and shallows or shoals in the crossings. "The rivers are deeper in the bends because of the concentration of stream power, turbulence, flow, and ability to transport sediment adjacent to the concave bank" (Simons, 1970). The characteristics of bends can be approximated using the following approach.

The first result of the currents being curved in plane is the appearance of a transverse inclination of the free water surface. To evaluate approximately the extent of this inclination, consider the equilibrium conditions of a column of fluid in the bend (Figure 63), whose base is dr by $rd\theta$ (where r is the radius and θ the angle of the center of the bend). Assume that in the vertical direction pressure is distributed according to the hydrostatic law. Then projected on to a vertical plane passing through the axis of the bend, the column of fluid will be subjected to the following forces:

A. Centrifugal forces

$$R_s = \alpha_o \frac{V^2}{r} \rho \; dr \; r \; d\theta \; D \tag{50}$$

where V is the mean velocity, D is the depth of the stream, ρ is the water density and α_o is an averaging factor, which allows for the uneven, vertical velocity distributions.

B. Force due to difference of pressure on sides of prism.

$$\Delta p = \frac{\partial}{\partial r} (\gamma \frac{D}{2} D \; r \; d\theta) dr$$

$$= r \; d\theta \; dr \quad \rho g \; D \frac{\partial D}{\partial r} \tag{51}$$

where g is the accelera ion due to gravity.

C. Reaction of the friction of the column under consideration against the bottom of the canal.

$$T = \tau_{or} \; rd\theta \; dr \tag{52}$$

where τ_{or} is the radial component of the frictional stress at the bottom. Rozovskii (1961) showed that this reaction is always directed from the center of the bend toward the concave or outer bank.

The condition of transverse equilibrium will then be written as follows:

$$R_s - \Delta P + T = 0. \tag{53}$$

Substituting the values for R_s, ΔP, and T

$$\alpha_o \frac{V^2}{r} \rho \; dr \quad rd\theta \quad D - r \; d\theta \; dr \; \rho \; g \; D \frac{\partial D}{\partial r} + \tau_{or} \; r \; d\theta \; dr = 0. \tag{54}$$

Whence we can determine the magnitude of the transverse inclination I_r of the free surface

$$I_r = \frac{\partial D}{\partial r} = \alpha_o \frac{V^2}{gr} + \frac{\tau_{or}}{\rho g D} \quad . \tag{55}$$

The last term of the right hand side of the equation was found to be relatively small by some experimenter (Rozovskii, 1961). If this is ignored, an approximate'equation is obtained:

$$I_r \simeq \alpha_o \frac{V^2}{gr} . \tag{56}$$

The above formula thus shows that, at any bend of a stream, there inevitably appears a transverse inclination of free surface. In that case the level of the free surface at the inner, convex bank, nearest to the center of curvature, is lowered while at the outer, concave bank, farthest from the center of curvature, it is raised.

The transverse inclination of water surface in the bend of a river as given by Equation (56) is

$$\frac{\partial D}{\partial r} = \alpha_o \frac{V^2}{rg} .$$

Noting that $\frac{\partial D}{\partial r} \simeq \frac{\Delta z}{W}$ we get

$$\Delta z = \frac{\alpha_o V^2 W}{rg} \tag{57}$$

where Δz is the transverse drop in water level.

From Equation (57)

$$r = \frac{\alpha_o V^2 W}{\Delta z g} . \tag{58}$$

Since Δz is proportional to V^2, it is also proportional to the longitudinal drop Δz_o along the reach of length L. Then

$$\Delta z = K_1 \Delta z_o . \tag{59}$$

Substituting the expression for slope

$$S = \frac{\Delta z_o}{L}$$

in the Chezy Equation

$V = C\sqrt{RS}$

and assuming $\alpha_o = 1$ one obtains the following equation for Δz_o.

$$\Delta z_o = \frac{V^2 L}{C^2 D} \tag{60}$$

where C is the Chezy coefficient and K_1 is a constant of proportionality.

Therefore,

$$\Delta z = K_1 \frac{V^2 L}{C^2 D} \ . \tag{61}$$

Expressing V in terms of slope $V = C\sqrt{RS}$ and the length of the bend in terms of the radius of curvature and the extermal angle of the bend,

$$L = 2\pi r \left(\frac{180 - \theta}{360}\right)$$

$$= \pi r \left(1 - \frac{\theta}{180}\right) \tag{62}$$

we obtain

$$\Delta z = K_1 \ \pi s r \left(1 - \frac{\theta}{180}\right) \ . \tag{63}$$

Rzhanitsyn, (1960) assumed a constant velocity in the bends, substituted the value of Δz from Equation (63) into Equation (58) and after proper transformation and simplification obtained the following equation.

$$r = \sqrt{K_o} \quad \frac{Q}{V_* \sqrt{A}(\pi - \theta)} \tag{64}$$

where

$$V_* = \sqrt{gDS}, \tag{65}$$

$$K_o = \frac{1}{K_1}$$

$$= \frac{L\ rg}{W\ C^2 D} \tag{66}$$

A = cross sectional area of flow.

As seen from expression (66) the value of K_o depends only on the geometric dimensions of the cross sectional area, the radius of the bend and the roughness coefficient, and as a result Rzhanitsyn (1960) stated that it is determined only by the morphometric characteristics of the river channel. He also stated that; "In hidden form, K_o depends (because the channel shape is the result of interaction of the stream and the river bed) also on the characteristics of the material composing the bed and the banks of the river. This coefficient can therefore, be called the morphometric parameter of the stream bend".

It is possible to compute the value of morphometric parameter of the bend for any river by using the relationship in Equation (66). Rzhanitsyn (1960) made field measurements and determined the values of K_o for several alluvial river bends. On the basis of those data he made the following conclusions:

1. The value of coefficient K_o is different for different types of channel bends. The limited bend has the highest value and the forced one has the lowest. For a limited bend the value of K_o is on the average between 18 and 22; it varies within wide limits (from 50 to 300% of the average value). The value of K_o for a free bend is about 4.0.

2. A comparison of the values of the morphometric parameter of the bend for different rivers shows that for less stable rivers the values of K_o are higher. This means that the development of channel shapes proceeds more intensively in more mobile rivers and that the shapes themselves are smoother, i.e., the mutual adjustment and the change of the channel shape and of the strucutre of the stream proceed faster in such rivers.

Rzhanitsyn (1960) stated: "The established morphometric parameter of a bend of natural channels is a definitve value; in a certain sense, it constitutes a manifestation of the principle of interaction between the stream and the bed material and also reveals the degree of development of the river channel in the bend".

Determination of K_o values - Values of K_o were determined by using the data collected for this study. Equation (66) was used for calculating the values of K_o. The length of the thalweg along the bend, radius of curvature of the bend, width of the channel, and the depth of flow was measured. Chezy C was computed by using values of average velocity, hydraulic radius and slope and substituting these values in Chezy Equation.

Values of K_o for free bends varied from about 0.5 to about 2. It appears that the type of sediment affects the value of K_o slightly. Lower values of K_o was observed for channels with predominantly bedload. Whereas a suspended load channel gave a slightly higher value of K_o. The average values of K_o for bedload and suspended load channels were 0.7 and 1.5 respectively.

Equation (66) shows that K_o is inversly proportional to width and depth of the channel. With predominantly bedload a channel develops wide and shallow cross section. Whereas with fine material a flow develops a much narrower and slightly deeper channel. Because of the much wider channel the value of K_o is smaller for predominantly bedload channels.

<u>Length of pools in bends</u> - As mentioned earlier, in a bend of a stream there is a transverse slope and transverse currents. These phenomena are greatest slightly downstream of the point of maximum amplitude. Upon emerging into the straight reach below the curve, the induced transverse currents slowly die out [Rzhanitsyn, 1960].

Rzhanitsyn (1960) developed the following equation for computing the length of pool L.

$$L = \frac{C^2 D}{g} \{ \ 2[\ 1 - (\frac{W}{2r})^2] - 1\} \ . \tag{67}$$

He made the following assumptions regarding the velocity distribution:

$$V_1^2 = V^2 \left(\frac{r}{r + \frac{W}{2}}\right) ,$$

$$V_2^2 = V^2 \left(\frac{r}{r - \frac{W}{2}}\right)$$

where V_1, and V_2 are the velocities at the banks in a bend, and V is the mean velocity. At the crossing he assumed $V_1 = V_2 = V$.

It has been found that Equation (67) gives a value of L which may differ from the actual one. The actual value can be more accurately approximated by multiplying Equation (67) by η, where η is the ratio of the actual length of the pool to the computed length.

$$L = \eta \ \frac{C^2 D}{g} \{ \ 2[\ 1 - (\frac{W}{2r})^2 \ ] - 1\} \ . \tag{68}$$

Figure 64 shows the variation of coefficient η with channel stability Y and with Lokhtins (1960) coefficient of channel stability equal to $\frac{W}{S}$.

Present study showed that the value of η varies between 0.80 and about 2 with about 85 percent of the values ranging between 0.8 and 1.25. The data could not be plotted in Figure 68 as stability coefficient and Lokhtins number for this study were greater than those values indicated in that figure.

Figure 65 shows that length of pool increases with discharge. Figure 66 shows a similar relationship between lenght of pool and maximum depth in the pool. It has already been shown that the meander length increases with discharge. Greater dimension for meander length means a longer bend and hence a longer pool. It has also been shown that maximum depth in a pool increases with discharge. Hence, length of pools increases with maximum depths in pools.

Longitudinal profile of the channel bottom in bend - Figure 67 shows the non-dimensional profile of pools and crossings in the bends of meandering channels. Data for several slopes and discharges were used for plotting this figure. The top figure was obtained by plotting the data for flow with predominantly bedload and little or no suspended load. The bottom figure applies for flow with high concentration of suspended load. This figure shows that the point of greatest depth occurs slightly downstream of the maximum point of bend. Flow carrying a predominantly bedload causes the bed profile to change gradually from a shallow depth in the crossing to a greater depth in the pool. But the bed profile changes rather abruptly for a flow carrying mostly suspended load. This abrupt change in bed profile is due to the greater depths in the bends of channels carrying predominantly suspended load.

Shapes of river channels with stable positions of pools and shoals were studied by Russian Engineers. Rzhanitsyn (1960) observed that the greatest depth of the stream is located below the section of greatest curvature, the smaller depth is approximately the same distance below the point of inflection. This relationship was checked by a number of Russian investigators on a large number of alluvial rivers of the European territory of the USSR, and was verified in the majority of cases. Rzhanitsyn's study also indicated that the bed profile of meandering streams depends on the type and concentration of sediment carried by the stream.

Though Rzhanitsyn (1960) stated that: "It is not possible to explain why the point of greatest depth lies downstream of the section of greatest curvature without further study of the problem", results of Ippen and Drinkers (1962) study can be used to explain this phenomenon. Ippen and Drinker (1962) investigated the distribution and the magnitudes of boundary shear stresses in the curved reaches of smooth trapezoidal channels under conditions of subcritical flow. The boundary shear patterns as obtained cannot be predicted quantitatively from the gross characteristics of the flow. Within the range of stream variables studied, it was found that local shears occur at intensities more than twice the mean tractive force computed for uniform flow. A one-dimensional mathematical treatment of the energy dissipation in the curve and downstream tangent failed to indicate either the peripherial location or the intensity of the greatest boundary stresses. But they observed that for a certain range of channel geometry, the areas of maximum local shear stresses were located along the outer bank in the downstream portion of the curve. A similar observation regarding the location of the zone of maximum trubulence intensity was made by Masiar (1967). It is obvious to expect the location of the greatest depth to coincide with the location of the zone of maximum shear and turbulence intensity.

Rzhanitsyn (1960) studied the shapes of longitudinal profiles for rivers that differ in size but are similar with respect to their bed material and mean annual concentration. Figure 68 is the outcome of his studies. The analysis of his data showed that in relative terms the shape of the longitudinal profiles of pool dimensions do not depend on the size of the stream. Figure 68 also shows that the data from the present study verifies Rzhanitsyn's work for the range of data covered under the present study.

Chapter VIII

EXAMPLES

In this chapter results of the present study will be used to explain some of the characteristics of natural rivers.

Straight Channel

In the field it is relatively easy to find illustrations of either meandering or braided channels. The same cannot be said of straight channels. Leopold and Wolman in their 1957 report stated: "In our experience truly straight channels are so rare among natural rivers as to be almost nonexistent. Extremely short segments or reaches of the channel may be straight, but it can be stated as a generalization that reaches which are straight for distances exceeding ten times the channel width are rare".

A good example of a straight alluvial river is the Illinois River in Illinois. Upon comparison with other streams of that area, the morphology of Illnois River is seen to be different in many respects. The most outstanding pecularity of the river is its extremely flat gradient or slope. In its lower 228 or 261 miles, from Utica or Peru to the Mississippi, Illinois River has an average slope of less than 1.5 inches to the mile ($S = 0.000237$). The mean velocity at average discharge is 1.3 feet per second. The data on the character of Illinois River is given in Table 2. This table was obtained from Rubey's 1952 paper.

Table 2. Illinois River from Kampsville, Illinois to Mouth

Average Discharge Q (cfs)	Mean Velocity at Average Discharge V (fps)	Normal Surface Width W (ft)	Mean Depth at Average Discharge D (ft)	Average Slope S	Froude Number F
15,000	1.30	1,100	11.00	1 inch/mile = 0.000237	0.07

Two other unusual features of Illinois River make this exceptionally flat gradient seem all the more remarkable. The flatness is due not at all to a meandering, roundabout stream course. Instead, the river is noticeably straighter and more direct in its route than any of the major streams of the general region. Furthermore, the current as marked by the main channel or deepest part of Illinois River has the almost unique characteristic of flowing, not like most streams against the outside, but close to the inside of curves in the river's course. This means that the thalweg follows the most direct course possible by hugging the inside of the bends. The channel of the Illinois River is much deeper and narrower than the channels of comparable discharge in the same area. The banks are stable. As a result of the flat gradient, the flow has a very low velocity.

Meandering and Braided Channels

It is very difficult to find meander pattern in nature which is as symmetrical as those obtained in the laboratory. Figure 69 shows the meander pattern of the Popo Agie River near Hudson, Wyoming. Leopold and Wolman (1957) stated that the meander pattern on the Popo Agie River is one of the most symmetrical that can be seen in the field. The main reason for including this figure is to show the pools and crossings in a meandering river. Such pools and crossings were observed in the laboratory meandering channel.

At a given discharge, various slopes are associated with varying channel shapes and patterns. Cottonwood Creek near Daniel, Wyoming, is a striking illustration of an abrupt change from one stream pattern to another (Figure 70). Above the gaging station, Cottonwood Creek is very sinuous. Immediately below the gage it becomes braided. As the profile in Figure 70 shows, the meander reach has a slope of 0.0011, while the braided section occurs on a slope of 0.0040. The break in the slope is most probably due to the channel adjustment caused by local deposition of coarser gravel in the valley alluvium. This example shows that for any given discharge, the slope of a braided reach is steeper than the slope of a meandering reach.

A similar phenomenon was observed in the laboratory during this experimental study program. At an average slope of 0.015, the flow developed a combination of meandering thalweg and braided channel patterns (Figure 71). The meandering thalweg pattern developed in the upstream portion of the laboratory flume and the braided channel developed in the downstream portion of the flume. The longitudinal profile along the thalweg showed that the slope in the braided reach was steeper than the reach where meandering thalweg pattern developed. Slope of the meandering reach was 0.012, whereas the slope of the braided reach was 0.016.

Sinuosity and Valley Slope

The present study showed that the sinuosity of a river increases with the increase of valley slope. Similar sinuosity-slope relationship can be observed in the cases of the Calamus River in Nebraska and the Mississippi River.

Figure 72 shows the river profile and valley profile of the Calamus River. Numbers on the figures are sinuosity indices. Sinuosity index is a measure of sinuosity of a river and was defined by Brice (1964) as "the ratio of length of channel to length of meandering axis". The above figure shows that the sinuosity of the river in the lower reaches is smaller in comparison to the sinuosity of the river in the upper reaches. Valley profile shows that the valley slope is flatter in the lower reaches where the sinuosity of the river is smaller.

Similar observations can be made in the case of the Mississippi River also. Valley slope between the junction of the Arkansas River and Greenville, Mississippi, is much steeper than the adjoining portions of the valley. As a result of this, the sinuosity of the Mississippi River is highest (about 3.30) in this portion of the valley. While computing sinuosities, length of the river along the old meandering channel was measured. Modern cutoffs were ignored. As a result of much flatter valley slope between Helena, Arkansas and the junction of the Arkansas River, the sinuosity of the Mississippi River in this reach is only 1.70. Valley slope is flattest between Donaldsonville, Louisiana, and the mouth of the Mississippi River. The sinuosity of the Mississippi River is only 1.27 in this reach.

Chapter IX

CONCLUSIONS

Four channel patterns; straight, meandering thalweg, meandering and braided were observed in the laboratory. Straight channels developed at very flat slopes (slopes flatter than 0.0047 or 0.0026 depending on whether the flow entered the channel straight or at an angle to the axis of the flume) with very low bedload concentrations (less than 740 ppm). Meandering thalweg channels developed for slopes between 0.0023 and 0.013 and for bedload concentrations of 740 and 2180 ppm. Such channels developed for slopes and bedload concentrations which were greater than those in straight channels and smaller than those in braided channels. Though the sinuosity of the banks was very low (less than 1.05) in these channels, the thalweg sinuosity was appreciable (see appendix B). Braided channels occurred at very steep slopes (slopes equal to or greater than 0.016) with high concentrations of bedload (equal to or greater than 3110 ppm). Such results show that there exists critical slopes at which an increase in slope causes rivers in non-cohesive materials to undergo changes in channel patterns (i.e. changes from straight to meandering thalweg or from meandering thalweg to braided pattern).

The present study verified Lane's (1957) and Leopold and Wolman's (1957) observations that for any given discharge, braided channels develop at steeper slopes than those in meandering channels. Moreover, the data fitted Lane's slope-discharge relations for meandering and braided channels (Figures 1 and 2).

One of the major conclusions of the present study is that meandering channels do not develop in non-cohesive materials. However, narrow, deep, and sinuous meandering channels developed during the present research program with high concentrations of clay in the flow.

The straight channels had deep and narrow cross sections and the banks were straight Due to its very low gradient the average velocity of flow and boundary shear stress was small in these channels. Because of low velocity and small boundary shear stress, the flow in a straight channel was incapable of causing any significant erosion and as a result it maintained its original straight alignment.

During this study meandering thalweg and braided channels developed with high bedload concentrations and with flow conditions such that there was pronounced erosion of the channel banks. Each bend and bar in a meandering thalweg channel developed as a result of impingement and deflection from the banks as a result of deposition of sand on the inside of the bend.

Friedkin (1945) stated that bank erosion is essential for the development of meandering channels. He did not discuss the role of bedload discharge in the development of meandering channels. It appears that bank erosion provided the flow with sufficient amount of bedload which deposited as alternate bars. He could not develop true meandering channels. His meandering channels were similar to the meandering thalweg channels of the present study. Friedkin (1945) noted, in fact, that in order to obtain photographs of his "meandering" channel, which are so frequently reproduced in engineering and geomorphology texts, the discharge was reduced until the water level had decreased sufficiently to expose the alternate bars.

Another major conclusion of this study is that initial disturbances in the channel are not sufficient to develop meandering thalweg pattern.

Moreover, the meandering tendency occurred at a flatter slope with initial bend. Ippen and Drinker (1962) showed that bends of open channels were subjected to very high shear stresses and the maximum shear stress in a bend exceeded in intensity the mean shear for uniform flow in a straight reach by over 200 percent. Such high local shear stress near the concave banks of bends caused significant erosion which supplied bedload for the formation of alternate bars.

As the slope of a meandering thalweg channel was increased over a certain limit, the thalweg cut through the bars and the channel became wide, shallow, and straight. The flow cut through alternate bars because of higher velocity associated with steeper slopes, and a braided channel formed.

Observations in the laboratory under the present study showed that the bars in a braided channel formed as a result of deposition of coarse particles at some portions of the channel. The stream could not transport those coarse particles under the local conditions existing in that reach. Some finer materials were trapped among the coarse particles and as a result the initial bars increased in size and it caused the discharge to flow in two or more interlacing channels. Similar observations regarding the development of braiding in rivers were made by Leopold and Wolman (1957), and Lane (1957). But Friedkin (1945) observed that braided rivers are "overloaded rivers" and are associated with steep slopes. He also stated that braided channels result when the banks are extremely easily eroded. In Friedkin's test with easily erodible channel, the erosion of the banks provided the stream with large amounts of bedload and the flow could not transport all of this bedload which resulted in the development of braiding of the stream. So braiding can be attributed to either incompetency or incapacity of a river. That is, either the total sediment load is too great or some portion of the load is too coarse to be transported by the river.

It was verified that thalweg sinuosity in a meandering thalweg channel depends on discharge, slope, and bedload concentration. At flatter slopes, thalweg sinuosity increases rapidly with slope and the rate of increase of sinuosity decreases progressively as the slope increases. With gradual increase of slope, sinuosity reaches a maximum value and then it decreases due to channel braiding at steep slopes. A similar relationship between thalweg sinuosity and bedload concentration was obtained.

Bedload transport is lowest in a straight channel, highest in a braided channel and intermediate in a meandering thalweg channel. The Froude number of the flow and stream power was very high in braided channels, very low in straight channels, and intermediate in meandering thalweg channels. Such variation of bedload transport, Froude number, stream power and shear with channel pattern is explained by the fact that velocities and boundary shear stresses in straight channels were very small, whereas meandering thalweg channels developed at slightly higher velocities and shear stresses than those recorded in straight channels, and braided channels developed when velocities and shear stresses were still higher.

The above mentioned variation of bedload discharge with channel pattern has important effect on principles of design of diversion works. Significant changes in the quantity of sediment load of streams or canals resulting from the diversion of flows might cause the streams or canals to undergo changes in channel pattern and channel geometry.

There is good correlation between mean velocity of flow and bedload discharge. Bedload transport increases with velocity. The rate of increase of bedload transport with velocity was greater in straight and meandering thalweg channels than in braided channels. Similar relationships were observed between rate of increase of bedload discharge, shear and channel pattern, and rate of increase of bedload discharge, stream power and channel pattern. Bedload in a braided channel was observed to be coarser than those in meandering thalweg and straight channels. This was due to greater velocities associated with braided channels. With coarser particles as bedload, the rate of increase of bedload discharge with mean velocity should decrease in a braided channel.

It was observed that bedload discharge, stream power, and shear increased with slope and the rates of increase for each of these with slope were highest in braided channels, lowest in straight channels, and intermediate in meandering thalweg channels. Mean velocity of flow also increased with slope and the rate of increase of velocity with slope was highest in braided channels, lowest in straight channels, and intermediate in meandering thalweg channels. The differences in the rates of increase of velocity with slope were due to characteristic channel cross sections and bed forms, (and hence bed roughness) associated with each of the channel patterns. Bedload discharge, stream power, and shear is proportional to mean velocity, and hence the rates of increase of each of these variables with slope and channel patterns were similar to the rate of increase of velocity with slope and channel pattern.

The research proved that high concentrations of clay in the flow transforms a wide, shallow, and less sinuous meandering thalweg channel into a narrow, deep, and more sinuous meandering channel. The channel became smoother due to deposition of clay among the coarser particles in the bed and banks and hence velocity of flow increased. The increased velocity caused scour of the bed. Moreover, some of the fine sediments deposited on the alternate bars and such deposition built up the bars. Due to the building up of the bars and channel scour, the flow was restricted in the thalweg. Continued building up of bars and scour of bed along the thalweg caused exposure of the bars above the water surface and the flow then took place in a narrow, deep, and more sinuous meandering channel.

These results support the field observations by Schumm (1968). He showed that changes in sediment characteristics of a channel are accompanied by changes in channel morphology. He also showed that a change from bedload to suspended load in a channel will cause an increase in sinuosity and a decrease of width-depth ratio.

During the present experiments, width-depth ratio of channels was found to increase with bedload concentration. If flow is turned into a small steep channel, the channel will be made wider by scour of the banks until the shear on the banks is reduced to a magnitude equal to that which the material composing them can resist. Consequently, when a natural stream with a steep slope is formed in erodible material, it tends to adopt a wide and shallow cross section. The bedload concentration in steeper channels were greater because of higher velocities and greater shear stresses. This explains why width-depth ratio increases with bedload concentration.

In practice, sediment characteristics in rivers are changed due to construction of reservoirs and diversion structures or development of catchment areas, and therefore rivers will undergo significant changes in geometry and sinuosity depending on the change in the sediment characteristics caused by the above mentioned factors.

Acker, P., 1964, "Experiments on Small Streams in Alluvium," American Society of Civil Engineers Proc. Journal of the Hydraulic Division, No. HY4, p. 36.

Ali, Al-Shaikh, 1964, "Flow Dynamics in Trapezoidal Channel Bends," Ph.D. dissertation, Colorado State University, Fort Collins, Colorado.

Ananyan, A. K., 1965, "Fluid Flow in Bends of Conduits," Translated from Russian by A. Baruch, Israel Program for Scientific Translation, Jerusalem.

Ananyan, A. K., 1967, "An Approximate Theory of Secondary Flows at the Bend of River Course," Proc. of the 12th Congress of the International Association for Hydraulic Research, Vol. 1, pp. 422-428.

Andreev, O. A., and I. A. Yaroslavtseu, 1953, reported in Kondratev, N.E., 1959, (Translation 1962), "River Flow and River Channel Formation," Israel Program for Scientific Translations, Jerusalem, p. 172.

Bagnold, R. A., 1956, "The Flow of Cohesionless Grains in Fluids," Royal Soc. of London Philosoph. Trans., Vol. 249, pp. 235-297.

Bagnold, R. A., 1960a, "Some Aspects of the Shape of River Meanders," Geological Survey Professional Paper 282-E.

Bagnold, R. A., 1960b, "Sediment Discharge and Stream Power -- A Preliminary Announcement," U.S. Geological Survey Circular 421, p.23.

Brice, J. C., 1964, "Channel Patterns and Terraces of the Loup Rivers in Nebraska: U.S. Geol. Survey, Prof. Paper 422-D, pp. D1-D41.

Callander, R. A., 1969, "Instability and River Channels," Journal of Fluid Mechanics, Vol. 36, Part 3, pp. 465-480.

Carlston, C. W., 1965, "The Relation of Free Meander Geometry to Stream Discharge and Its Geomorphic Implications," American Journal of Science, Vol. 263, pp. 864-885.

Colby, B. R., 1957, "Relationship of Unmeasured Sediment Discharge to Mean Velocity," American Geophysical Union Transactions, Vol. 38, pp. 708-717.

Colby, B. R., 1964a, "Practical Computations of Bed-Material Discharge," American Society of Civil Engineers Proc., Journal of Hydraulics Div., Vol. 90, No. HY2, pp. 217-246.

Colby, B. R., 1964b, "Discharge of Sands and Mean Velocity Relationships in Sand Bed Streams," U.S. Geological Survey Professional Paper 462-A.

Cook, H. L., 1935, "Outline of the Energetics of Stream-Transportation of Solids," American Geophysical Union Transactions, Part 2, pp. 456-463.

Delleur, J. W., and D. S. McManus, 1959, "Secondary Flow in Straight Open Channels," Proc. 6th Midwestern Conference on Fluid Mechanics, University of Texas, Austin, p. 81.

Eakin, H., 1935, "Diversity of Current Direction and Load Distribution on Stream Bends," Transaction of the American Geophysical Union, Part II, p. 467.

Einstein, H. A. and N. L. Barbarossa, 1952, "River Channel Roughness," American Society of Civil Engineers Transactions, Vol. 117, pp. 1121-1132.

Einstein, H. A., and H. Li, 1958, "Secondary Currents in Straight Channels," Transactions, American Geophysical Union, Vol. 39, pp. 1058-1088.

Einstein, H. A., and H. W. Shen, 1964, "A Study on Meandering in Straight Alluvial Channels," Journal of Geophysical Research, Vol. 69, No. 24, pp. 5239-5247.

Elata, C., and A. T. Ippen, 1961, "The Dynamics of Open-Channel Flow with Suspensions of Neutrally Buoyant Particles," Cambridge, Massachusetts, Massachusetts Inst. Tech., Dept. Civil and Sanitary Eng. Tech. Report 45.

Fox, J. A. and D. J. Ball, 1968, "The Analysis of Secondary Flow in Bends in Open Channels," Proc. Institution of Civil Engineers, Vol. 39, pp. 467-475.

Friedkin, J. F., 1945, "A Laboratory Study of the Meandering of Alluvial Streams," U.S. Waterways Experiment Station, p. 40.

Gessler, J., 1970, "Self-Stabilizing Tendencies of Alluvial Channels," Journal of the Waterways and Harbors Division, May 1970, No. WW2, pp. 235-249

Gilbert, G. K., 1914, "Transportation of Debris by Running Water," U.S. Geological Survey Professional Paper 86, p. 263.

Goldstein, S. (Editor), 1965, "Modern Developments in Fluid Dynamics," Dover Publications, Inc., New York, pp. 85-87.

Hansen, E., 1967, "The Formation of Meanders as a Stability Problem," Basic Research Report No. 13, Technical University of Denmark, Copenhagen.

Henderson, F. M., 1961, "Stability of Alluvial Channels," ASCE, Proc. Vol. 87, Jour. HYD Div., pp. 109-138.

Hino, Mikio, 1963, "Turbulent Flow with Suspended Particles," American Society of Civil Engineers Proc., Vol. 89, No. HY4.

Ippen, A.T., and P.A. Drinker, 1962, "Boundary Shear Stresses in Curved Trapezoidal Channels," American Society of Civil Engineers Proceedings, Vol. 88, No. HY5, p. 143.

Jefferson, M.S.W., 1902, "Limiting Width of Meander Belts," National Geographic Magazine, Vol. 13, pp. 373-384.

Kennedy, J.F., and N.H. Brooks, 1965, "Laboratory Study of an Alluvial Stream at Constant Discharge," W.M. Keck Laboratory of Hydraulics and Water Resources, Division of Engineering and Applied Science, California Institute of Technology, Pasadena, Report No. KH-R-17.

Komura, S., 1966, "Alternate Scours in Straight Alluvial Channels," Master's Thesis, Colorado State University, Fort Collins, Colorado, 72 p.

Kondratev, N.E. (Editor), 1959, "River Flow and River Channel Formation", Translated from Russian by Y. Prushansky, Published for the National Science Foundation, Washington, D.C. and the Dept. of the Interior by the Israel Program for Scientific Translations, Jerusalem, 1962, Available from the office of Technical Services, U.S. Department of Commerce, Washington,25,D.C., 172 p.

Lane, E.W., and Carlson, E.J., 1953, "Some Factors Affecting Canals Constructed in Coarse Granular Material," International Association for Hydraulic Research Proc., Minnesota International Hydraulics Convention, 1953.

Lane, E.W., 1955, "The Importance of Fluvial Morphology in Hydraulic Engineering," Proc. ASCE, Vol. 81, No. 745.

Lane, E.W., 1957, "A Study of the Shape of Channels Formed by Natural Streams Flowing in Erodible Material," M.R.D. Sediment Series No. 9, U.S. Army Engineer Division, Missouri River, Corps of Engineers, Omaha, Nebraska.

Langbein, W.B., 1964, "Geometry of River Channels," Journal of the Hydraulics Division, Proc. ASCE, No. HY2, pp. 301-312.

Langbein, W.B., and L.B. Leopold, 1966, "River Meanders -- Theory of Minimum Variance," U.S. Geol. Survey Prof. Paper 422-H, H1-H15.

Leopold, L.B., 1953, "River Meanders and Vorticity Theorem," Transactions, American Geophysical Union, Vol. 34, No. 6, pp. 955-958.

Leopold, L.B., and M.G. Wolman, 1957, "River Channel Patterns: Braided, Meandering and Straight," Geological Survey Professional Paper 282-B.

Leopold, R. A., and M. G. Wolman, 1960, "River Meanders," Geological Society American Bulletin, Vol. 71, pp. 769-794.

Leopold, L. B., and W. B. Langbein, 1962, "The Concept of Entropy in Landscape Evolution," U.S. Geol. Survey Prof. Paper 500A.

Leopold, L. B., M. G. Wolman, and J. P. Miller, 1964, "Fluvial Processes in Geomorphology," W. H. Freeman and Company, San Francisco and London, p. 522.

Lokhtins, 1960, (Rzhanitsyn, N. A., 1969), "Morphological and Hydrological Regularities of the Structure of the River Net," Translated by D. B. Krimgold, USDA, Agricultural Research Service, Soil and Water Conservation Research Division.

Mäsiar, E., 1967, "The Effect of Bend on the Distribution and Development of the Macroturbulence Intensity in Open Channel-Beds," Proc. of the 12th Congress of IAHR, Vol. 2, pp. 154-162.

Meyer-Peter, R., and R. Müller, 1948, "Formulas for Bed-Load Transport," International Assoc. Hydraulic Structures Research, 2nd mtg., Stockholm, Sweden, pp. 39-64.

Morisawa, M., 1968, "Streams," McGraw-Hill Book Company, New York.

Nagabhushanaiah, H. S., 1967, "Meandering of Rivers," International Assoc. Scientific Hydrology Bull., Vol. 7, pp. 28-43.

Neu, H. A., 1967, "Transverse Flow in a River Due to Earth's Rotation," Journal of the Hydraulics Division, Vol. 93, No. HY5, pp. 149-165.

Prus-Chacinski, T. M., 1956, "Patterns of Motion in Open Channel Bends," Journal of Institution of Water Engineers, Vol. 10, pp. 420-426.

Rathbun, R. E., and E. V. Richardson, 1969, "Response of a Laboratory Alluvial Channel to Changes of Hydraulic and Sediment-Transport Variables," Geological Survey Professional Paper 562-D, p. 32.

Raudkivi, A. J., 1967, "Loose Boundary Hydraulics," First Edition, Pergamon Press Ltd., London.

Raudkivi, A. J., 1967, "Analysis of Resistance in Fluvial Channels," Am. Soc. of Civil Engineers Proc., Journal of Hydraulics Div., Vol. 93, No. HY5, pp. 73-84.

Reynolds, A. J., 1965, "Waves on the Erodible Bed of an Open Channel," Journal of Fluid Mechanics, Vol. 22, pp. 113-133.

Rottner, J., 1959, "A Formula for Bed-Load Transportation," La Houille Blanche, pp. 301-307, (After Colby, 1964).

Rozovskii, I. L., 1957, "Flow of Water in Bends of Open Channels," Published by the Academy of Sciences of the Ukrainian SSR, p. 233.

Rubey, W. W., 1952, "Geology and Mineral Resources of the Hardin and Brussels Quadrangles (in Illinois)," U.S. Geol. Survey Prof. Paper 218, 179 p.

Rzhanitsyn, N. A., 1960, "Morphological and Hydrological Regularities or the Structure of the River Net," Translated by Dr. D.G. Krimgold, USDA, Agricultural Research Service, Soil and Water Conservation Research Div.

Scheidegger, A. E., 1967, "A Thermodynamic Analogy for Meander Systems," Water Resources Research, Vol. 3, No. 4, pp. 1041-1046.

Scheidegger, A. E., and W. B. Langbein, 1966, "Probability Concepts in Geomorphology," U.S. Geological Survey Professional Paper 500-C, p. 14.

x Schumm, S. A., 1960, "The Shape of Alluvial Channels in Relation to Sediment Type," U.S. Geol. Survey Prof. Paper 352-B, pp. 17-30.

x Schumm, S. A., 1963a, "A Tentative Classification of Alluvial River Channels," U.S. Geol. Survey Circ. 477, 10 p.

x Schumm, S. A., 1963b, "Sinuosity of Alluvial Rivers on the Great Plains," Geol. Soc. America Bull., Vol. 74, pp. 1089-1100.

Schumm, S. A., 1968, "River Adjustments to Altered Hydrologic Regimen -- Murrumbidgee River and Paleochannels, Australia," U-S. Geological Survey Professional Paper 598, p. 65.

Schumm, S. A., 1969, "River Metamorphosis," American Soc. of Civil Engineers, Proc. Journal of the Hydraulic Div., No. HY1, pp. 255-273.

Shen, H. W., 1961, "A Study of Meandering and Other Bed Patterns in Straight Alluvial Channels," Hydraulic Laboratory, University of California, Berkeley, Water Resources Center Contribution No. 33.

Shen, H. W., and S. Komura, 1968, "Meandering Tendencies in Straight Alluvial Channels," Journal of the Hydraulic Division, No. HY4, pp. 997-1016.

Simons, D. B., 1957, "Theory and Design of Stable Channels in Alluvial Material," Ph.D. dissertation, Colorado State University, Fort Collins, Colorado.

Simons, D. B., and E. V. Richardson, 1962, "Resistance to Flow in Alluvial Channels," American Society Civil Engineers, Trans., Vol. 127, pp. 927-1006.

Simons, D. B., E. V. Richardson, and W. H. Haushild, 1963, "Some Effects of Fine Sediment on Flow Phenomena," U.S. Geol. Survey Water-Supply Paper 1498-G, 46 p.

Simons, D. B. and E. V. Richardson, 1963, "Forms of Bed Roughness in Alluvial Channels, Amer. Soc. Civil Eng., Trans. Vol. 128, pp. 284-302

Simons, D. B., and E. V. Richardson, 1966, "Resistance to Flow in Alluvial Channels," USGS Professional Paper 422J.

Simons, D. B., 1970, "River and Canal Morphology," Presented at the Institute of River Mechanics, Colorado State University, Fort Collins, Colorado.

Tanner, W. F., 1960, "Helical Flow, A Possible Cause of Meandering," Journal of Geophysical Research, Vol. 65, pp. 993-995.

Thakur, T. R., and A. E. Scheidegger, 1968, "A Test of the Statistical Theory of Meander Formation," Water Resources Research, Vol. 4, No. 2, April, pp. 317-329.

Tiffany, J. B., and G. A. Nelson, 1939, "Studies of Meandering of Model-Streams," Transactions, American Geophysical Union, Part IV, August, pp. 644-649.

Vanoni, V. A., 1946, "Transport of Suspended Sediment by Water," American Society Civil Engineers Trans., Vol. 111, pp. 67-102.

Vanoni, V. A. and N. H. Brooks, 1967, "Laboratory Studies of the Roughness and Suspended Load of Alluvial Streams," Pasadena, California, California Institute Technology Report E-68, 121 p.

Vanoni, V. A. and G. N. Nomicos, 1960, "Resistance Properties of Sediment-Laden Streams," American Society Civil Engineers Trans., Vol. 125, pp. 1140-1175.

Vanoni, V. A., and L. S. Hwang, 1967, "Relation Between Bed Forms and Friction in Streams," American Society of Civil Engineers Proceedings, Journal of Hydraulic Division, Vol. 93, No. HY3, pp. 121-144.

Velikanov, M. A., 1950, Reported in Kondratev, N. E., 1959, (Translated 1962), "River Flow and River Channel Formation," Israel Program for Scientific Translations, Jerusalem, p. 172.

von Schelling, H., 1951, "Most Frequent Particle Paths in a Plane," Transactions American Geophysical Union, Vol. 32, pp. 222-226.

von Schelling, H., 1964, "Most Frequent Random Walks," General Electric Co., Report 64, GL 92, Schenectady, New York.

Warner, P. W., 1951, "On the Origin of River Meanders," Transactions, American Geophysical Union, Vol. 32, No. 6, pp. 898-901.

X White, C. M., 1940, "Equilibrium of Grains on Bed of Streams," Royal Society (London) Philos, Trans., Ser. A., Mathematical and Physical Sciences, Vol. 174, pp. 322-334.

Williams, G. P., 1967, "Flume Experiments on the Transport of a Coarse Sand," Geological Survey Professional Paper 562-B, p. 31.

Yen, Ben Chien, 1967, "Some Aspects of Flow in Meandering Channels," Proceedings Twelfth Congress of the International Association for Hydraulic Research, Vol. 1.

APPENDIX A

Figures

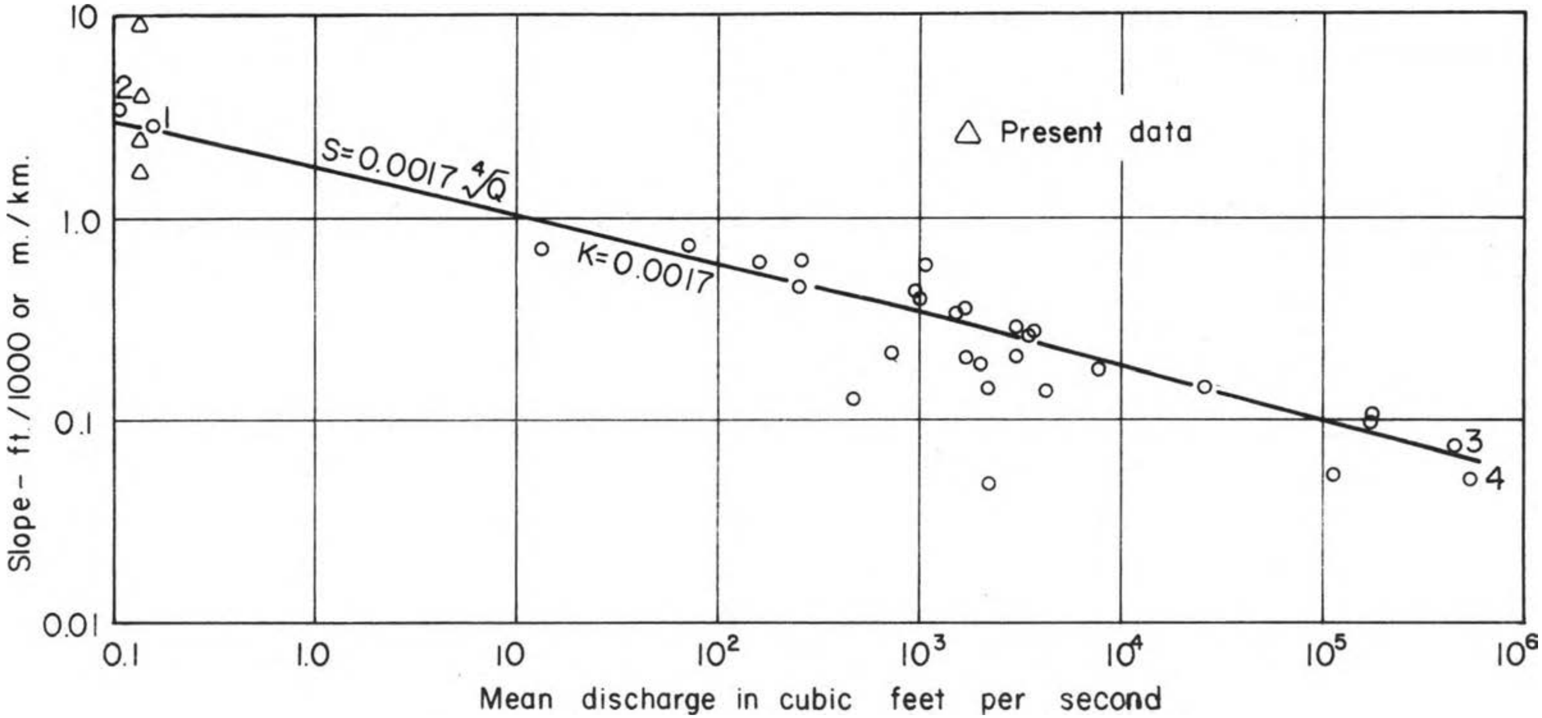

Figure 1. Slope-discharge relations for meandering streams in sand (after Lane, 1957)

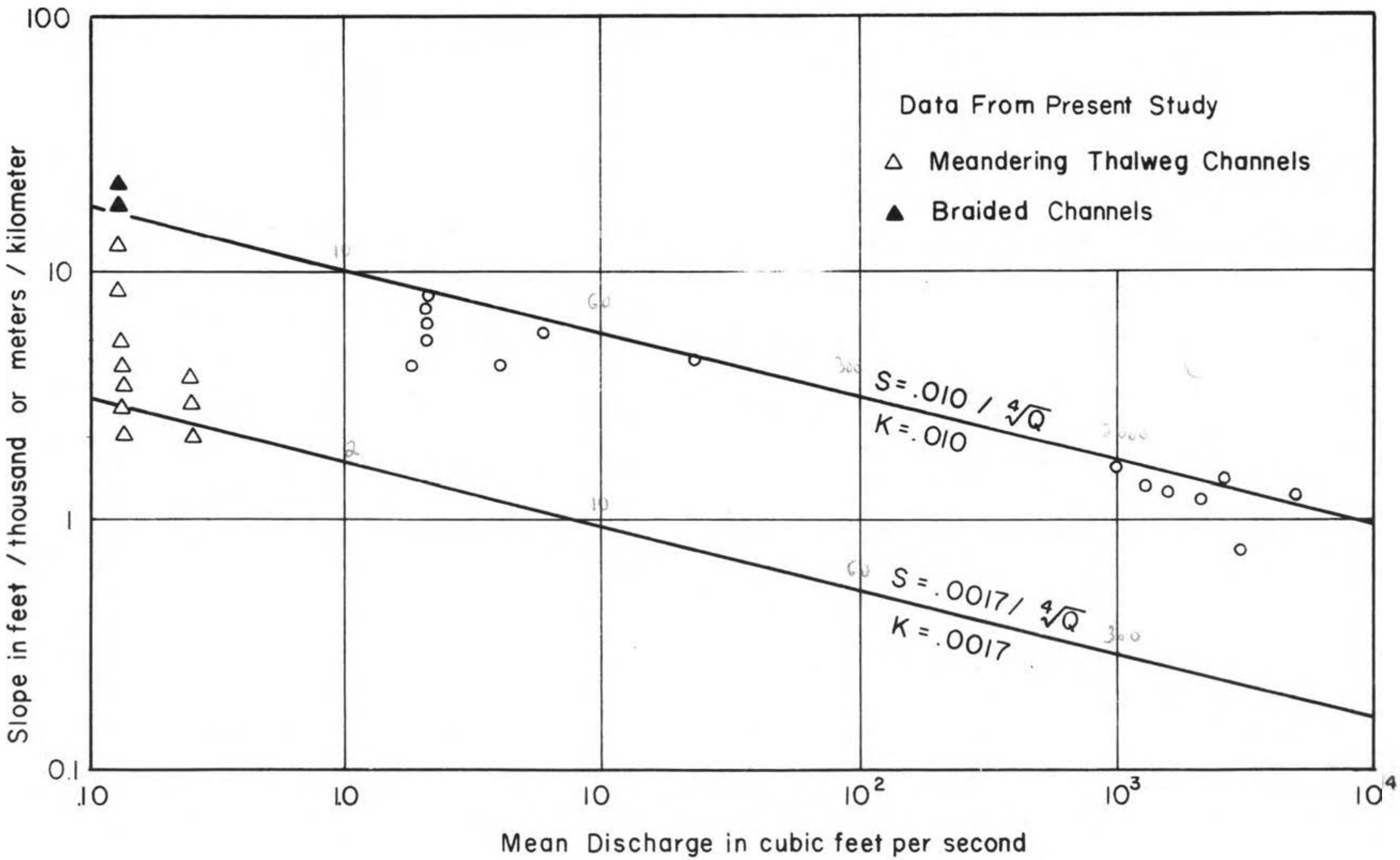

Figure 2. Slope-discharge relations for braided streams (after Lane, 1957)

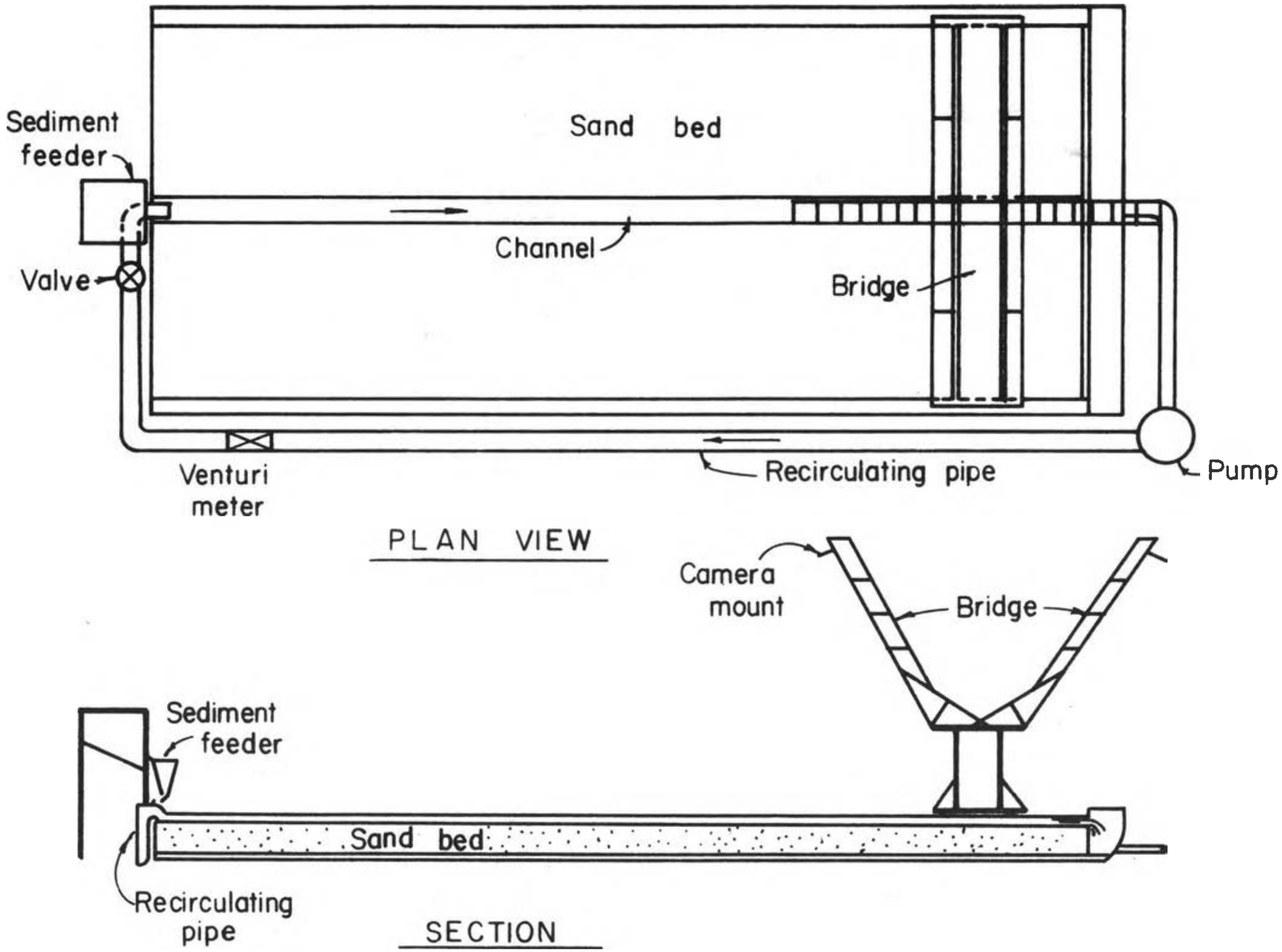

Figure 3. Experimental set up.

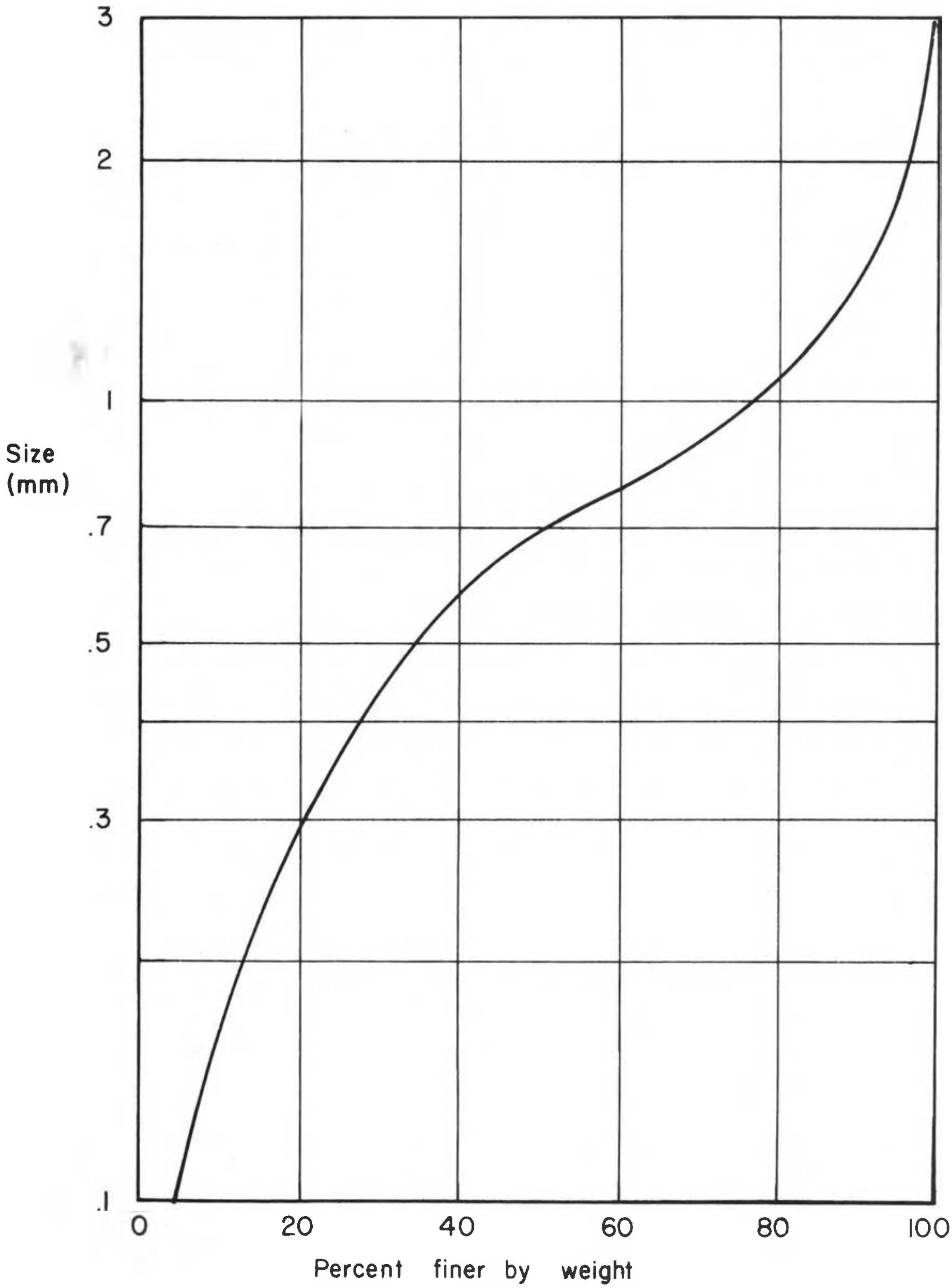

Figure 4. Size distribution of bed material

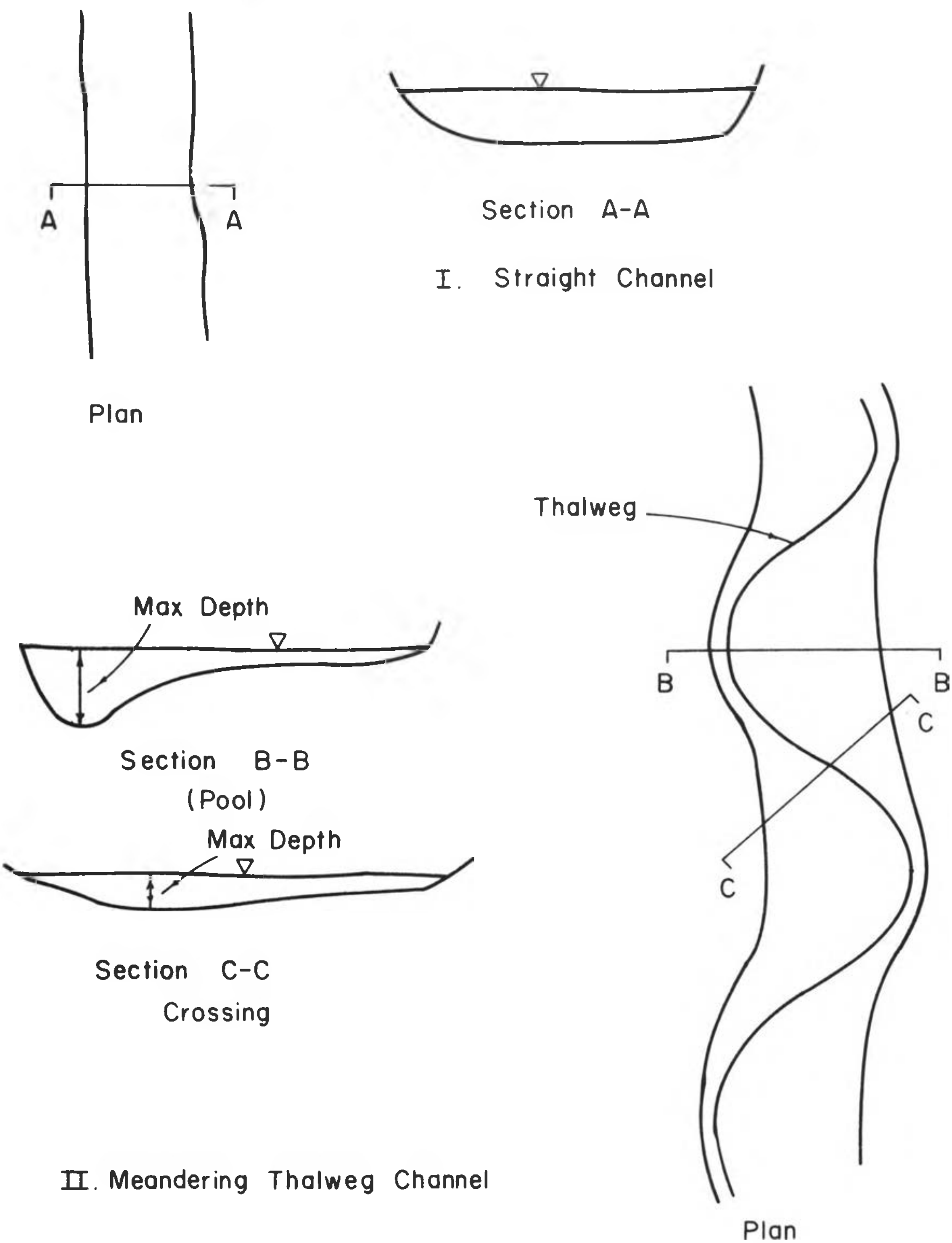

Figure 5. Different channel patterns

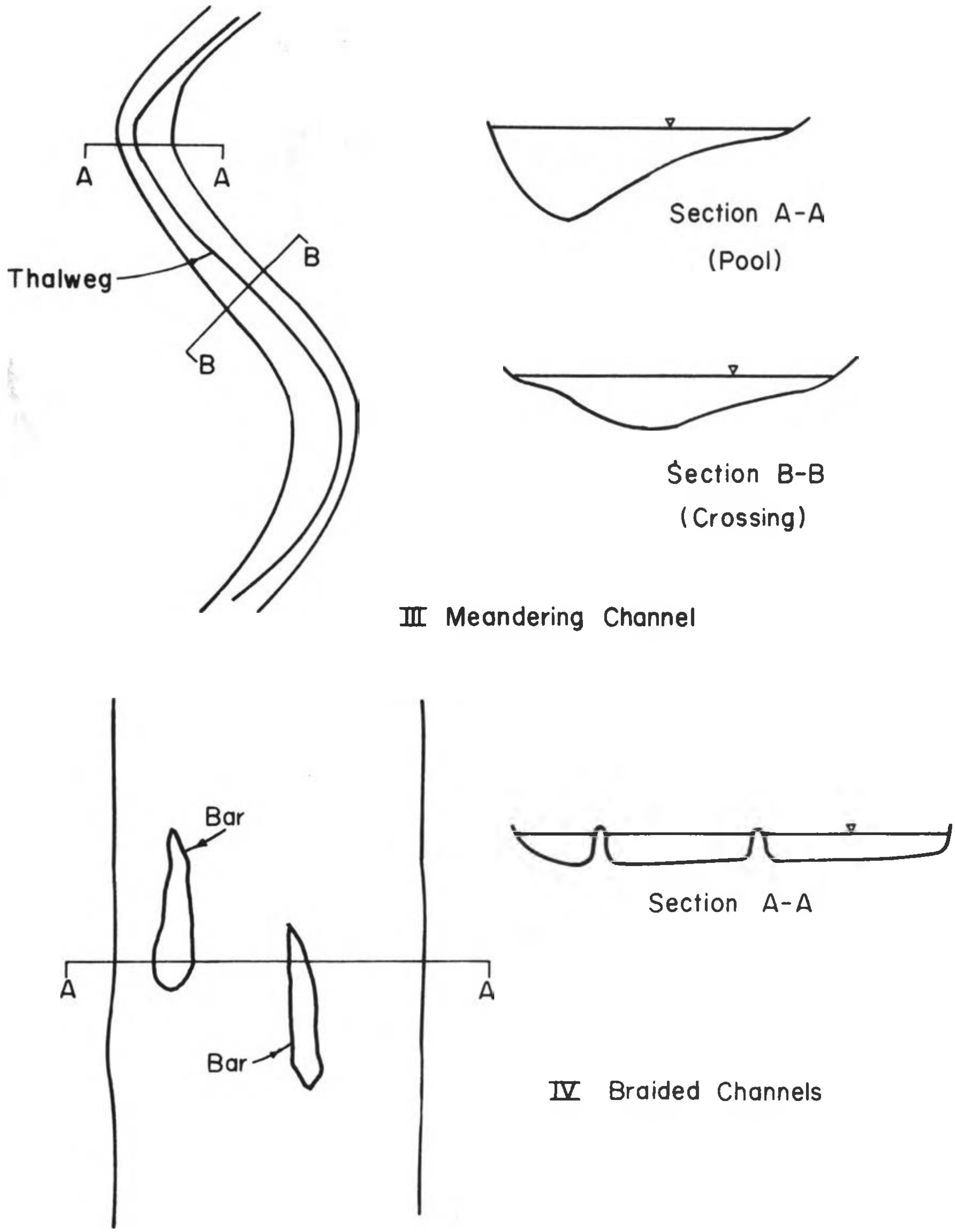

Figure 5 (cont). Different channel patterns

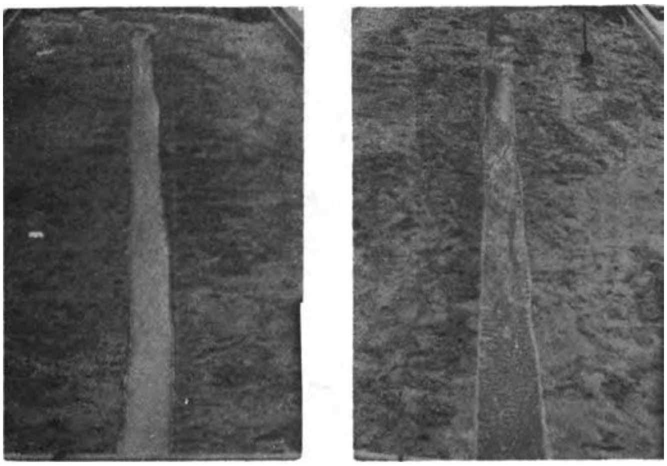 

(a) Straight channel (b) Meandering thalweg channel

 

(c) Meandering channel (d) Braided channel

Figure 5 (cont). Photographs of different channel patterns

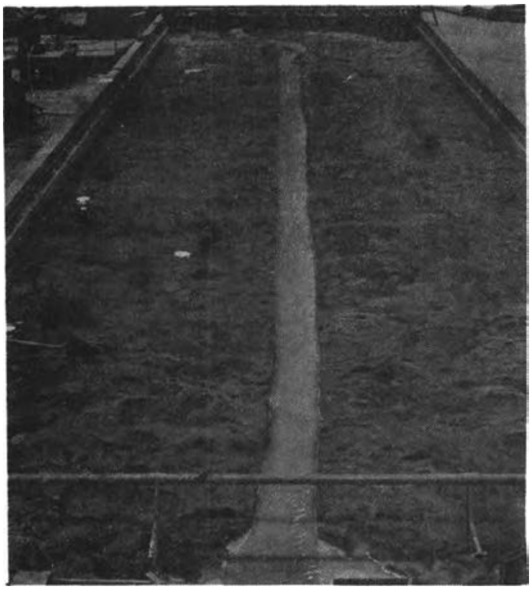

(a) time 1/2 hr.

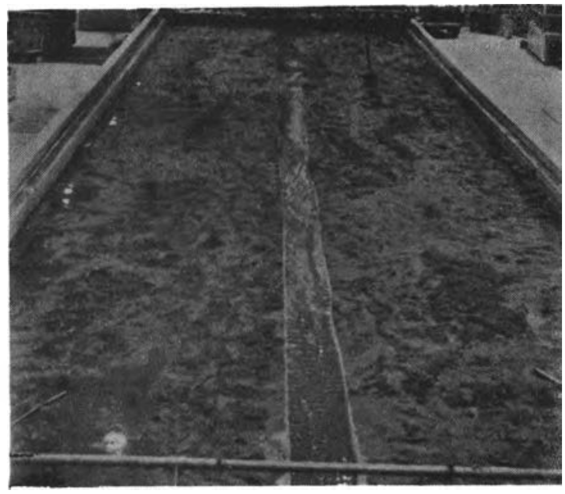

(b) time 1 1/2 hr.

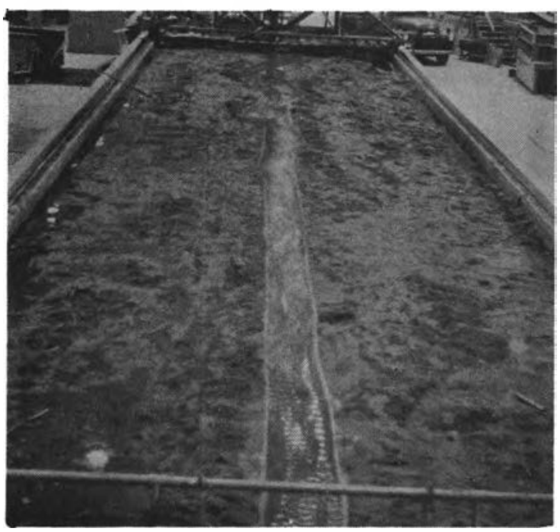

(c) time 2 1/4 hr.

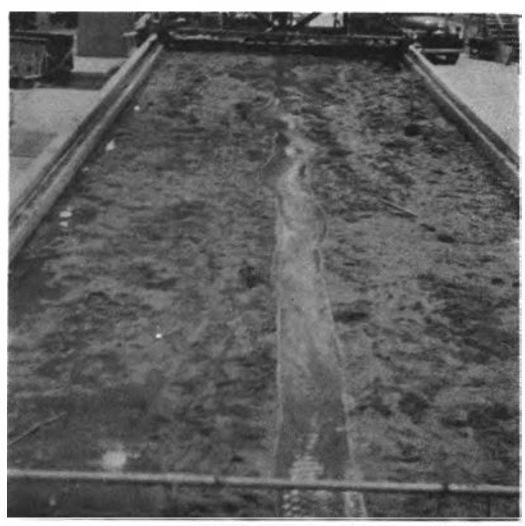

(d) time 4 hr.

Figure 6. Photographs showing gradual development of alternate bars

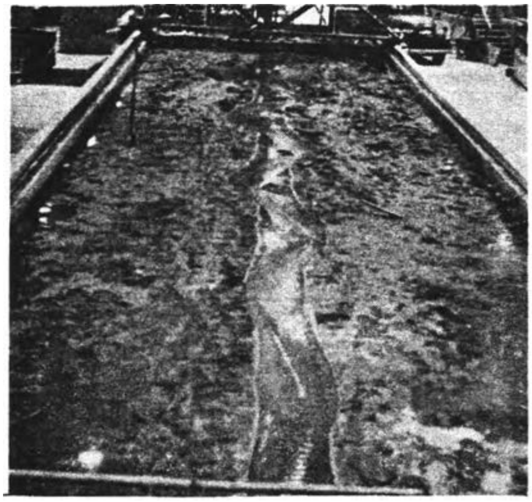

(e) time 6 1/2 hr.

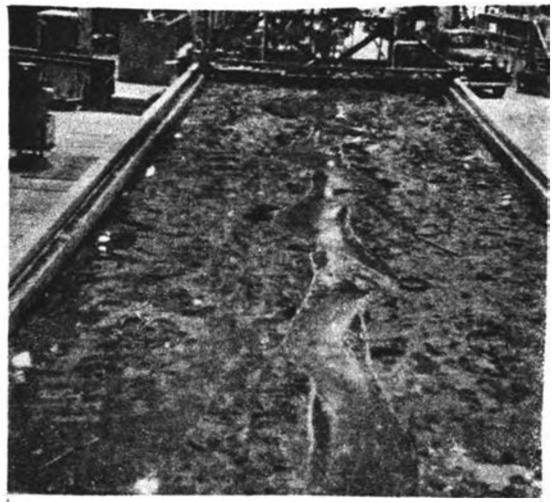

(f) time 8 hr.

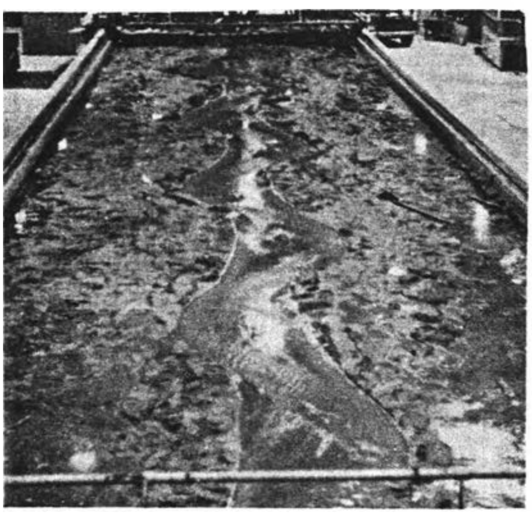

(g) time 12 hr.

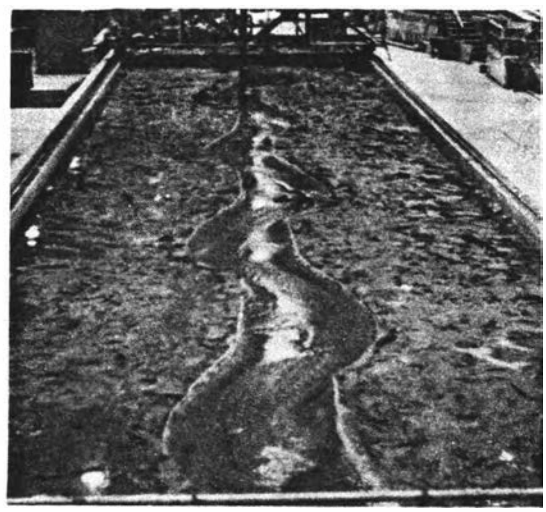

(h) time 21 hr.

Figure 6 (cont). Photographs showing gradual development of alternate bars

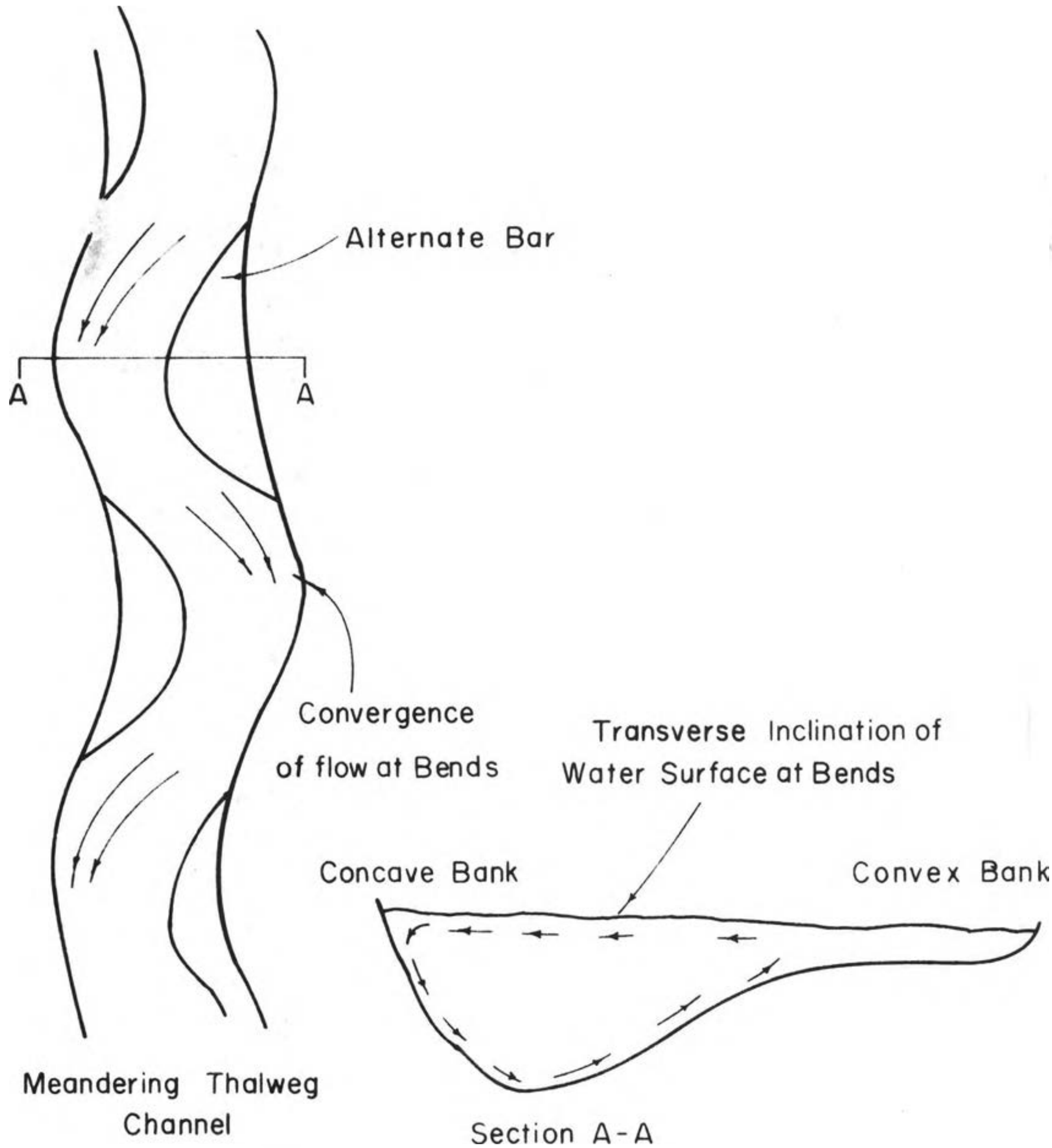

Figure 7. Flow in the bend of a meandering thalweg channel

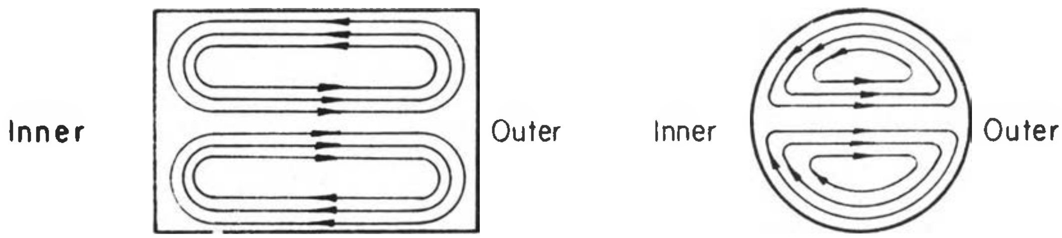

Figure 8. Secondary currents in pipes (after Goldstein, 1965)

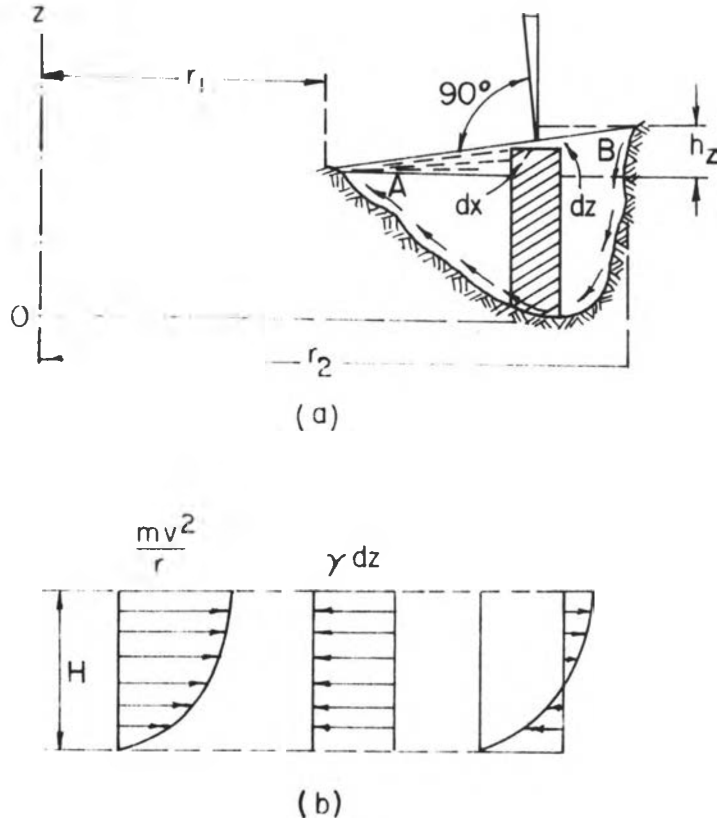

Figure 9. Secondary currents at bends of open channels (after Simons, 1970)

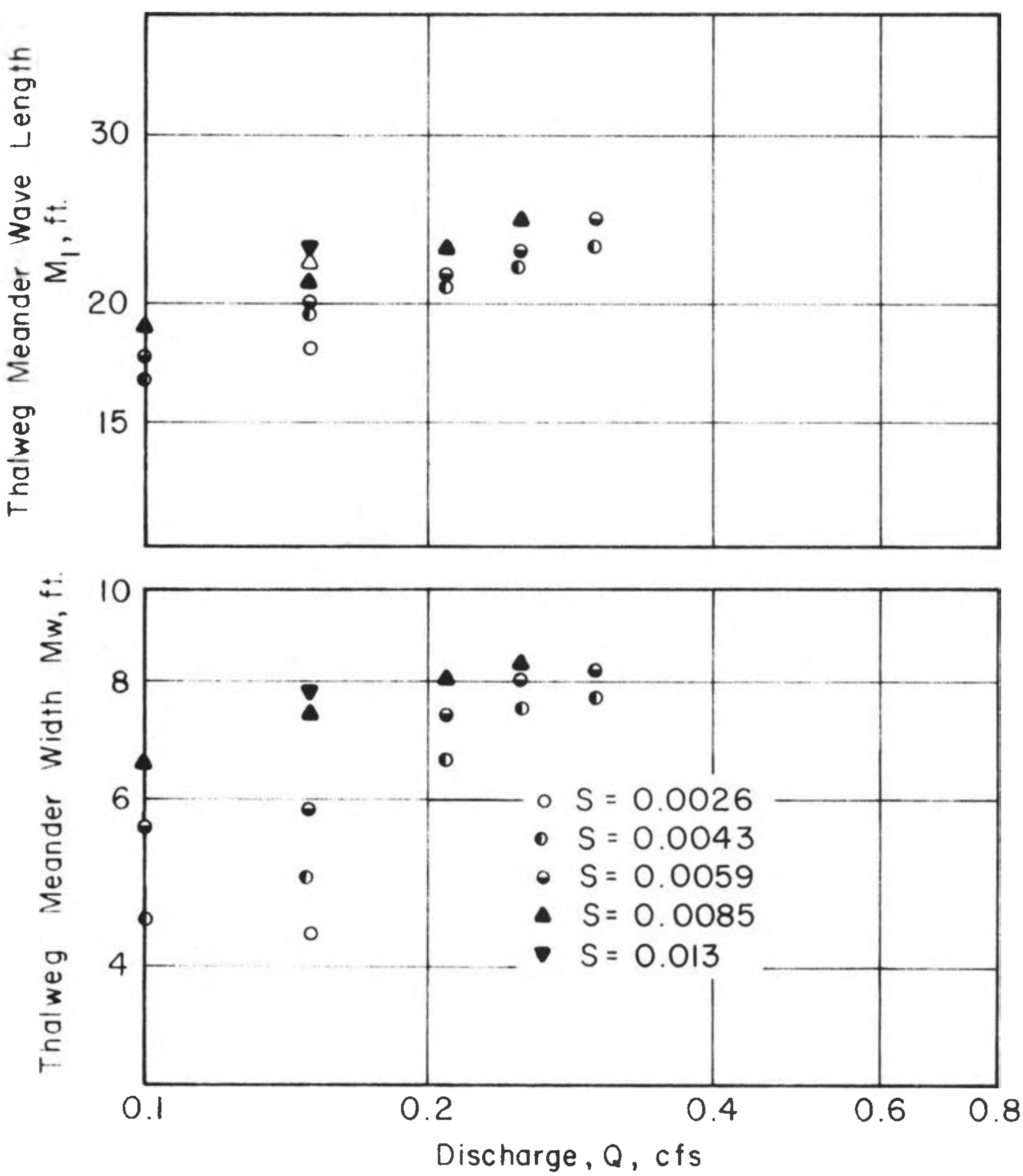

Figure 10. Variation of thalweg meander dimensions with discharge and slope

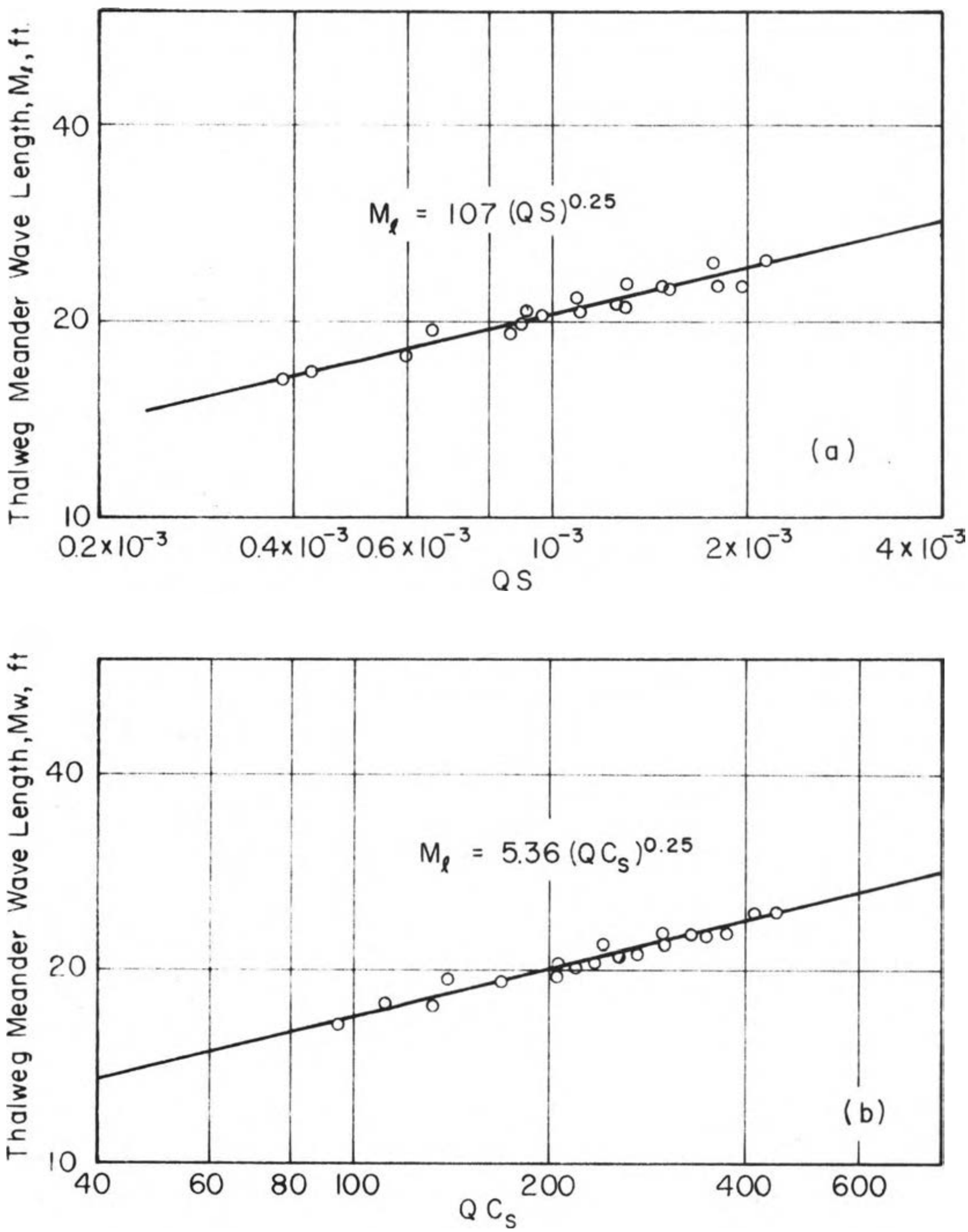

Figure 11. Relationship among (a) thalweg meander wave length, discharge, and slope, and (b) thalweg meander wave length, discharge, and bedload concentration

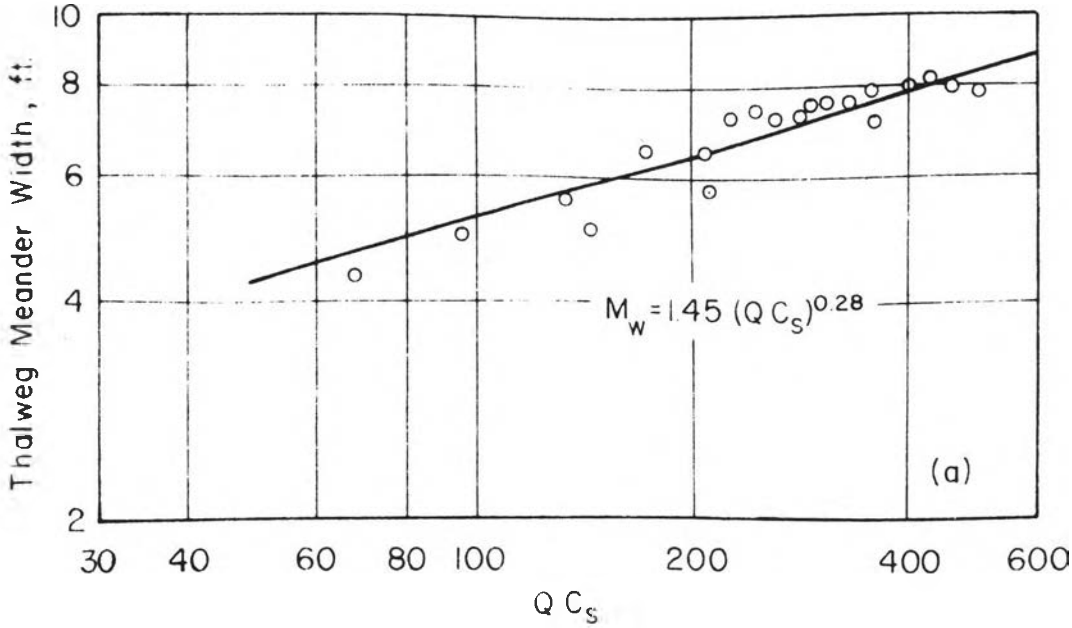

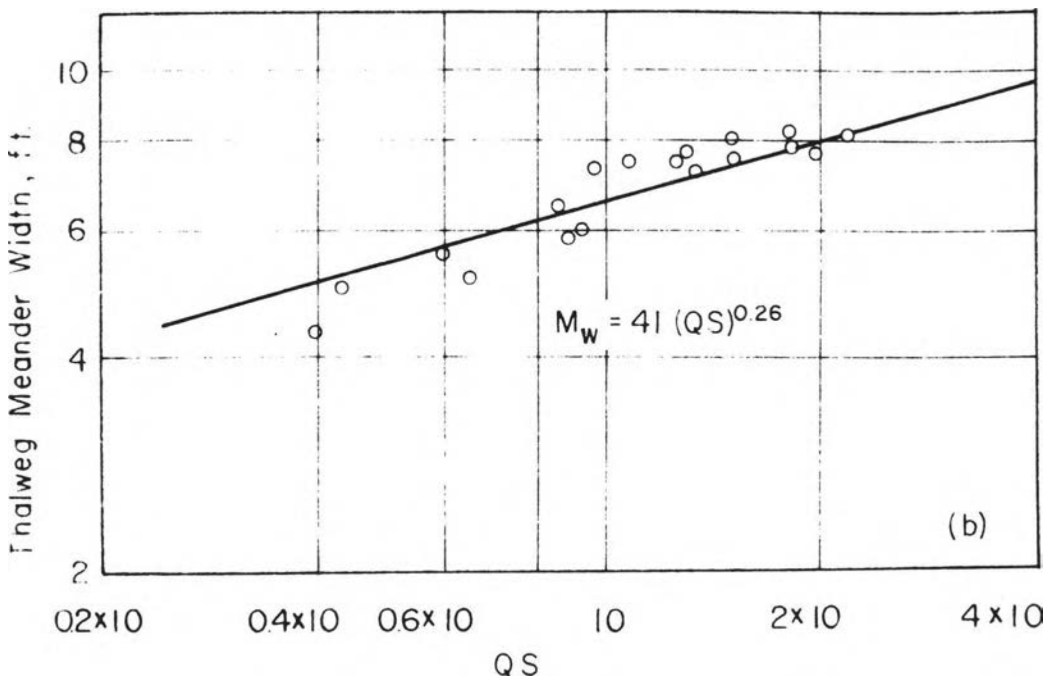

Figure 12. Relationship among (a) thalweg meander width, discharge, and bedload concentration, and (b) thalweg meander width, discharge, and slope

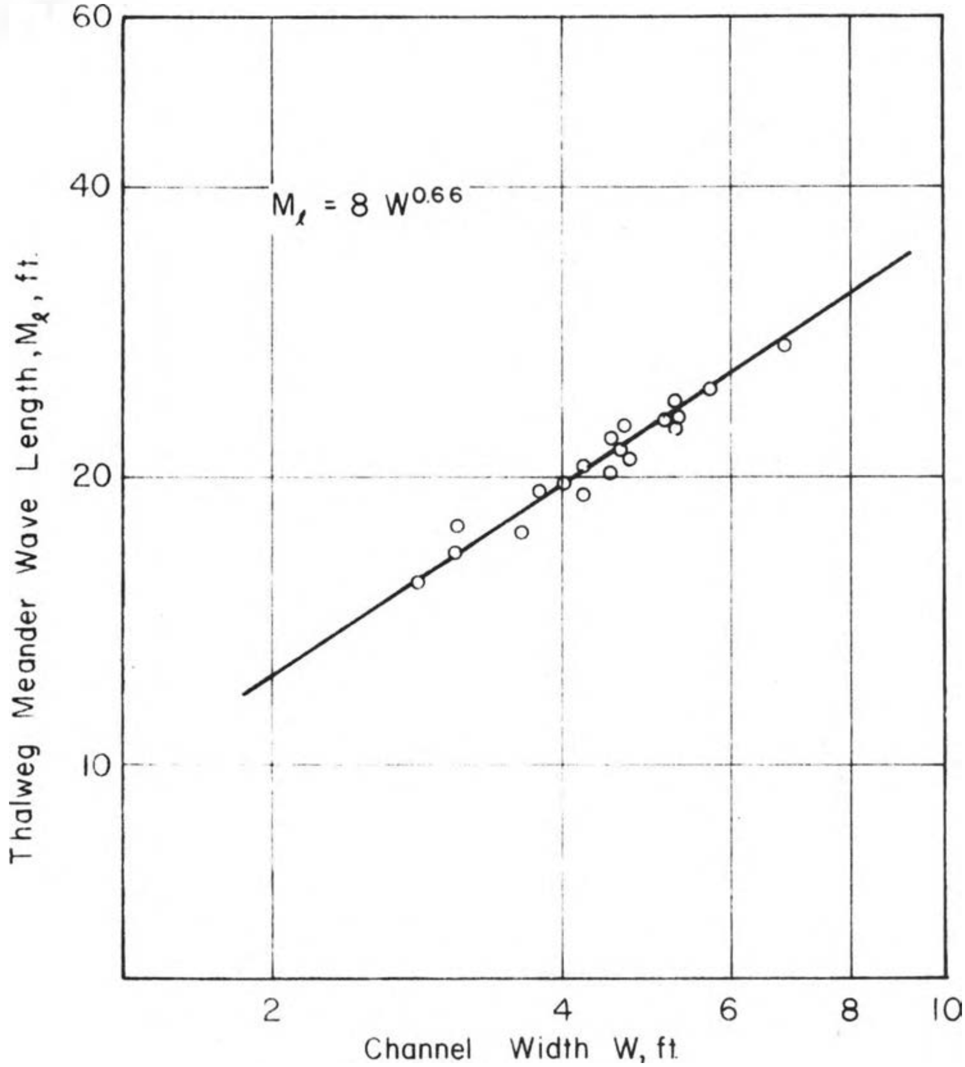

Figure 13. Relationship between thalweg meander wave length and channel width

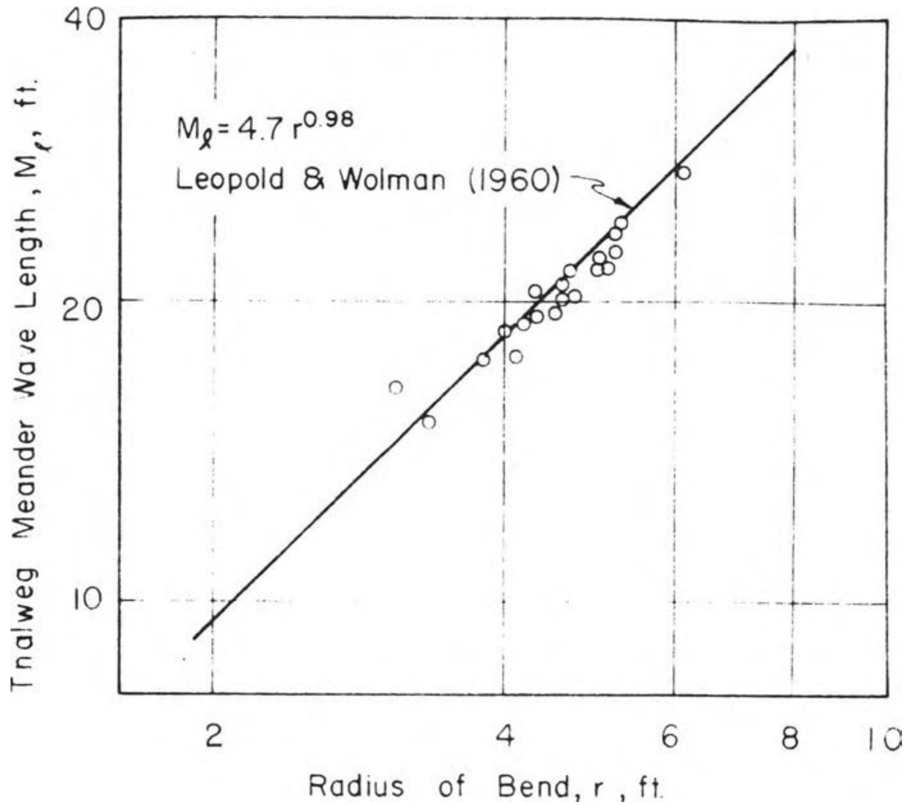

Figure 14. Relationship between thalweg meander wave length and radius of bend

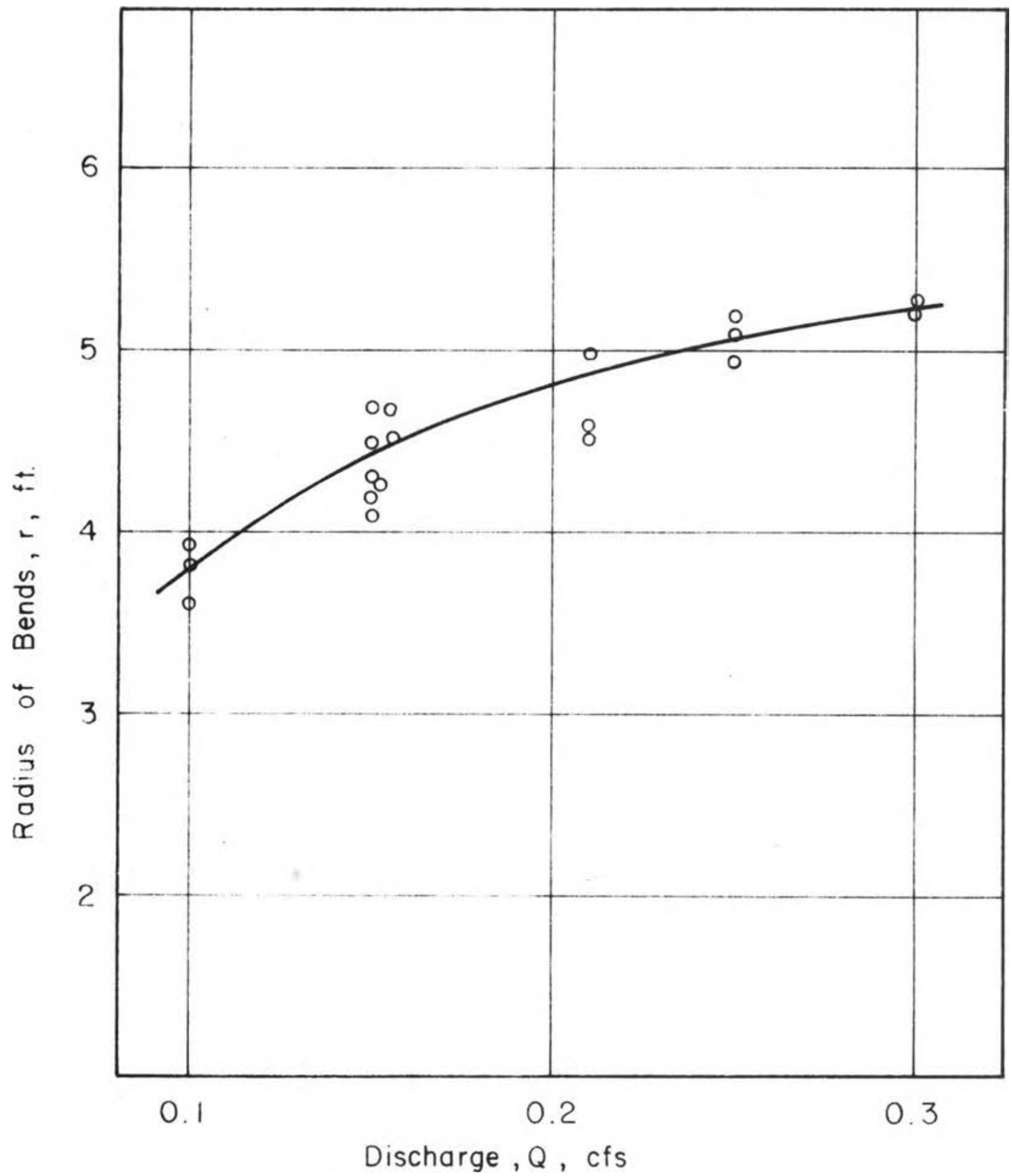

Figure 15. Variation of radius of bend with discharge

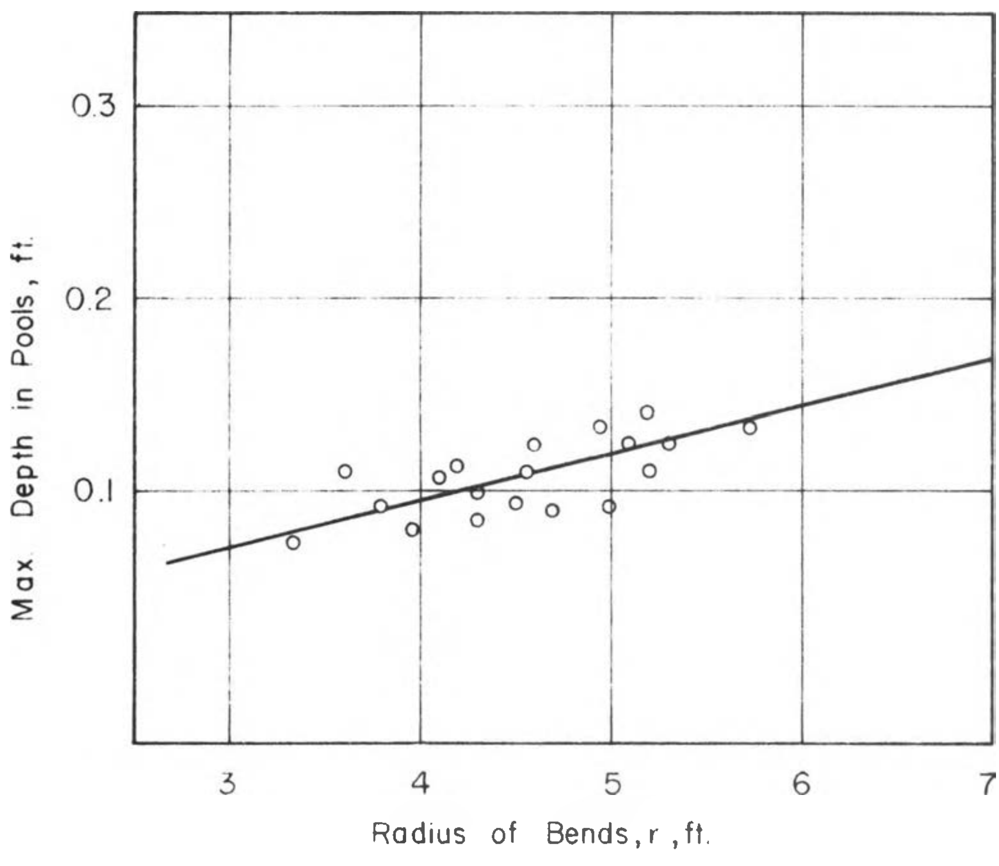

Figure 16. Variation of maximum depths in pools with radius of bends

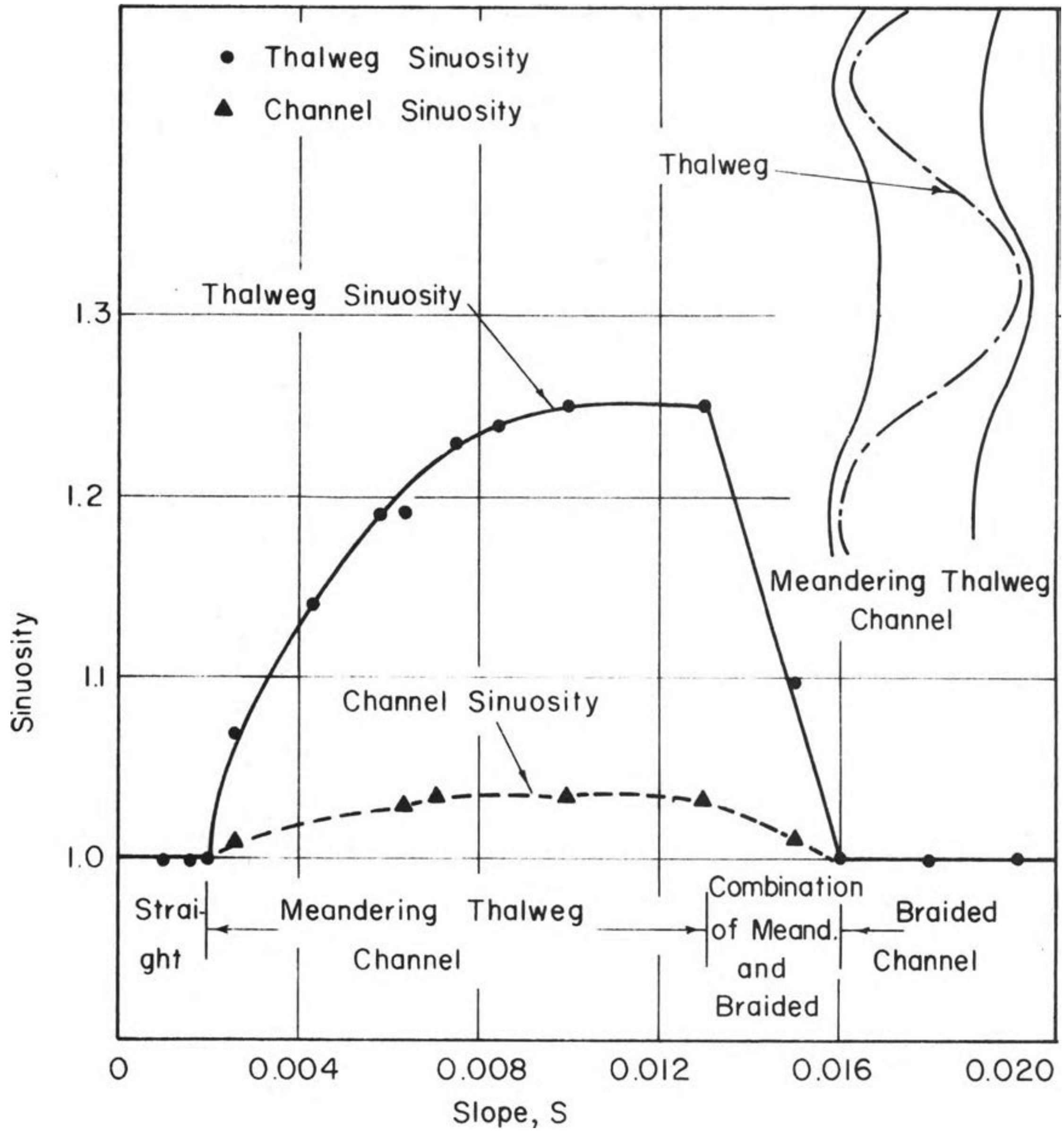

Figure 17. Sinuosity versus slope for a constant ~~slope~~ Q of 0.15 cfs

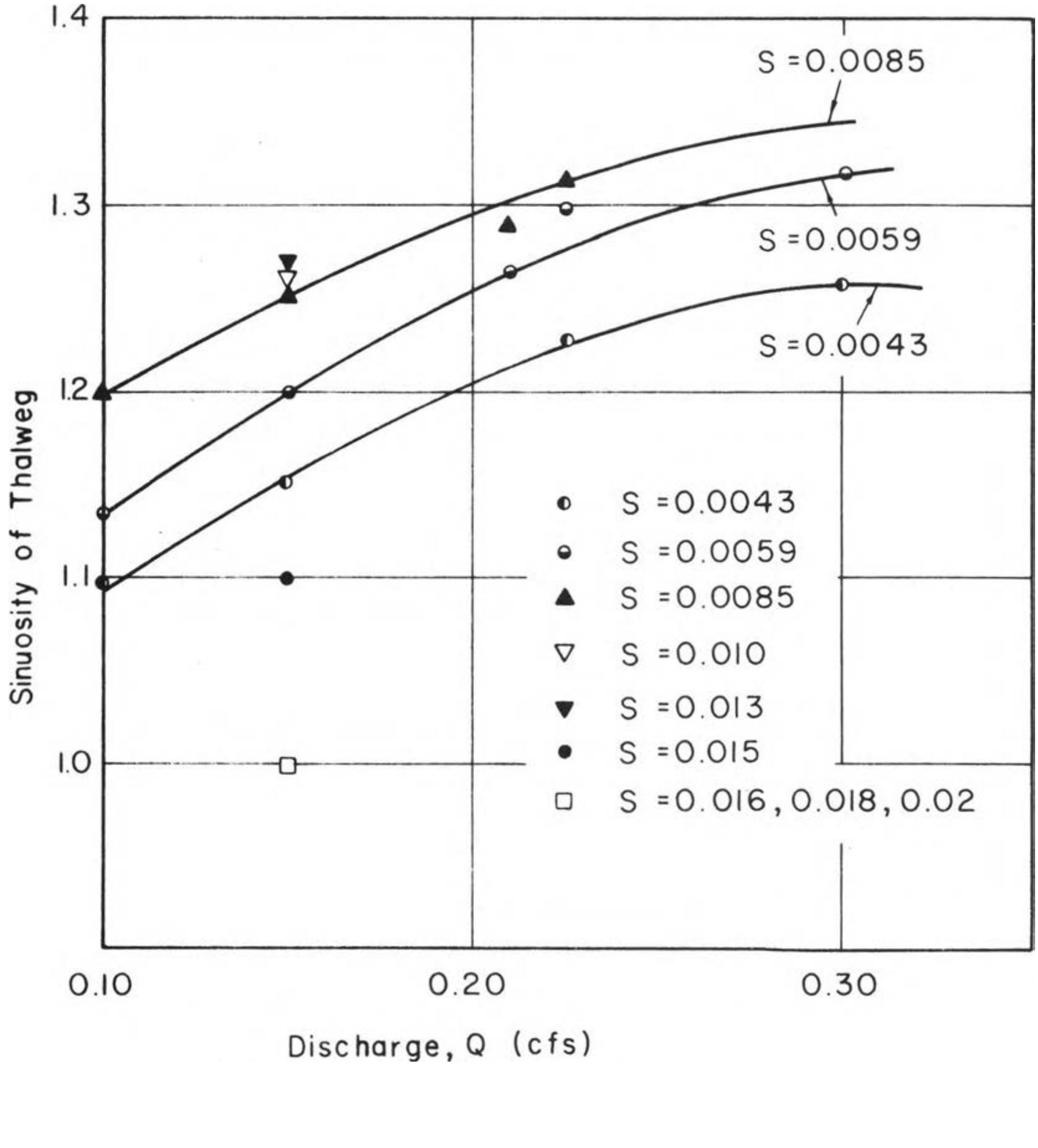

Figure 18. Variation of thalweg sinuosity with discharge and slope

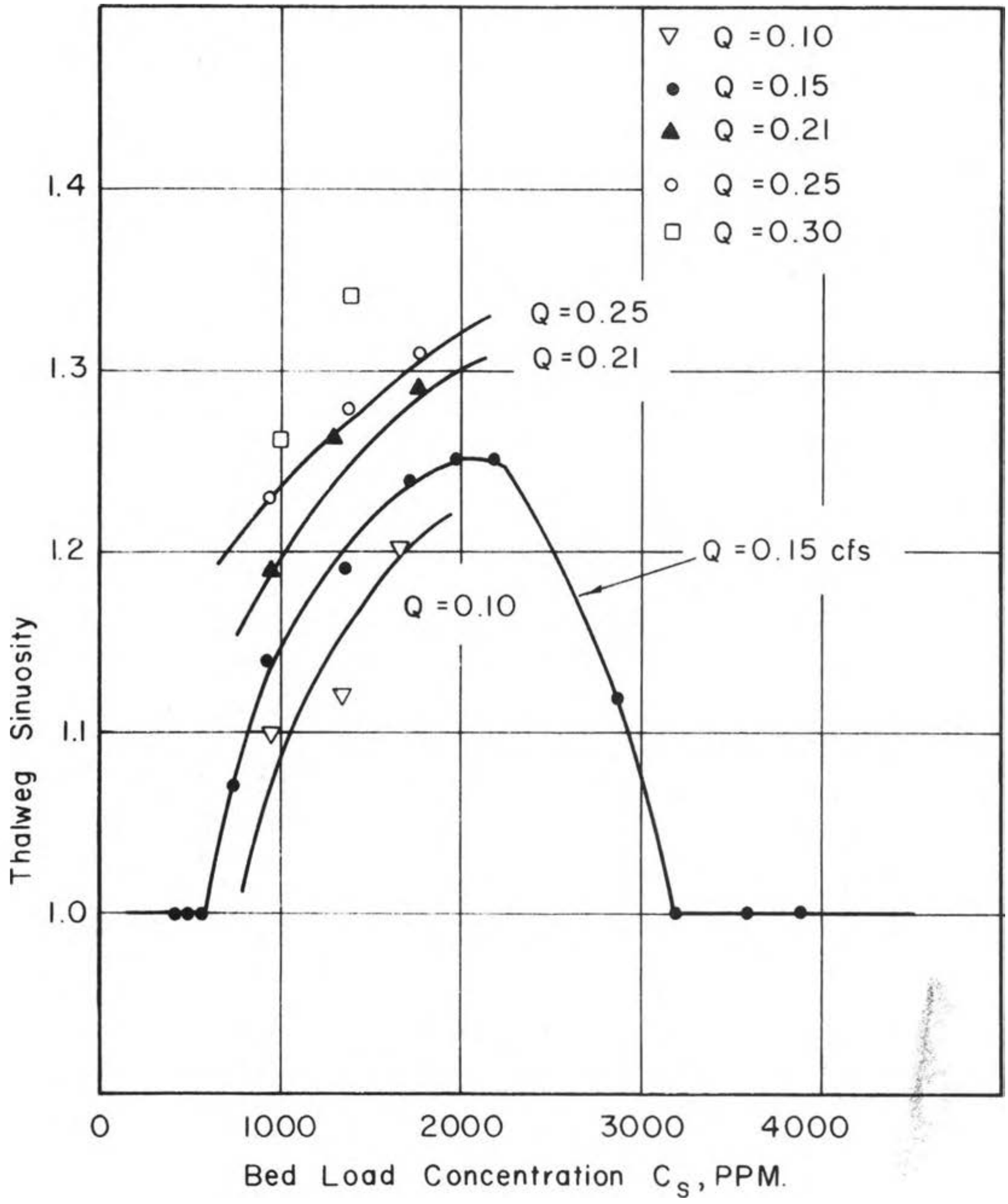

Figure 19. Variation of thalweg sinuosity with discharge and bed-load concentration

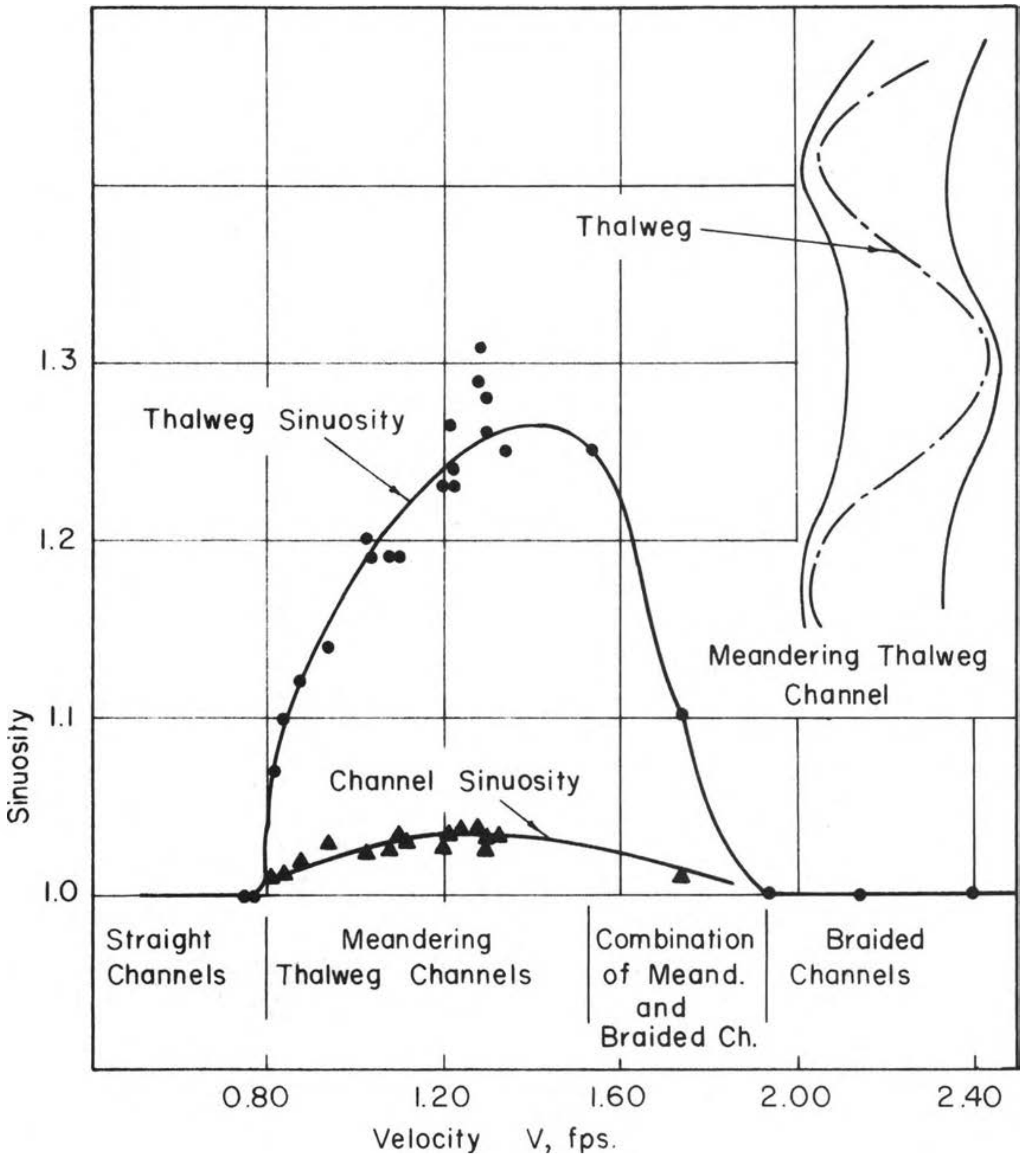

Figure 20. Variation of sinuosity with mean velocity

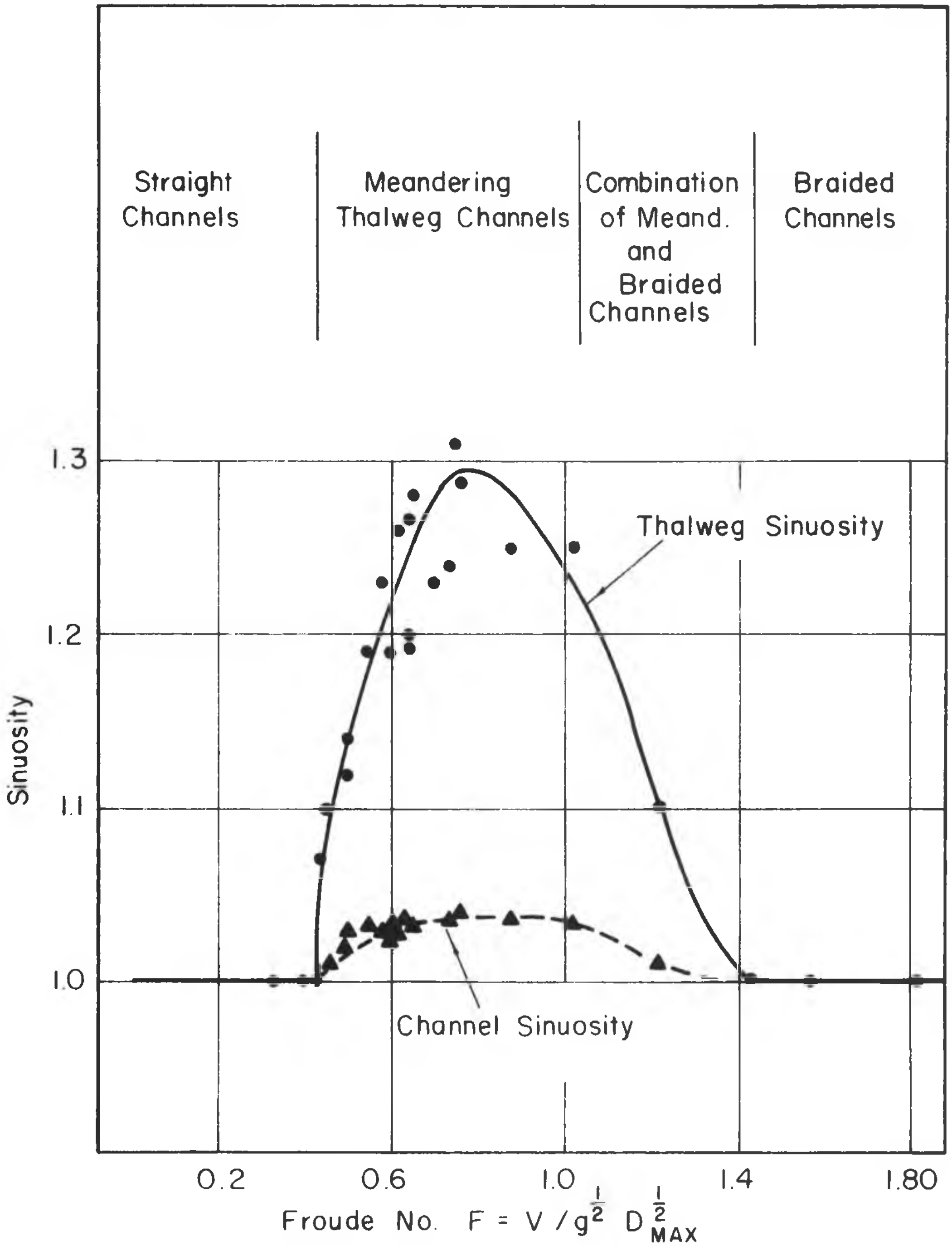

Figure 21. Variation of sinuosity with Froude number

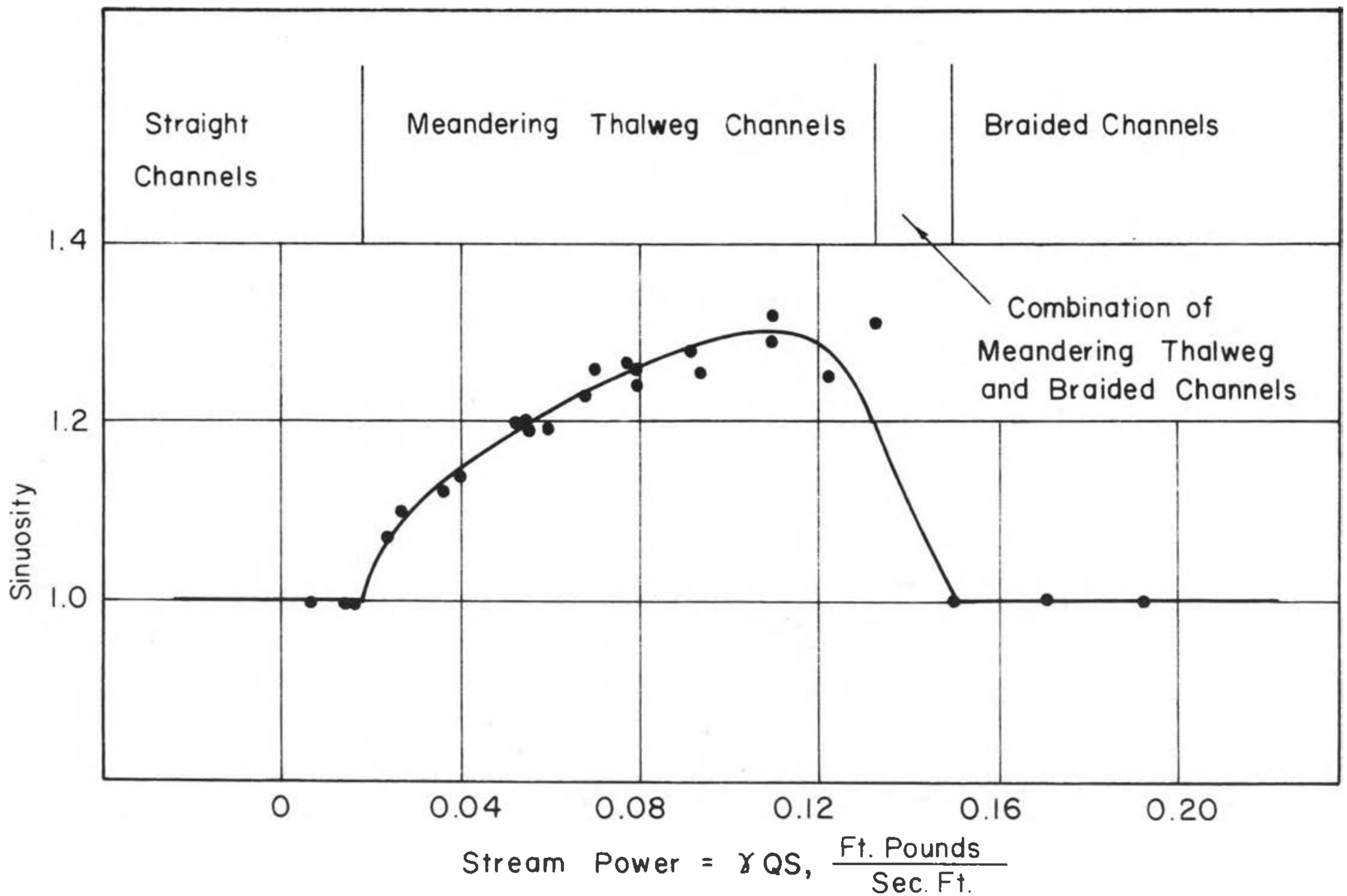

Figure 22. Variation of sinuosity with stream power

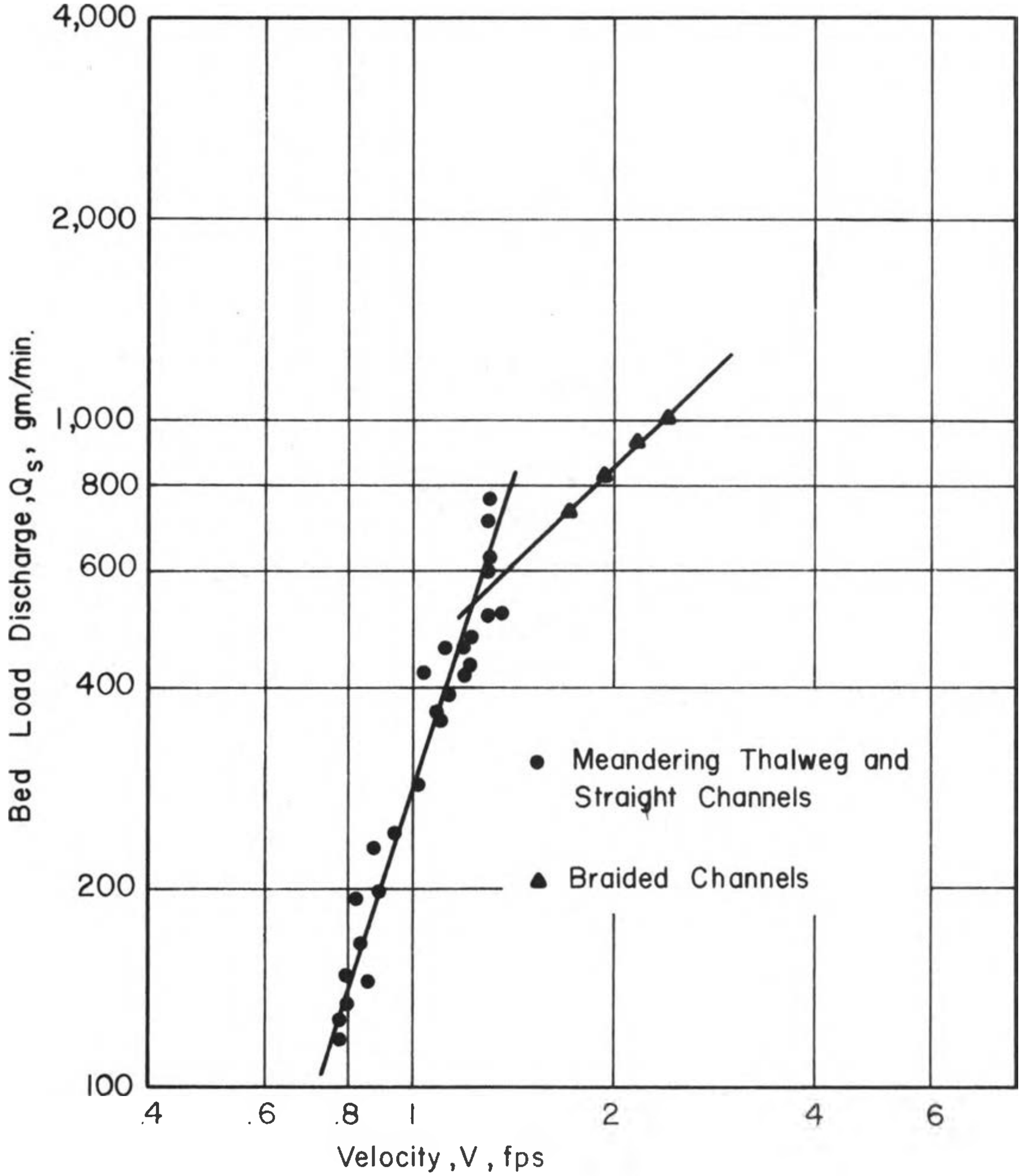

Figure 23. Variation of bedload discharge with mean velocity and channel pattern

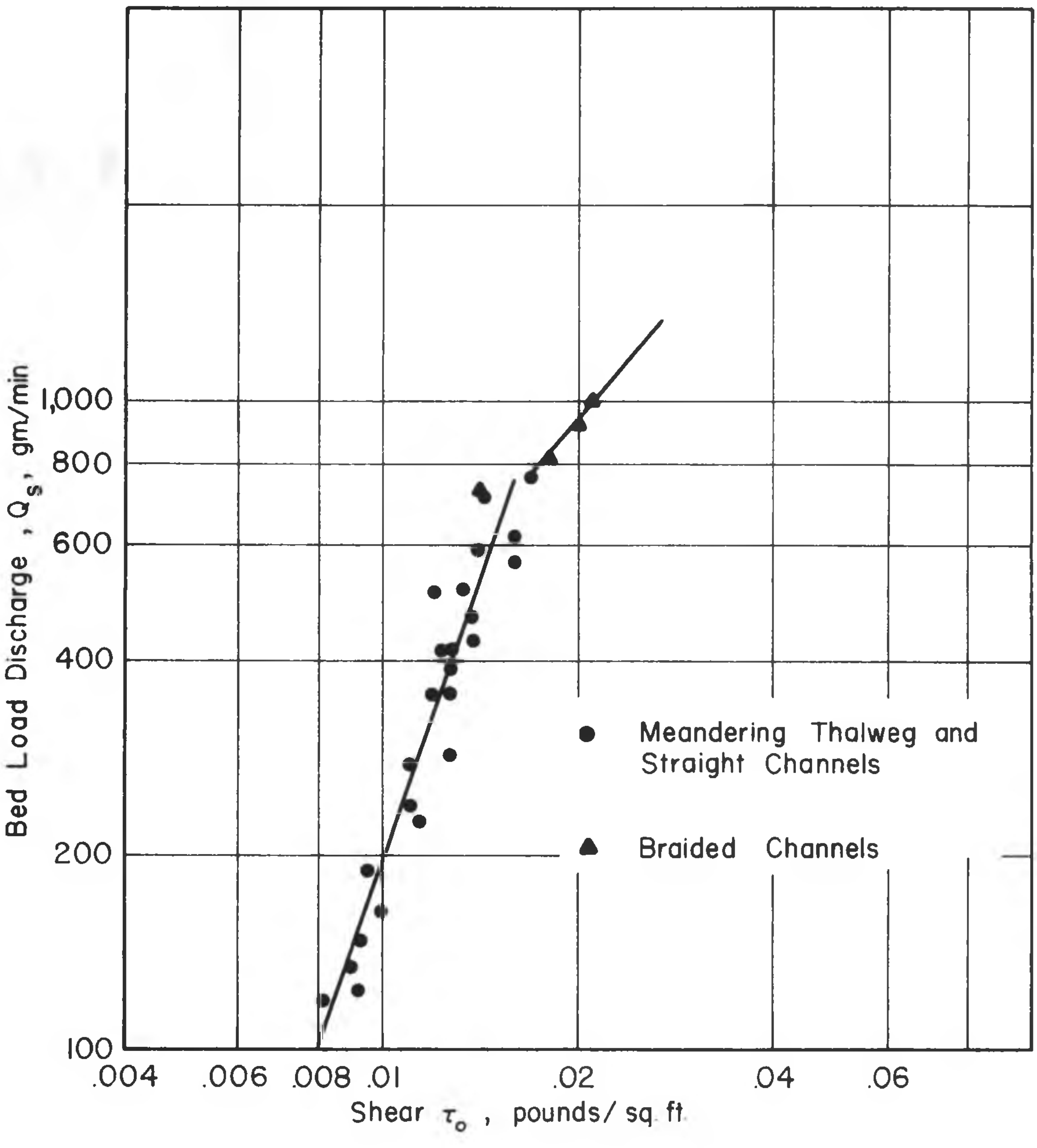

Figure 24. Variation of bedload discharge with shear and channel pattern

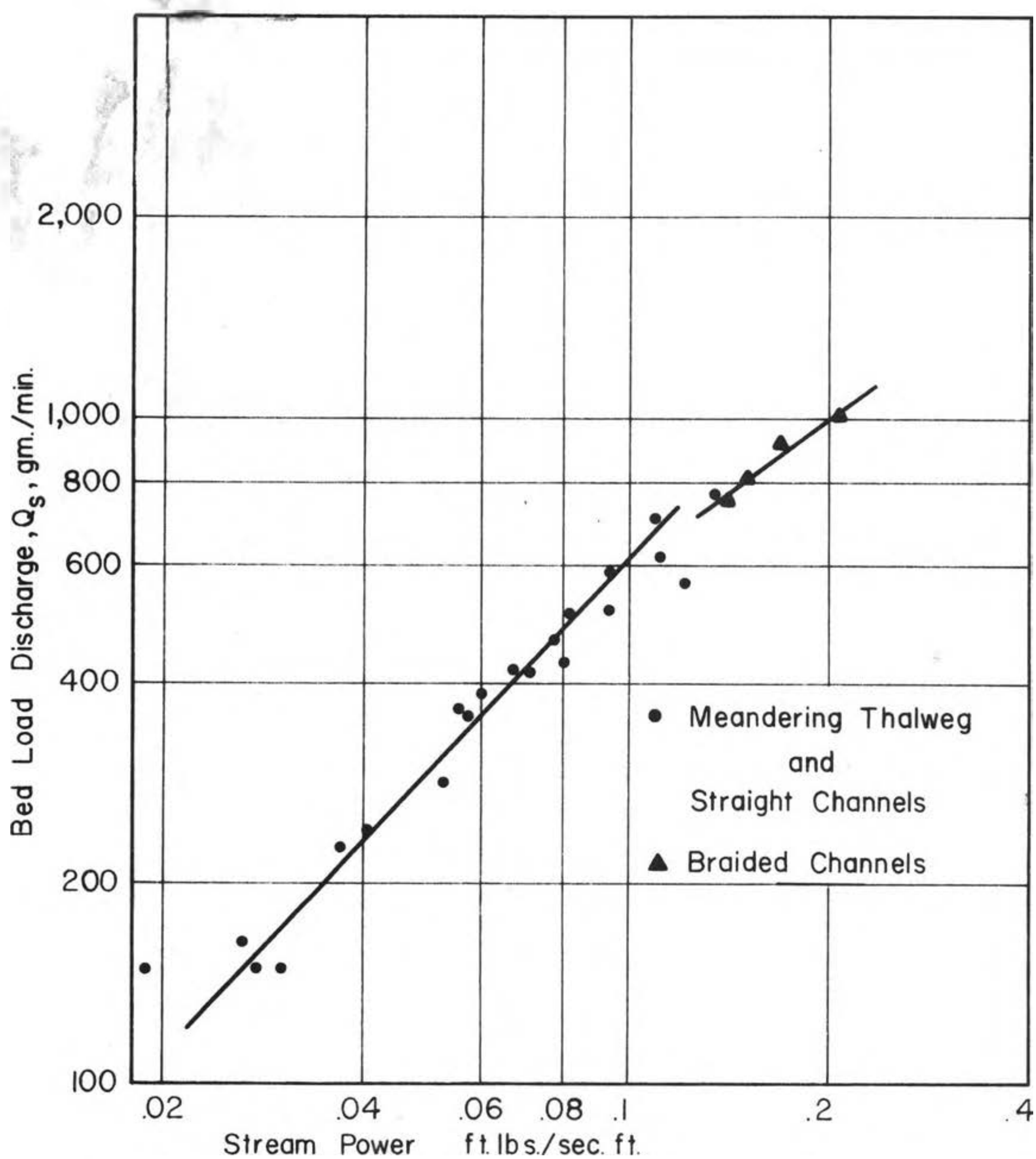

Figure 25. Variation of bedload discharge with stream power and channel pattern

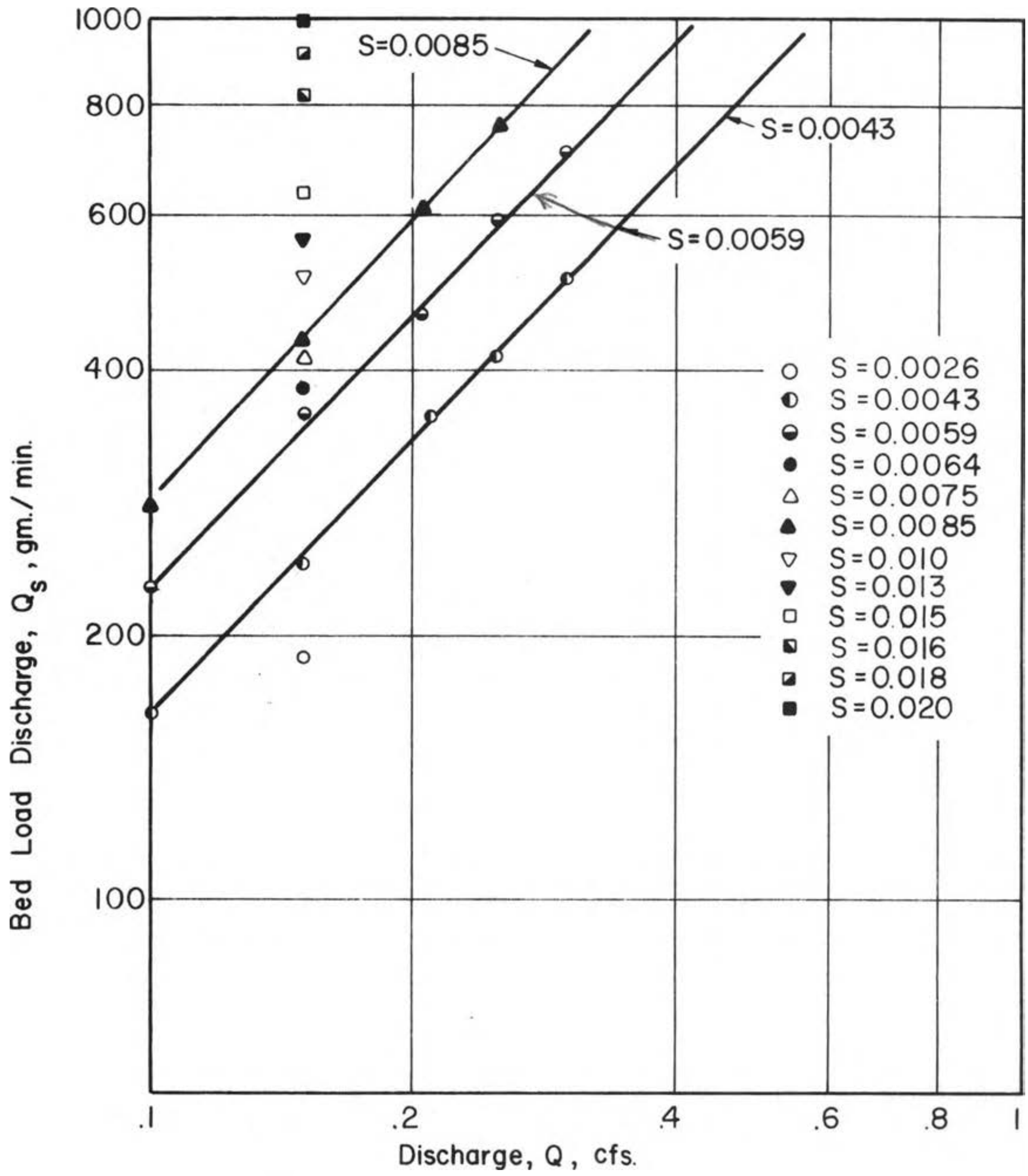

Figure 26. Variation of bedload discharge with discharge and slope

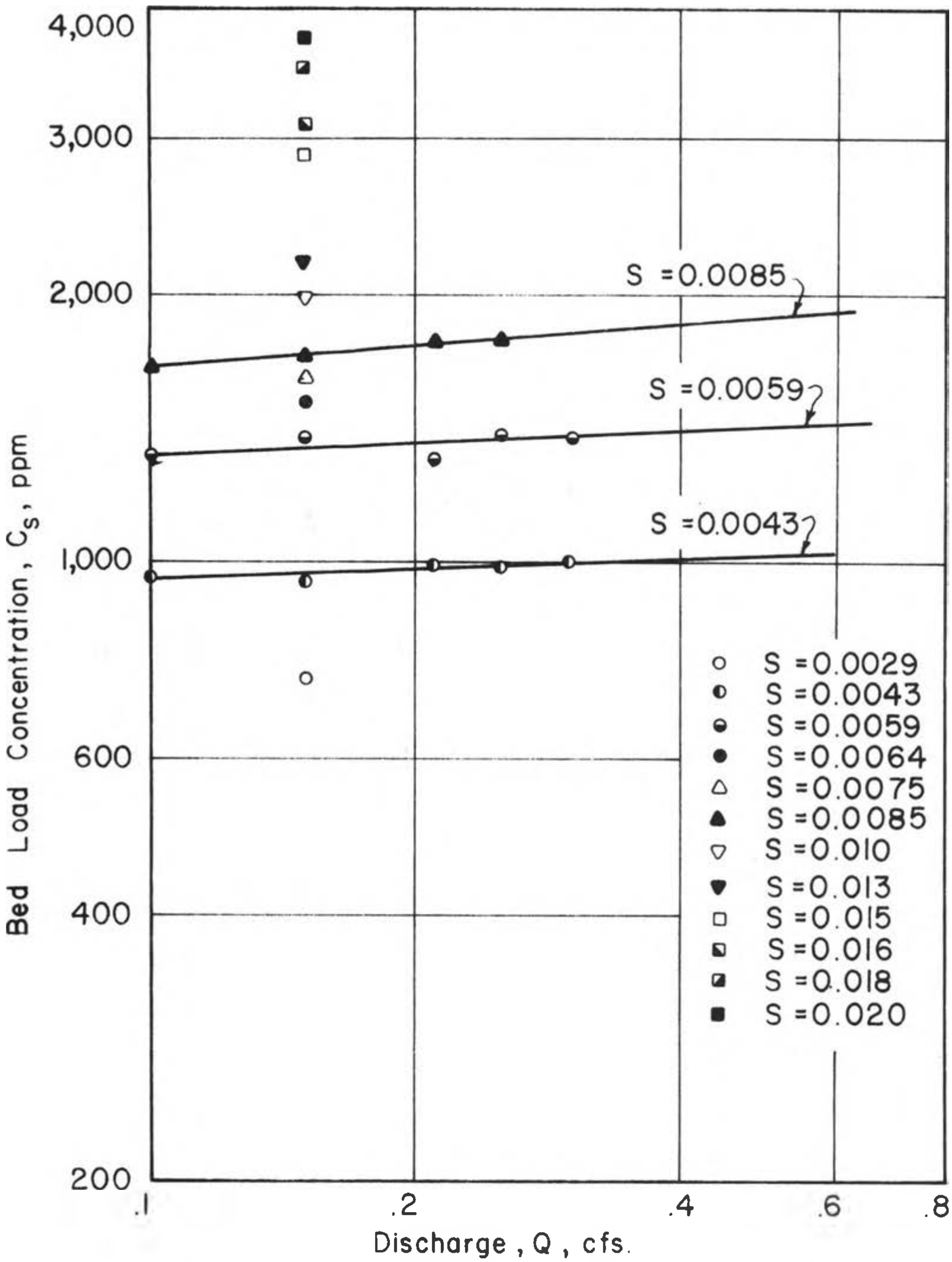

Figure 27. Variation of bedload concentration with discharge and slope

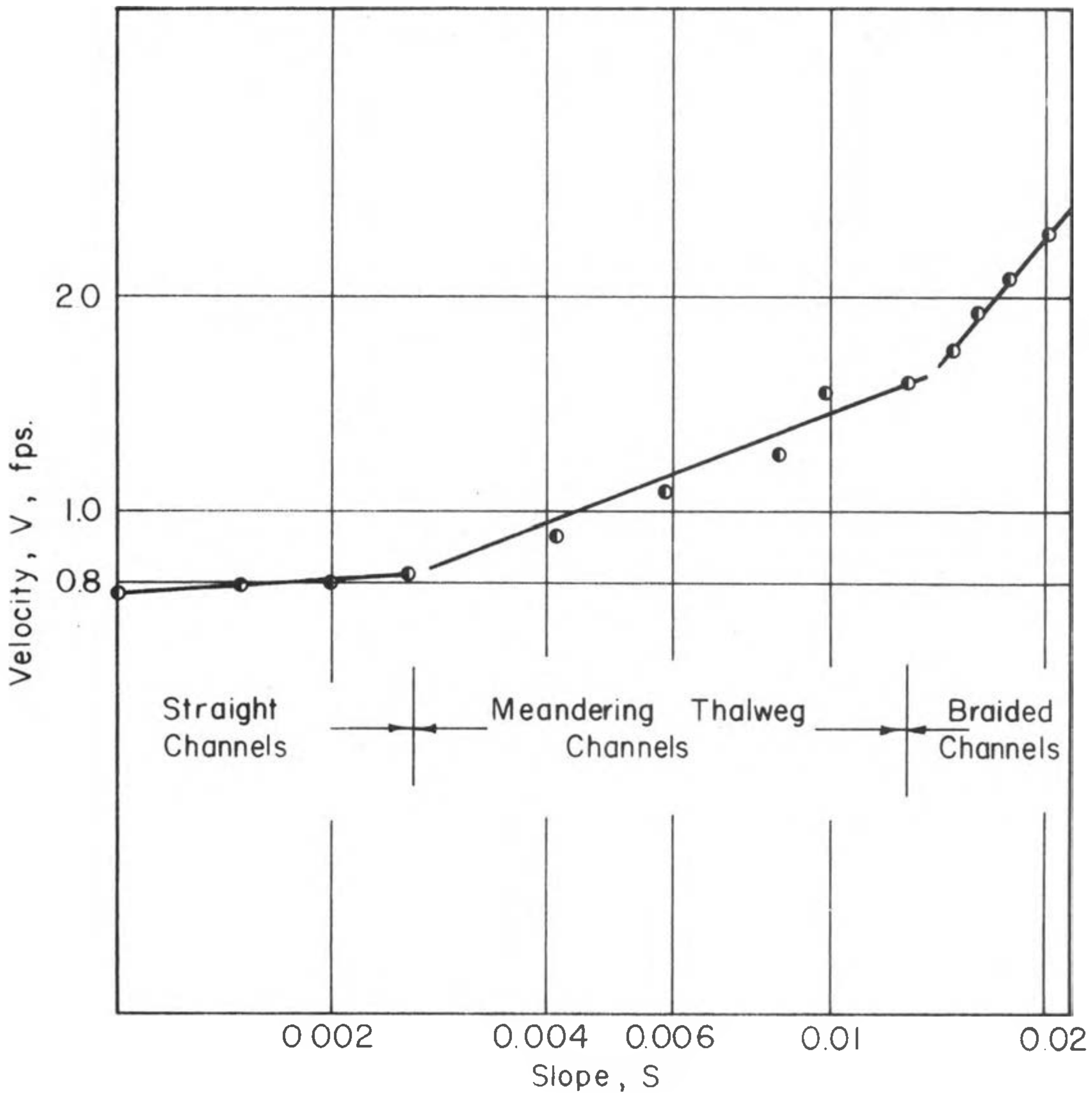

Figure 28. Variation of velocity with slope and channel pattern for a constant discharge of 0.15 cfs

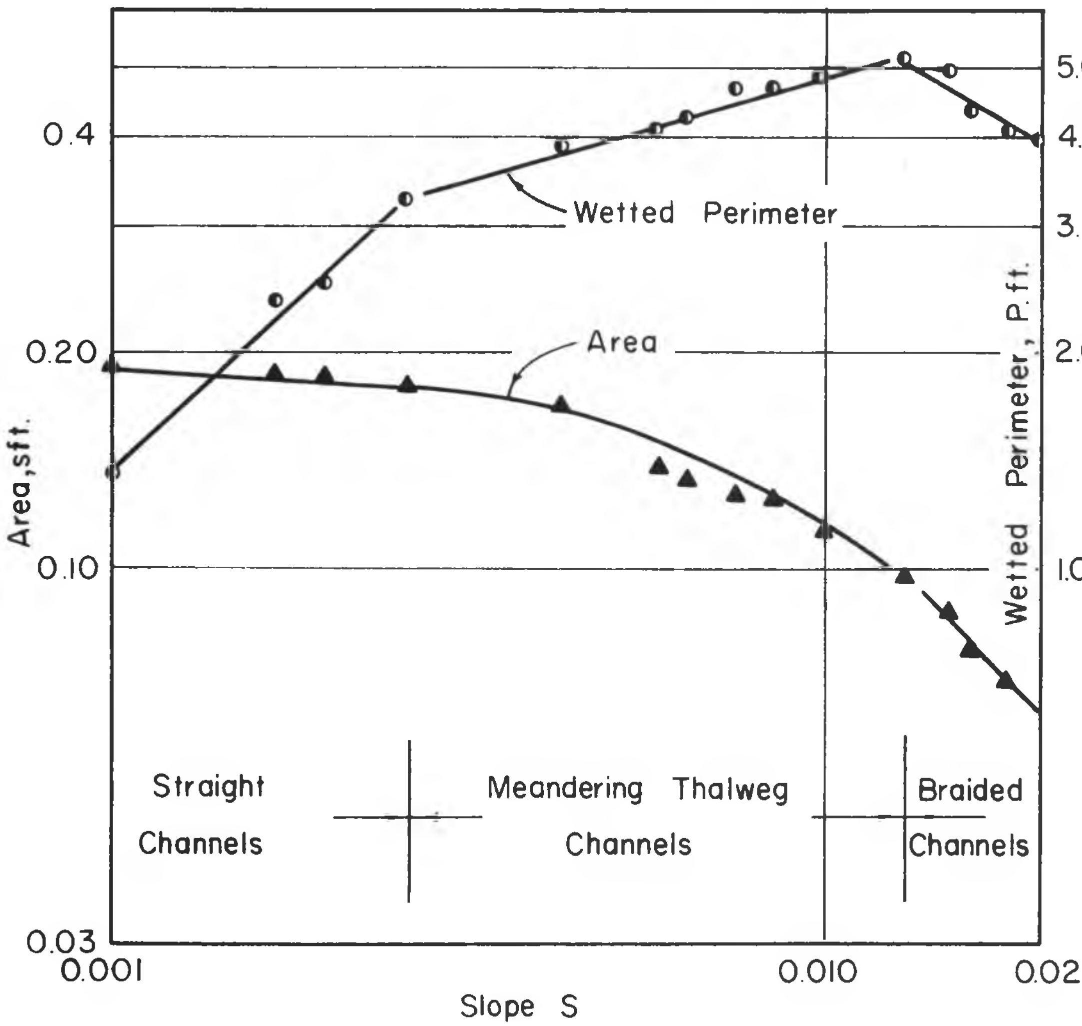

Figure 29(a). Variation of area and wetted perimeter with slope and channel pattern for a constant discharge of 0.15 cfs

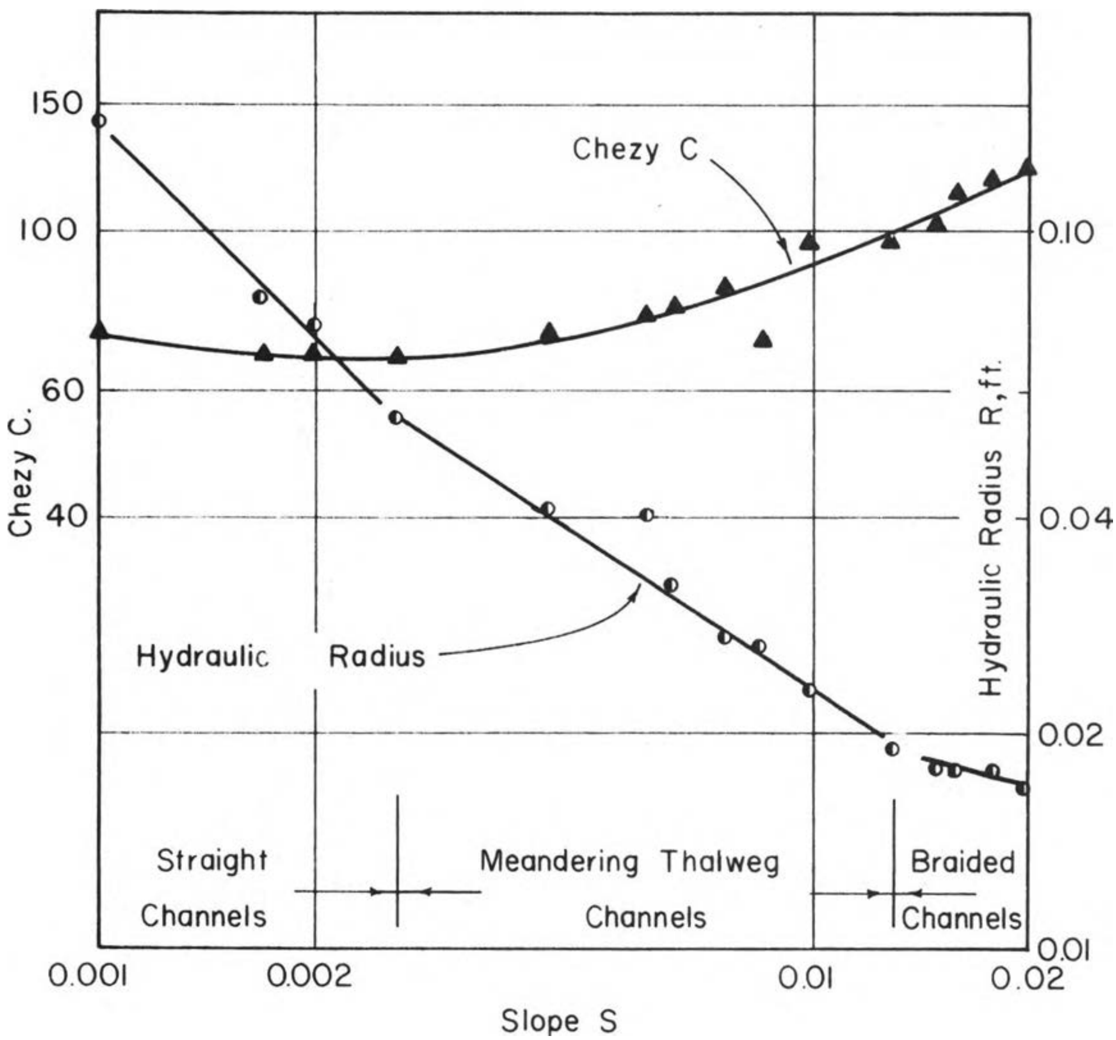

Figure 29(b). Variation of hydraulic radius, and Chezy C with slope and channel pattern for a constant discharge of 0.15 cfs

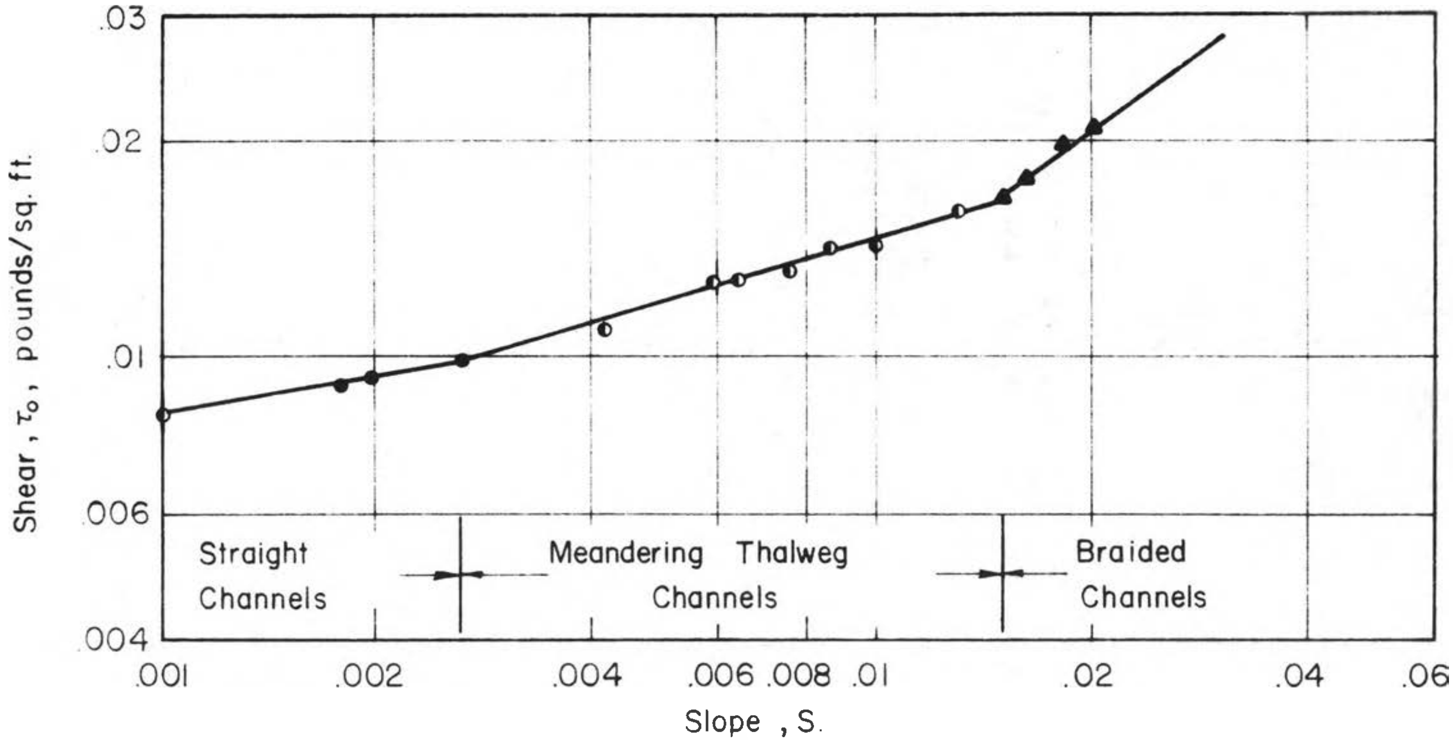

Figure 30. Variation of shear with slope and channel pattern for a constant discharge of 0.15 cfs

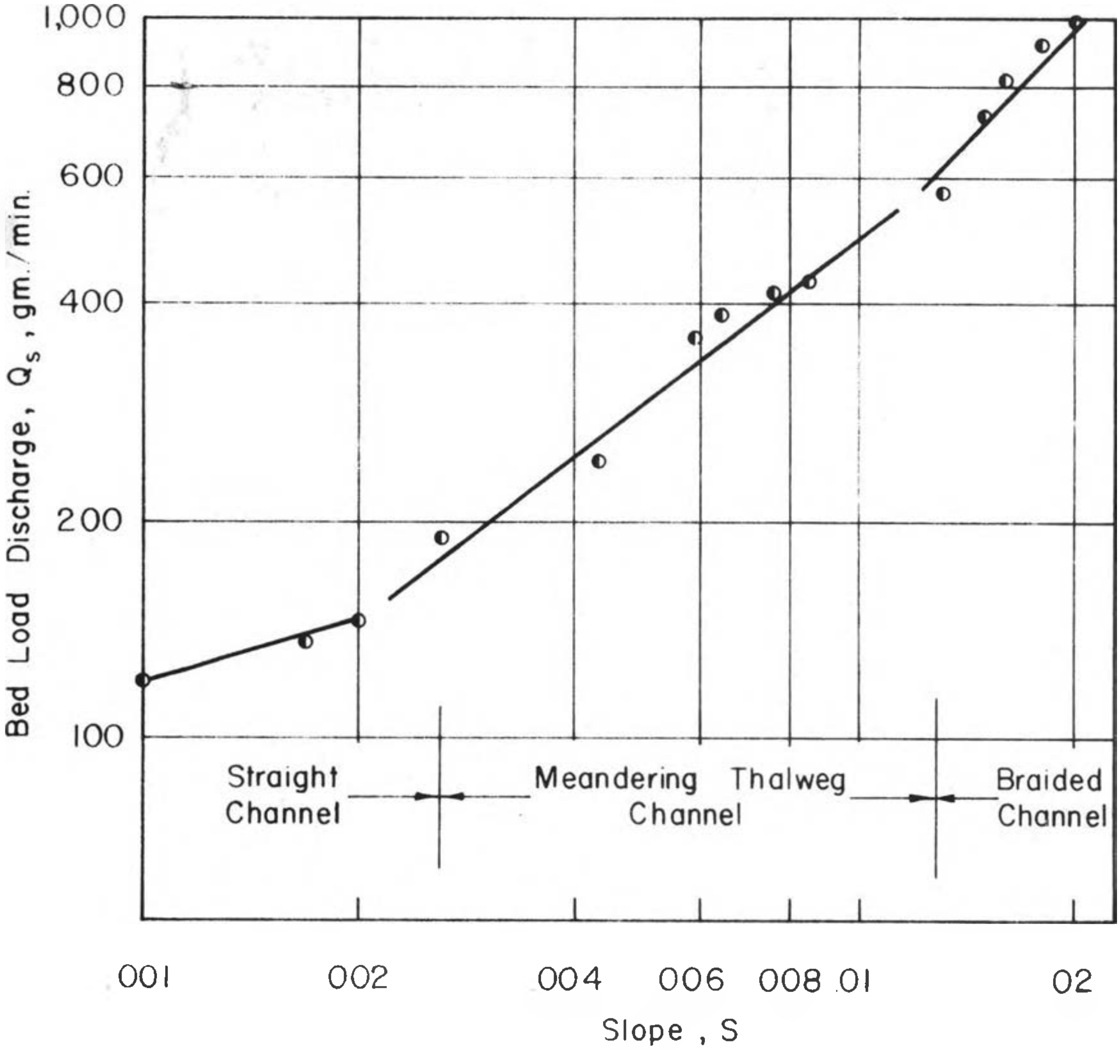

Figure 31. Variation of bedload discharge with slope and channel pattern for a constant discharge of 0.15 cfs

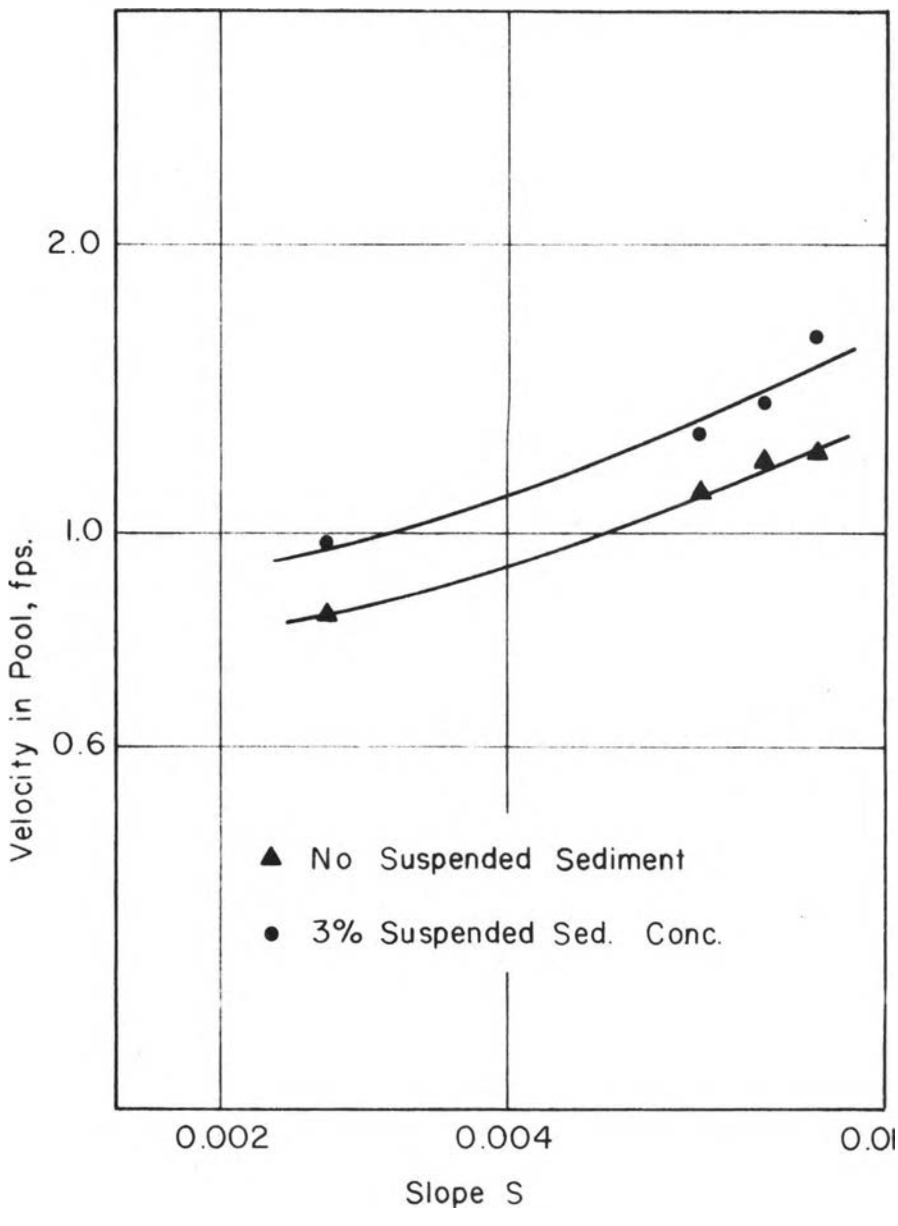

Figure 32. Effect of suspended sediment concentration on mean velocity

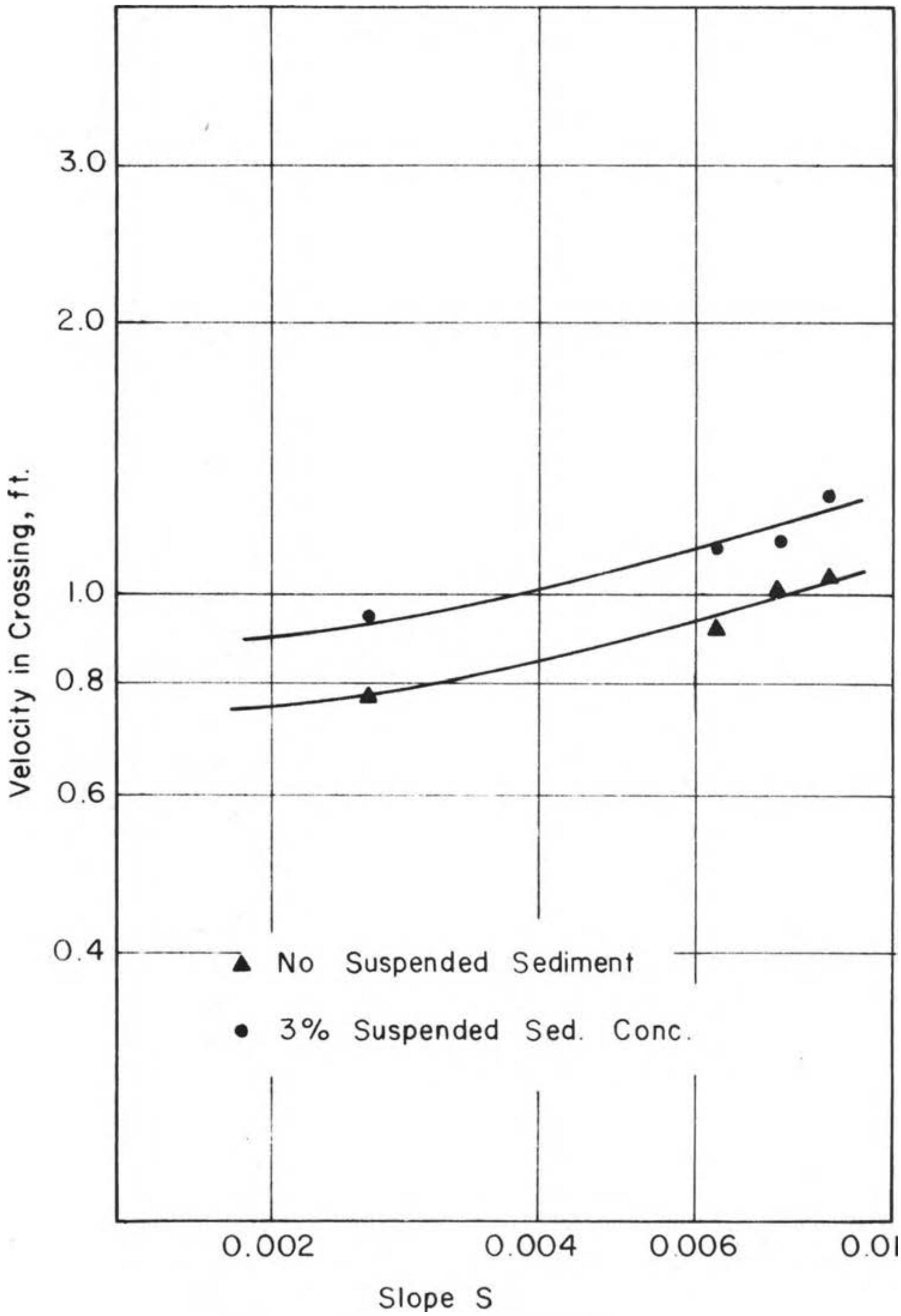

Figure 33. Effect of suspended sediment concentration on mean velocity

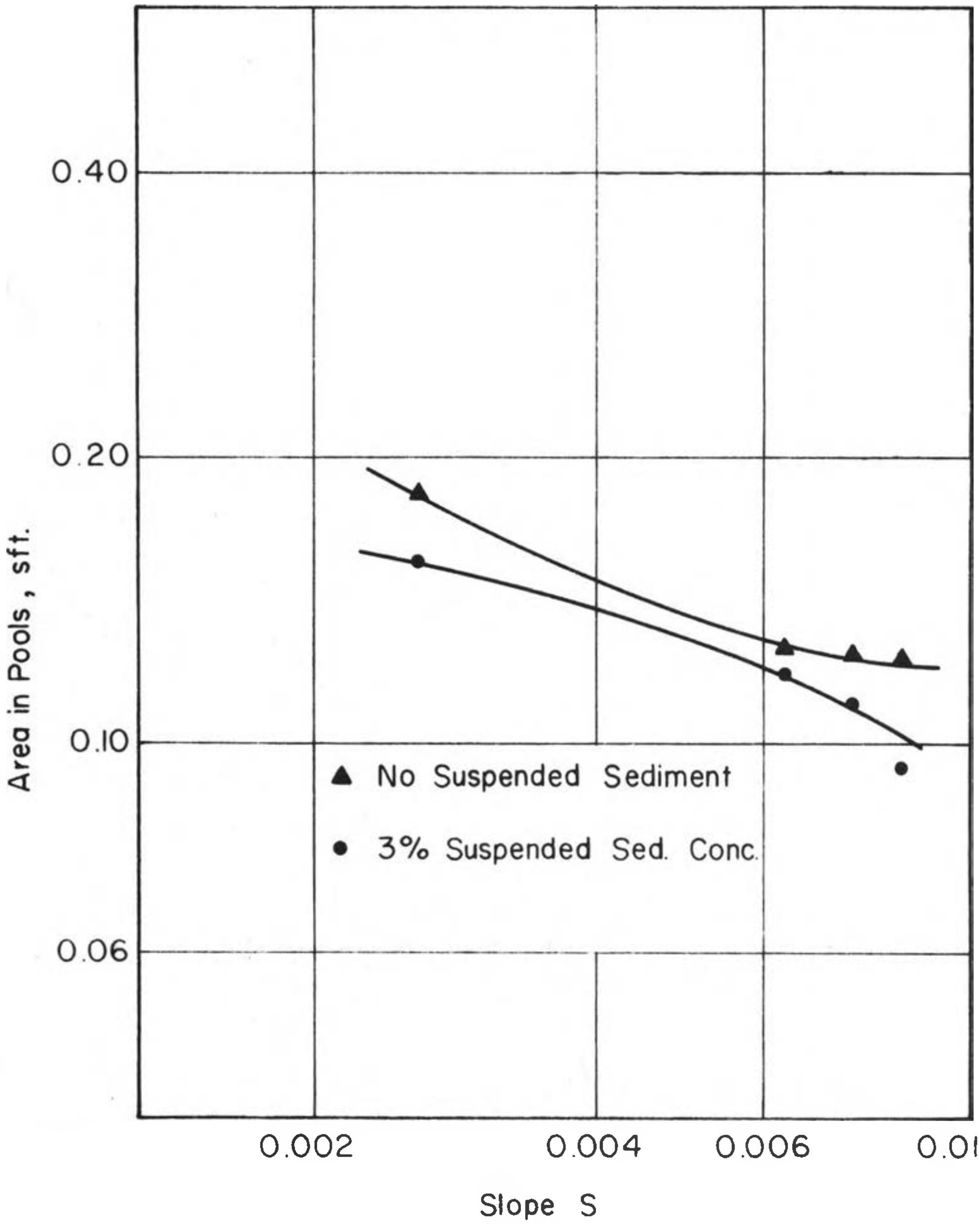

Figure 34. Effect of suspended sediment concentration on cross sectional area

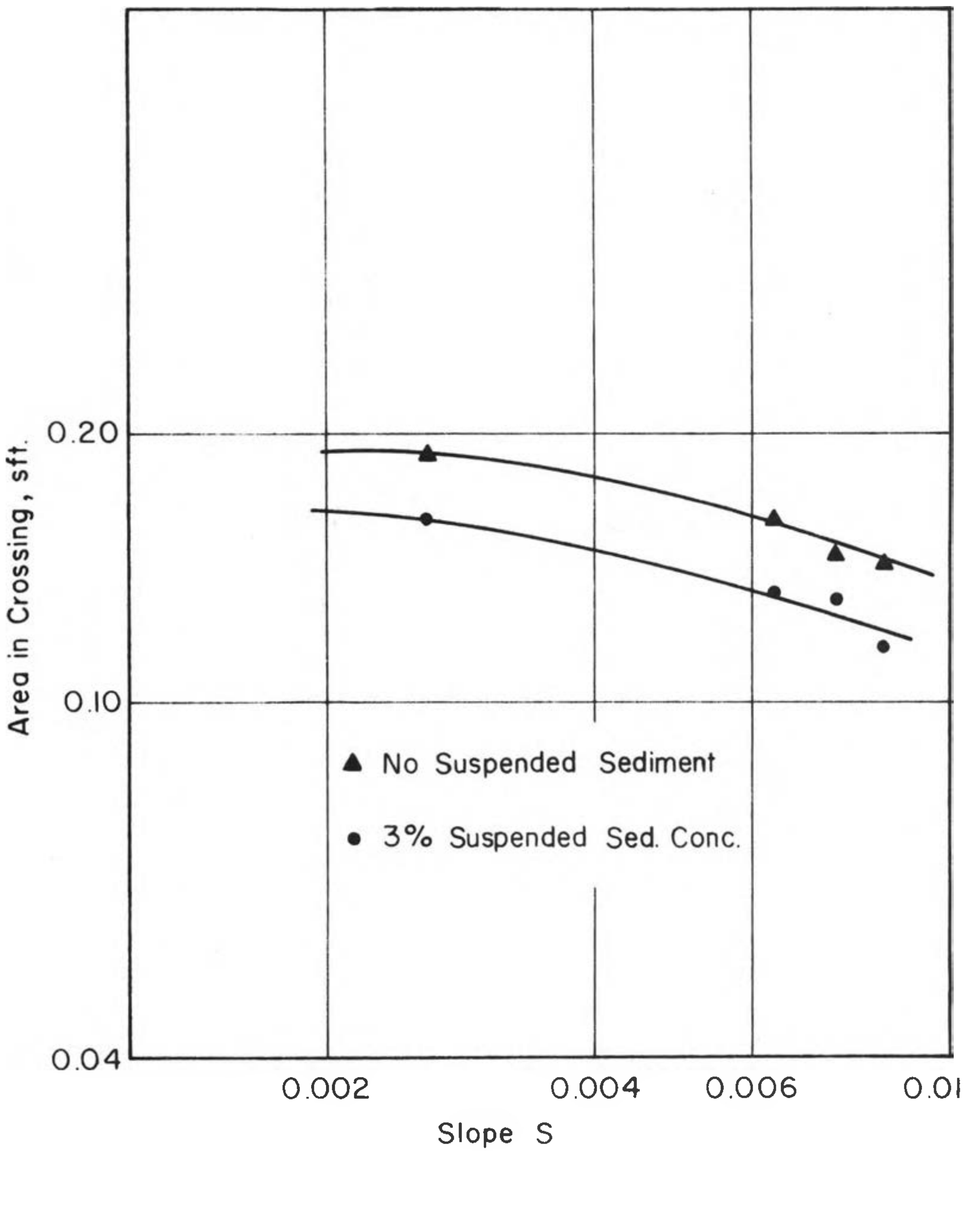

Figure 35. Effect of suspended sediment concentration on cross sectional area

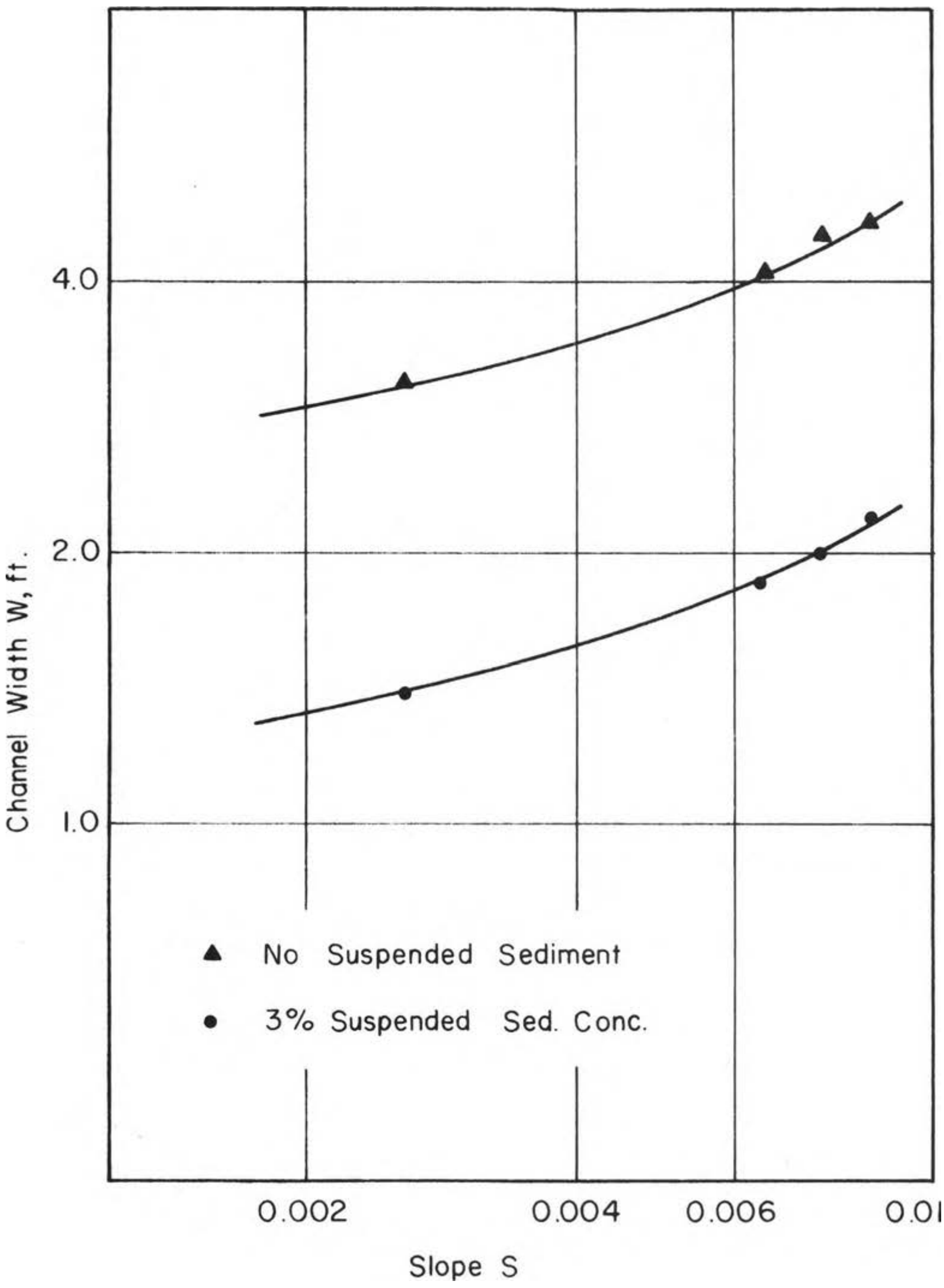

Figure 36. Effect of suspended sediment concentration on channel width

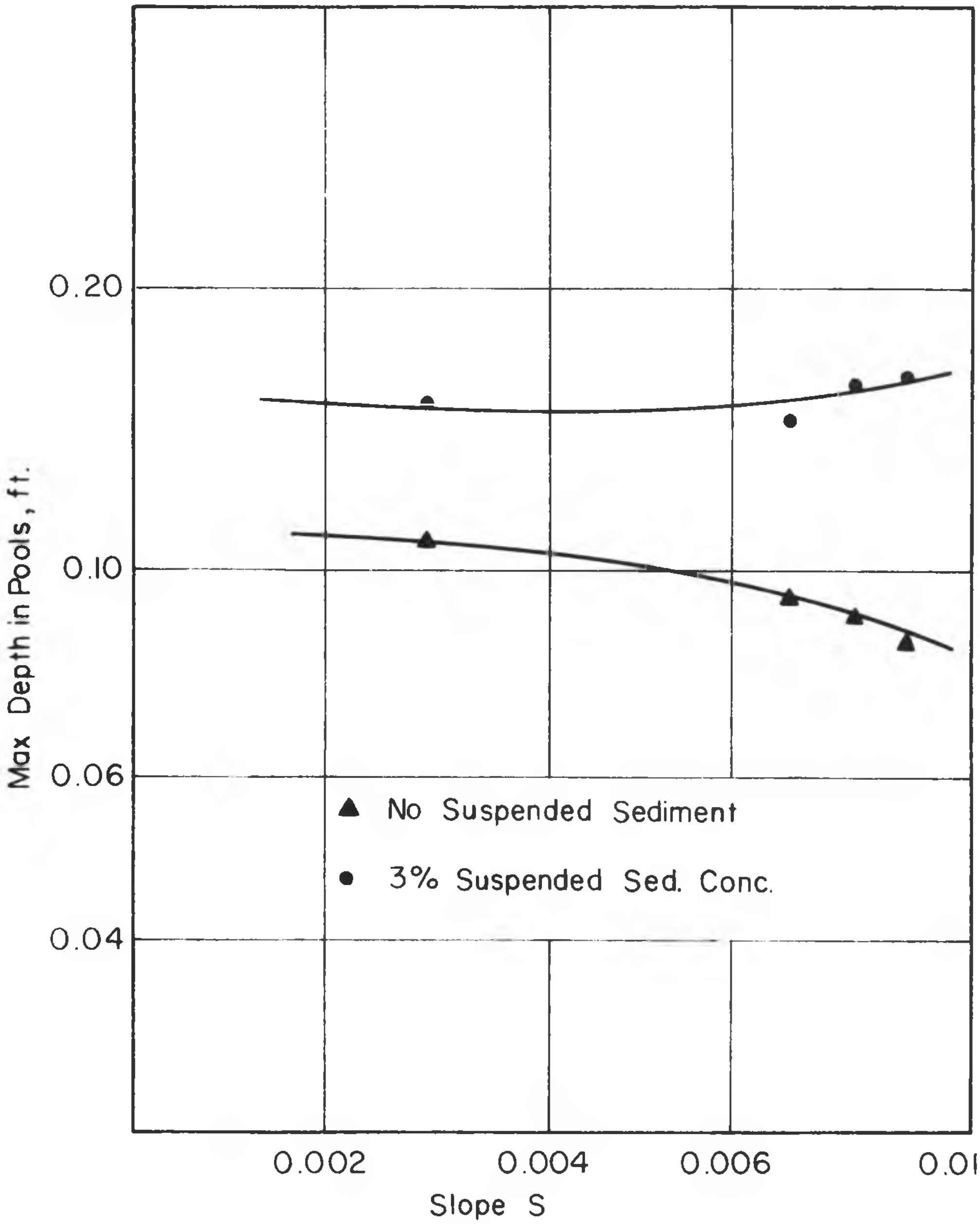

Figure 37. Effect of suspended sediment concentration on maximum depths in pools

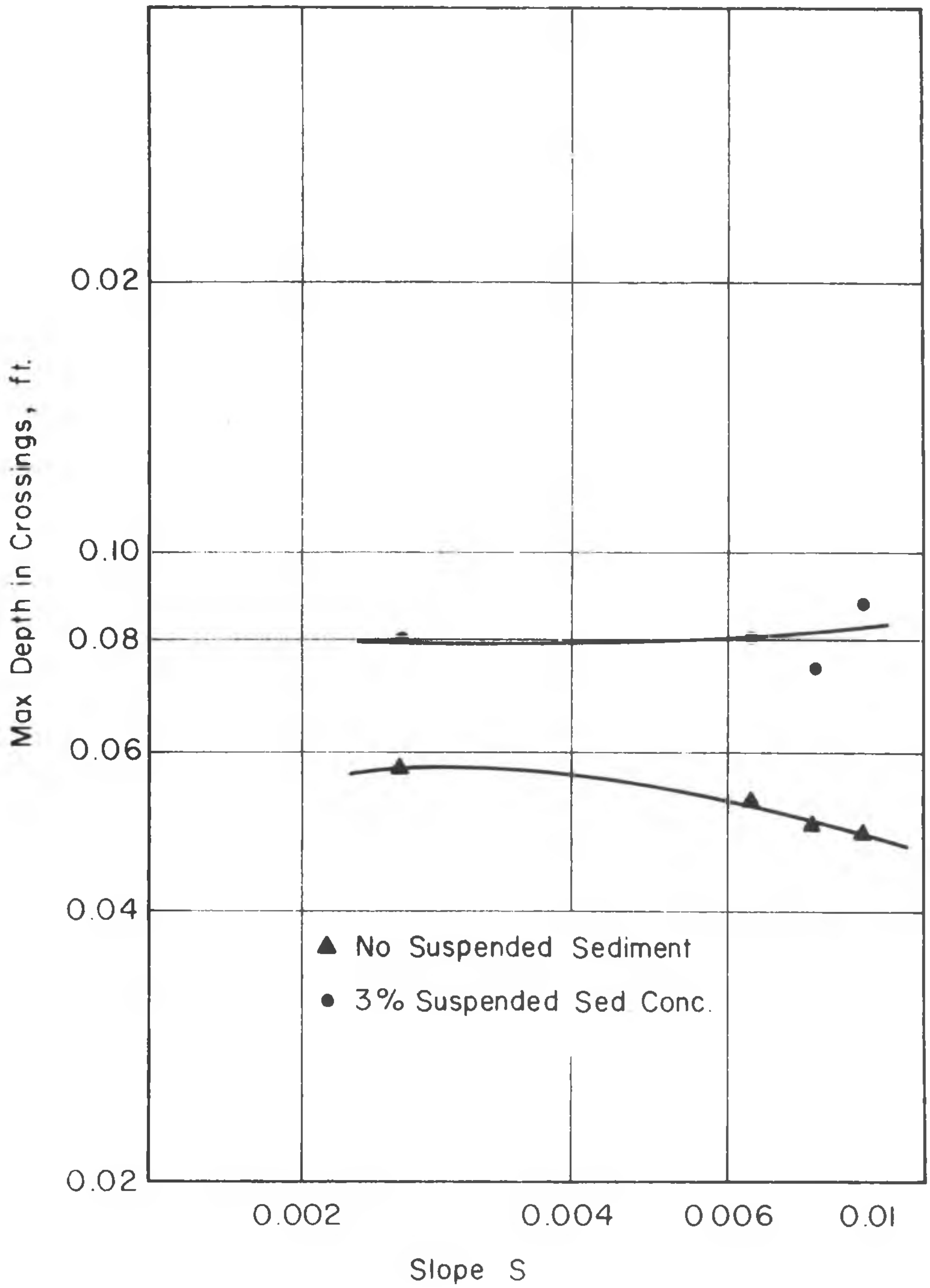

Figure 38. Effect of suspended sediment concentration on maximum depths in crossings

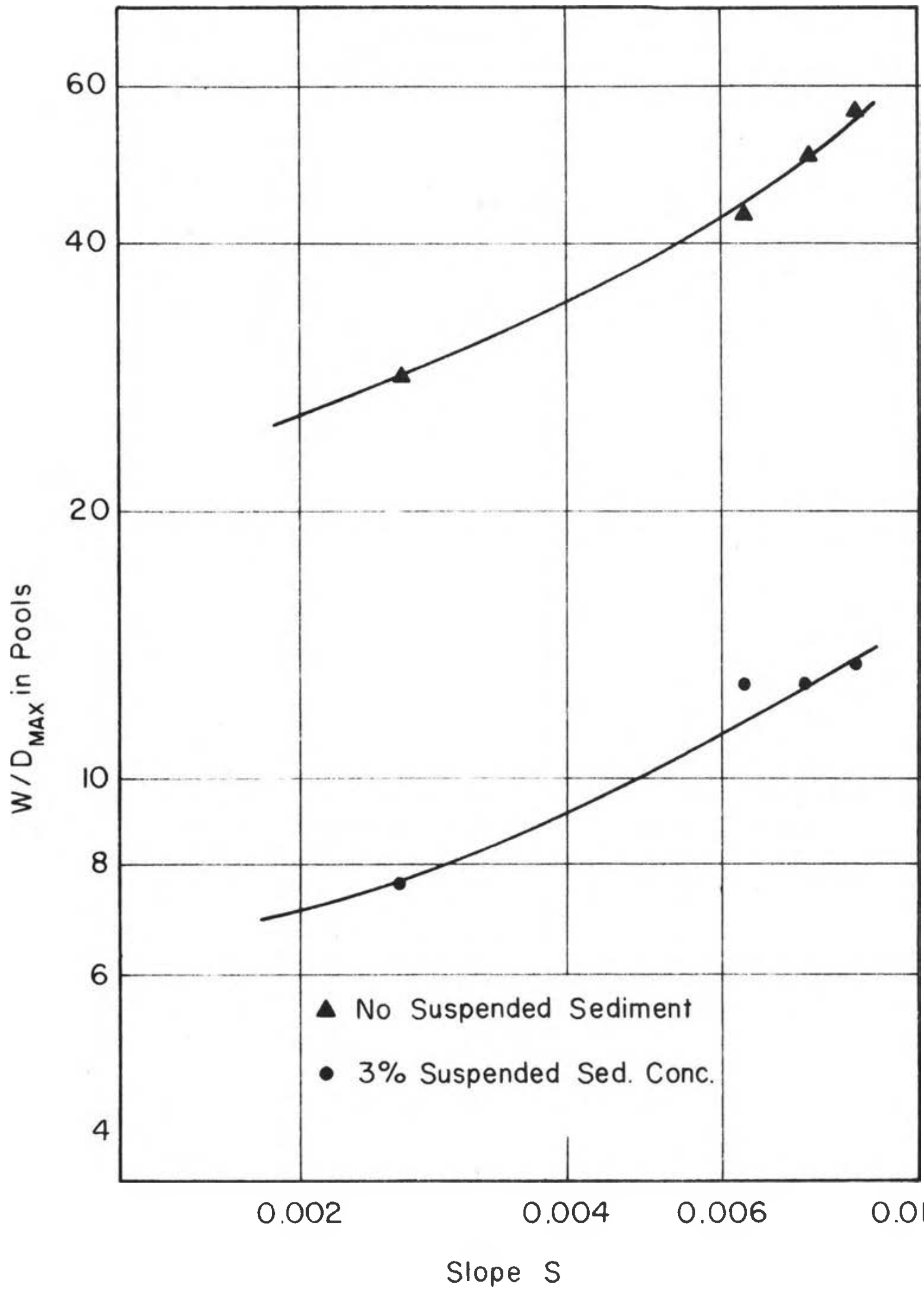

Figure 39. Effect of suspended sediment concentration on $\frac{W}{D_{max}}$ in pools

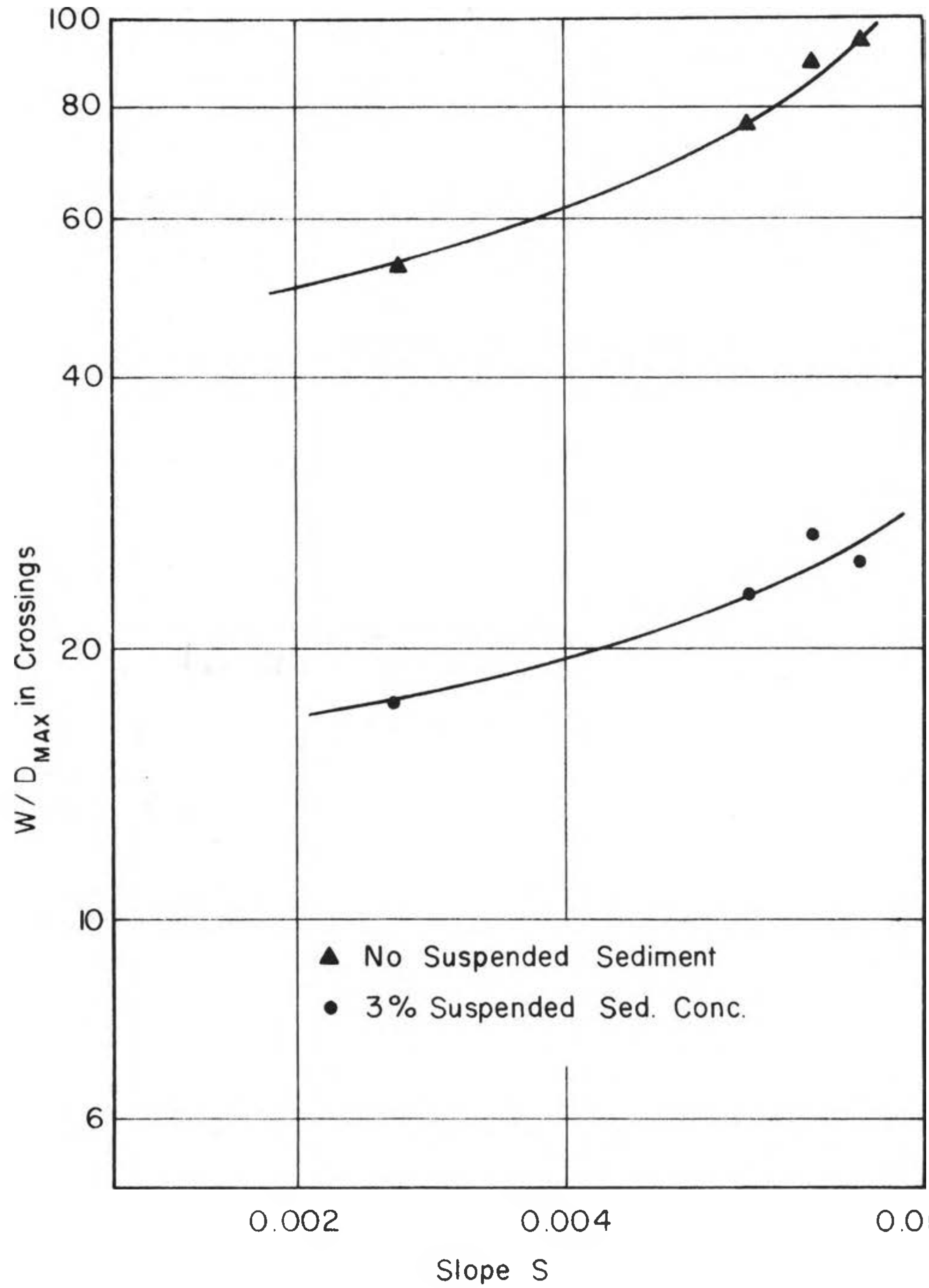

Figure 40. Effect of suspended sediment concentration on $\frac{W}{D_{max}}$ in crossings

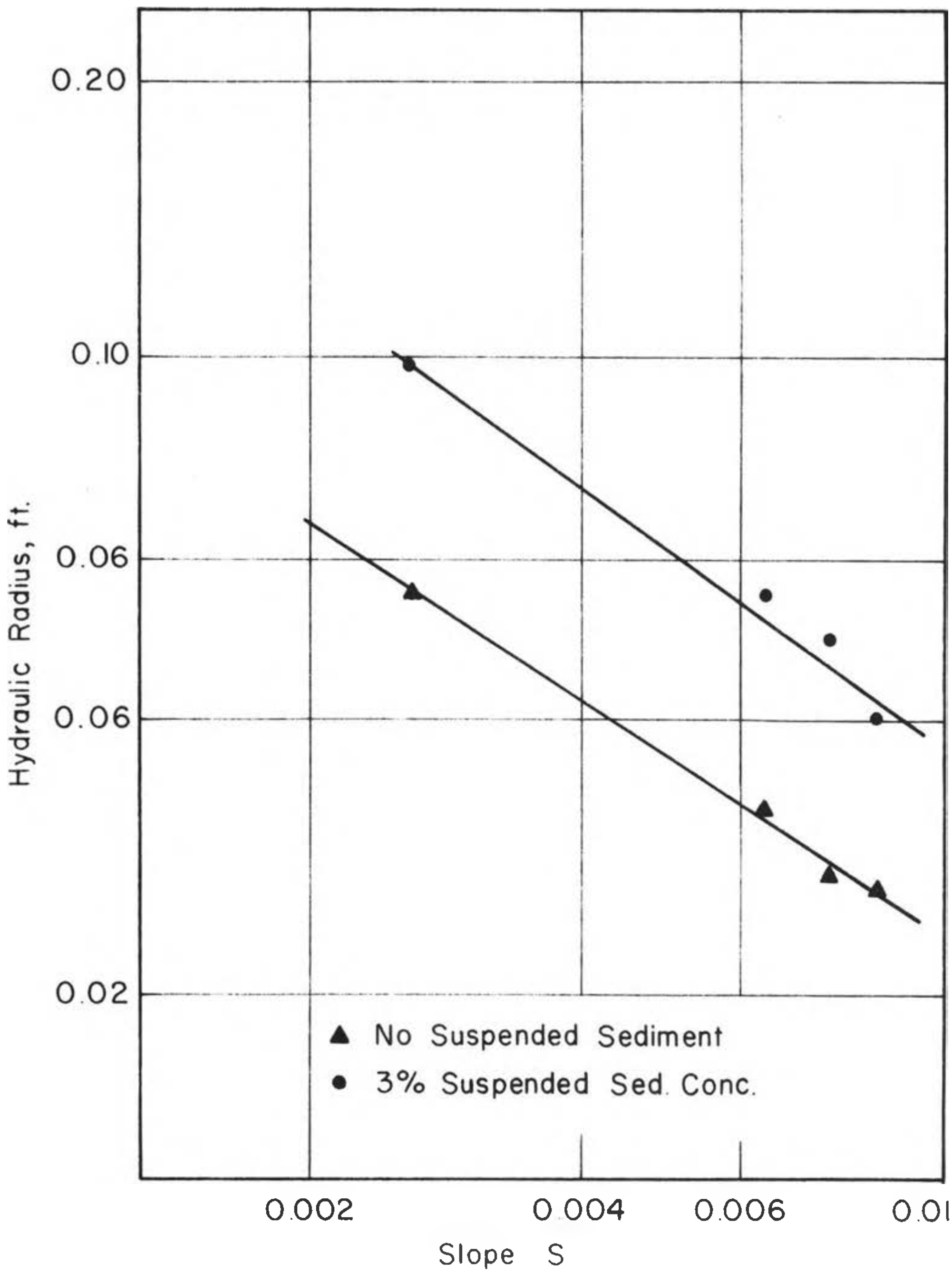

Figure 41. Effect of suspended sediment concentration on hydraulic radius

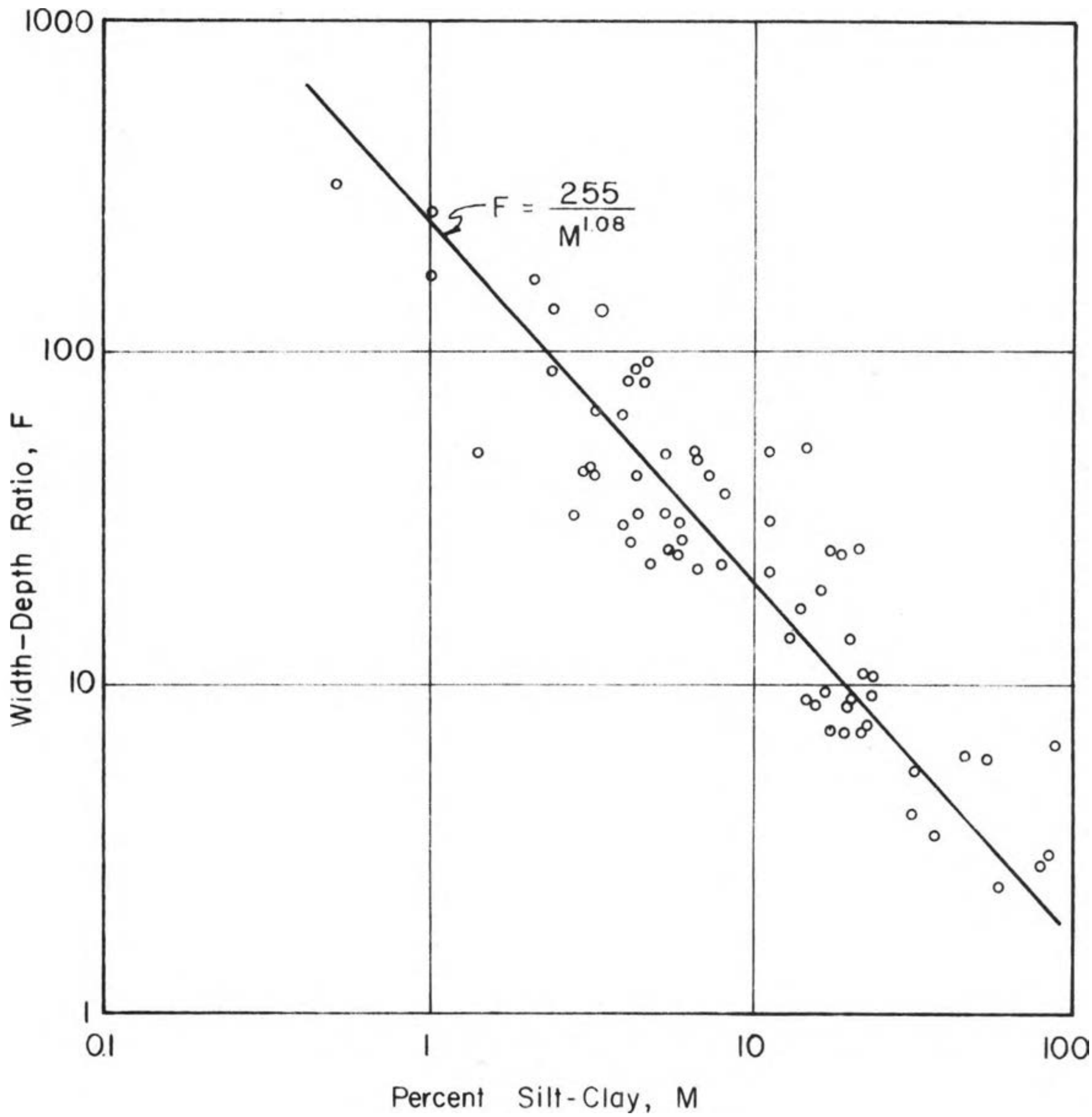

Figure 42. Relation of width-depth ratio to weighted mean percent silt-clay (after Schumm, 1960)

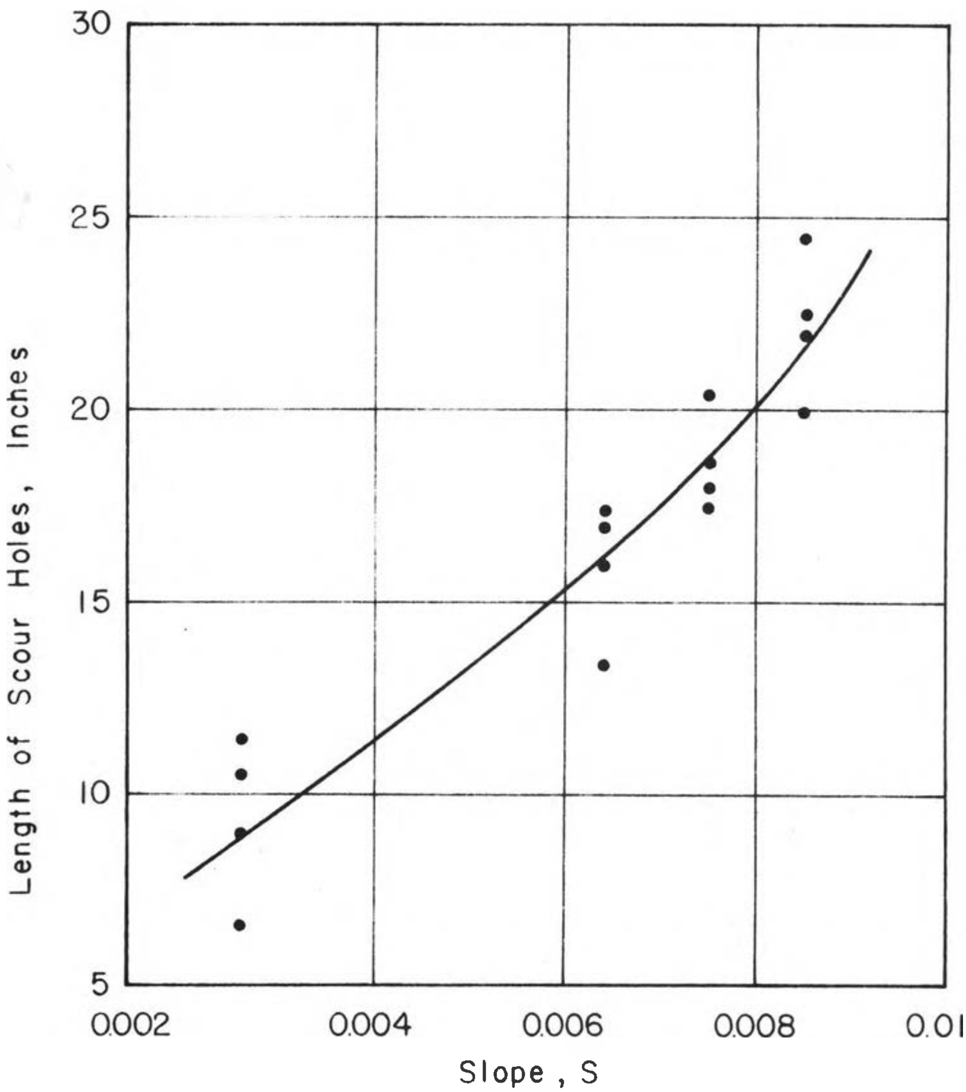

Figure 43. Length of scour holes in bends of meandering channels

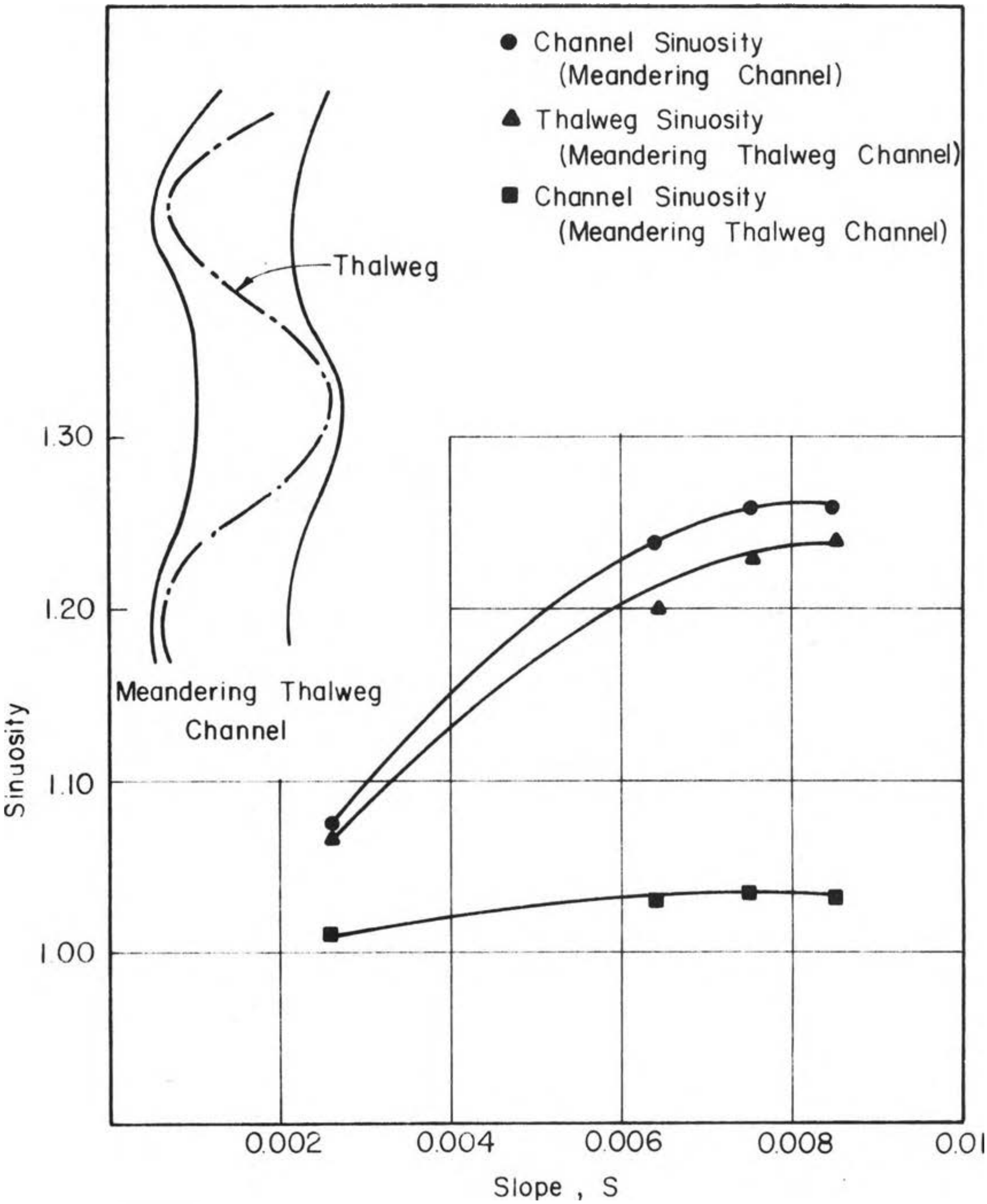

Figure 44. Sinuosity versus slope

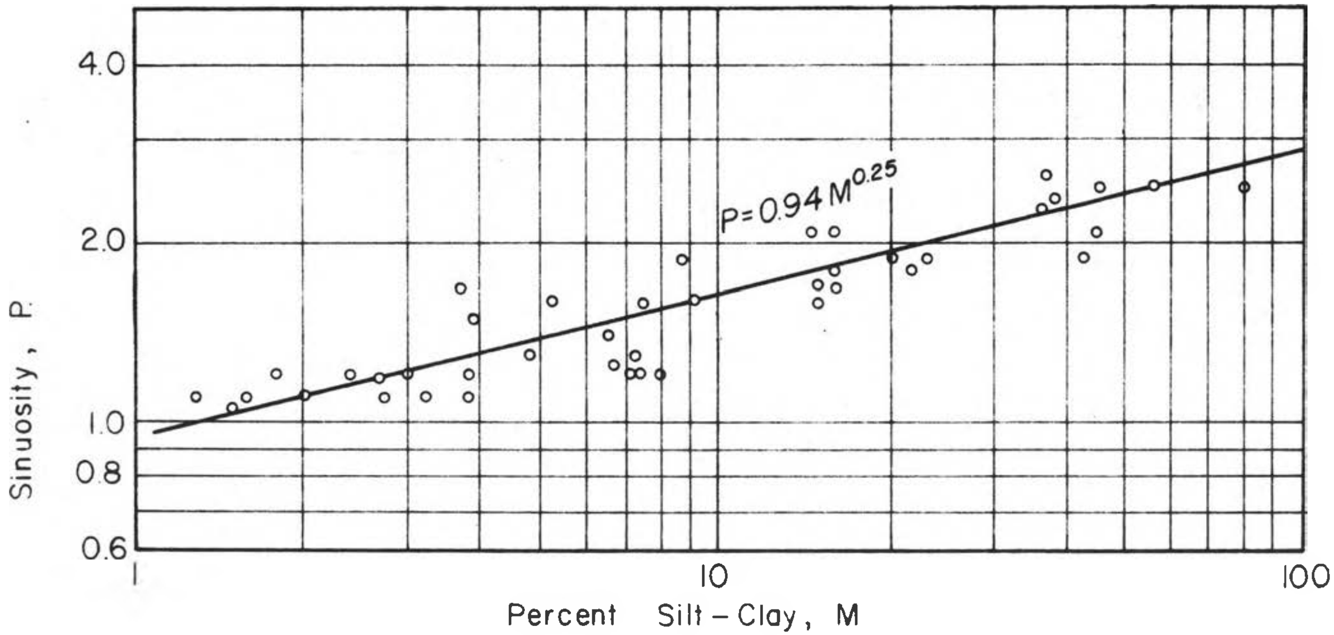

Figure 45. Relation of sinuosity to silt-clay in perimeter of channel (after Schumm, 1963b)

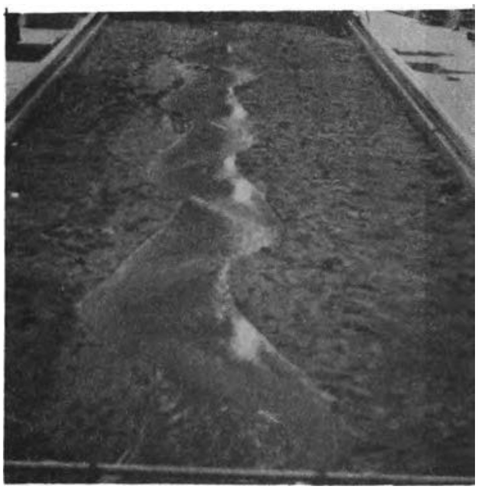

(a) meandering thalweg channel with very little or no suspended sediment

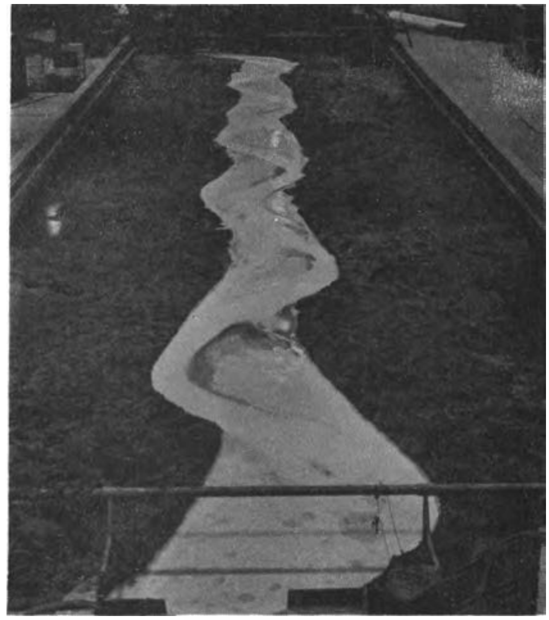

(b) meandering channel with 3% concentration of suspended sediment

(c) close view of a bend

(d) thalweg and scour holes in bends of meandering channels

Figure 46. Effect of high concentration of suspended sediment on channel morphology

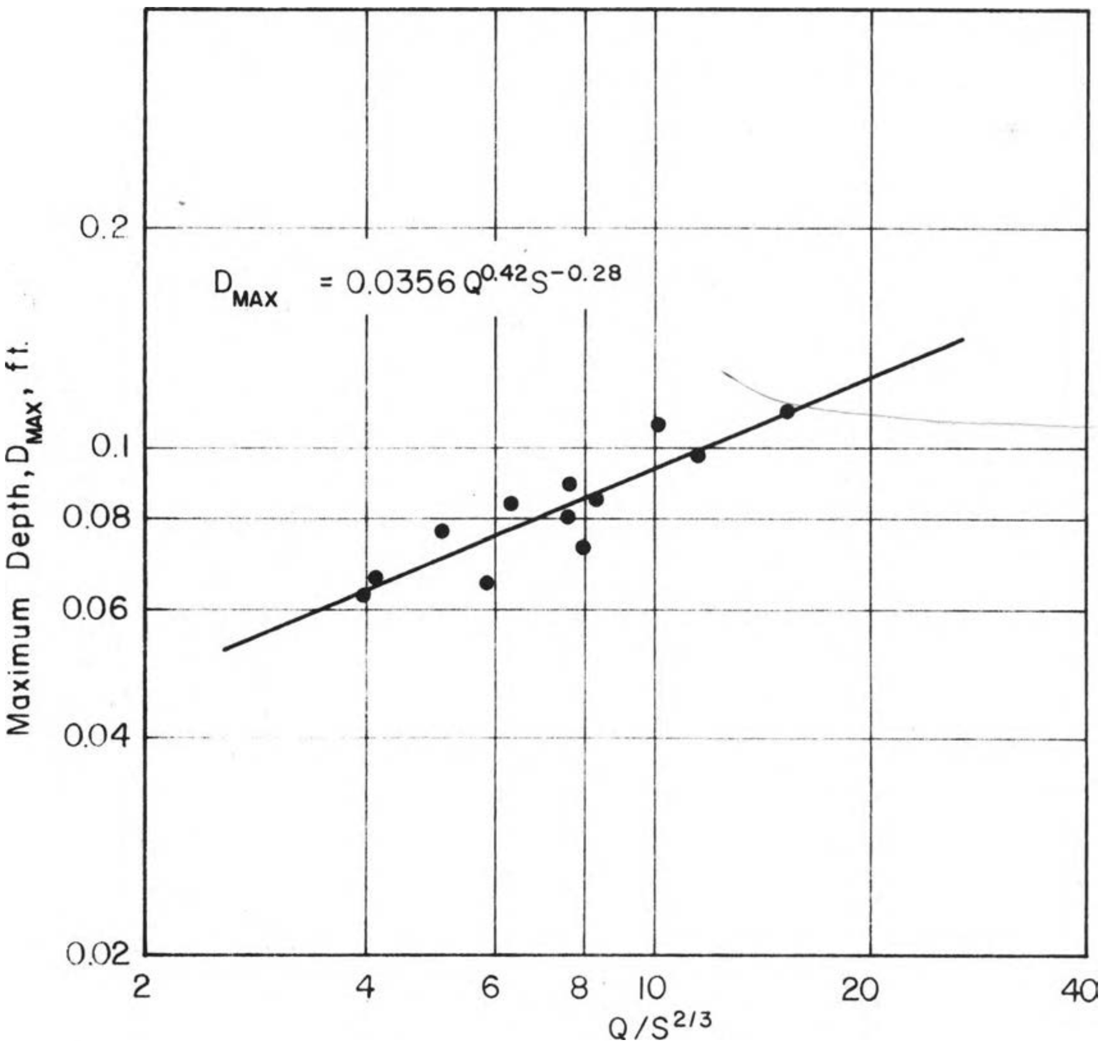

Figure 47. Maximum depths versus $Q/S^{2/3}$ in straight channels

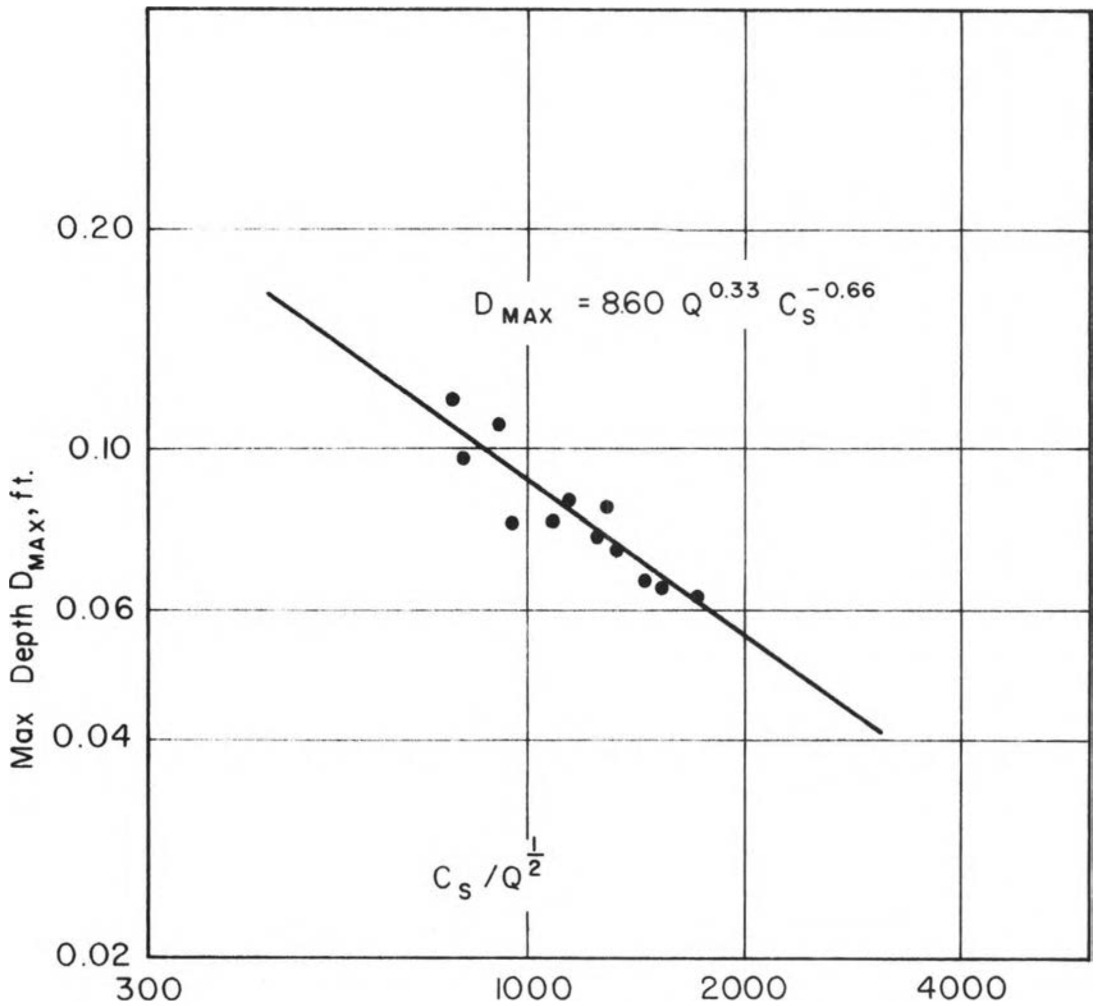

Figure 48. Relationship among maximum depth, discharge, and bedload concentration in straight channels

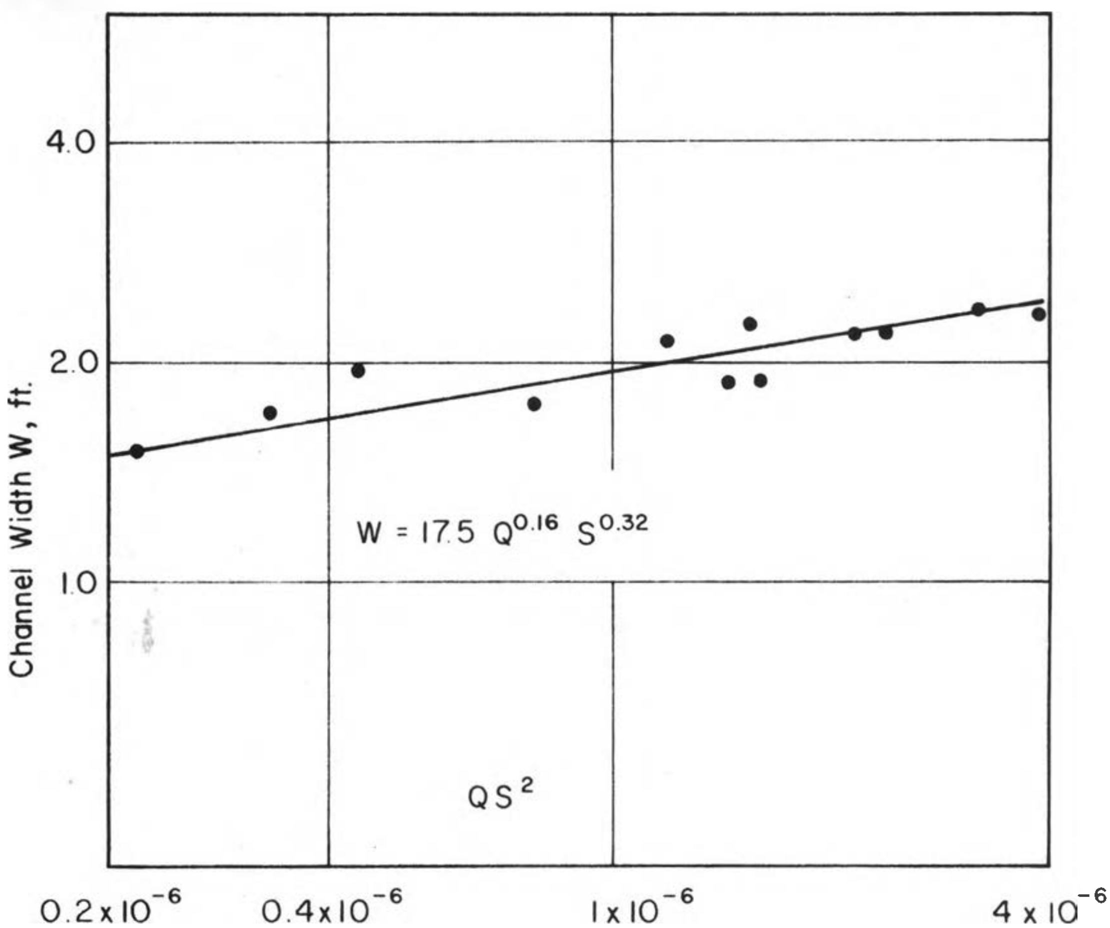

Figure 49. Relationship among channel width, discharge, and slope in straight channels

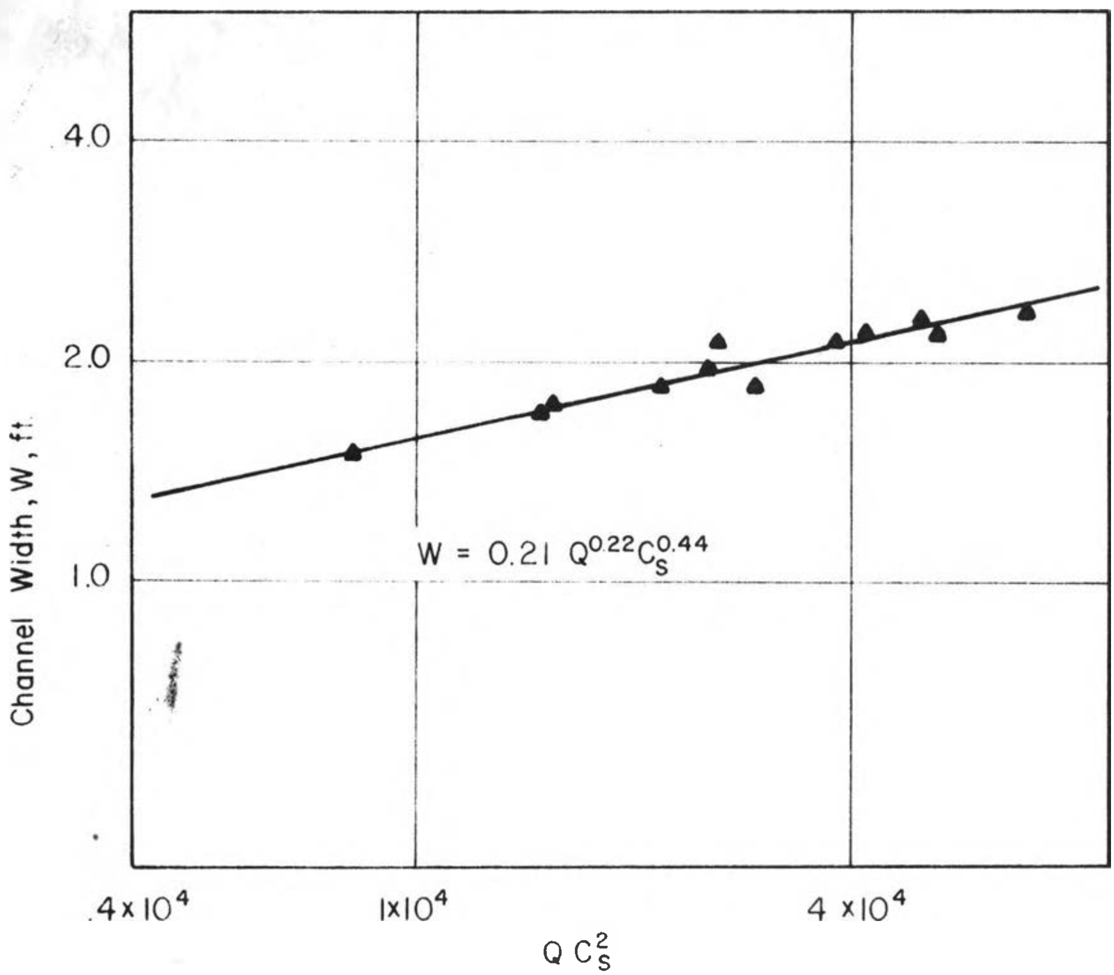

Figure 50. Relationship among channel width, discharge, and bedload concentration in straight channels

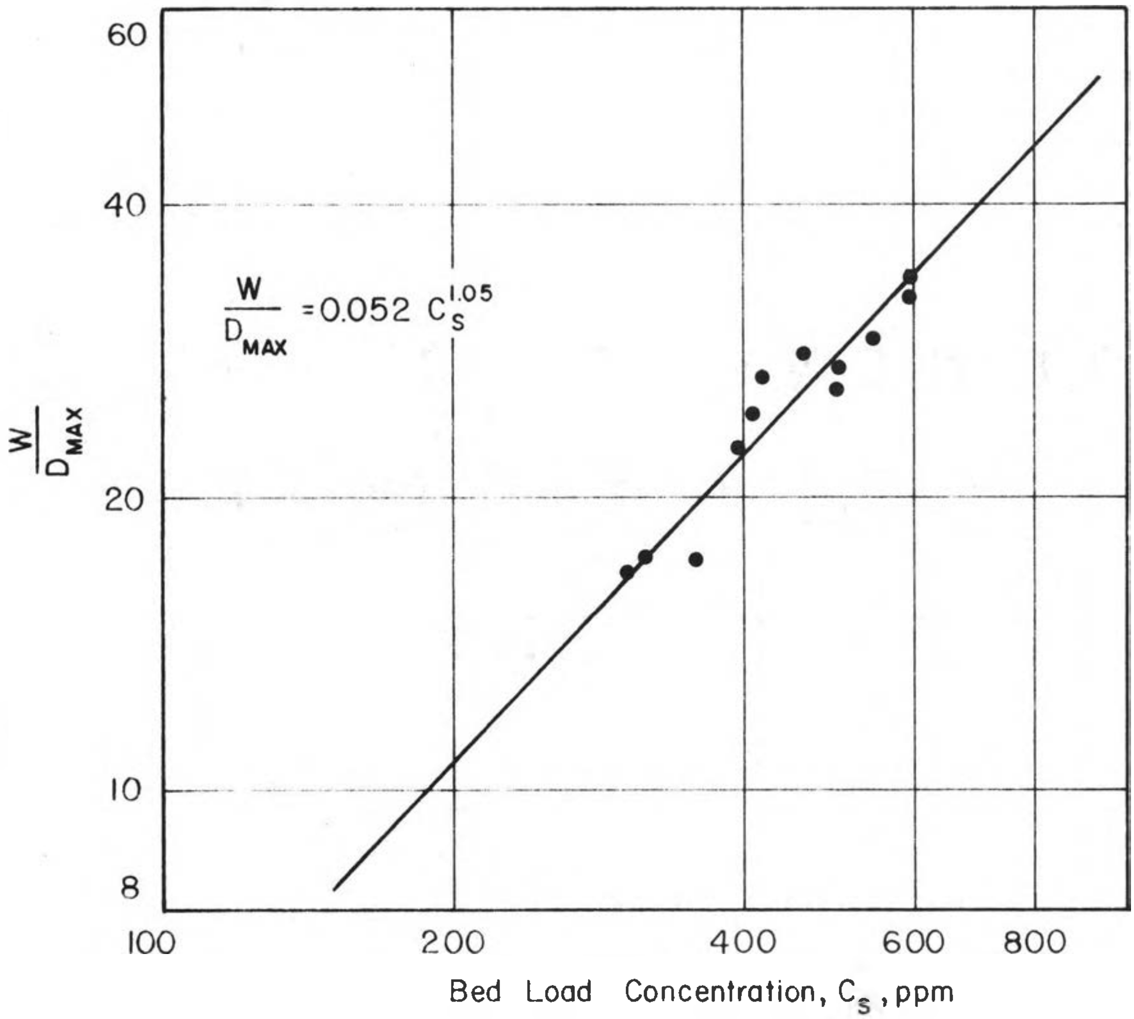

Figure 51. Relationship between $\frac{W}{D_{max}}$ and bedload concentration in straight channels

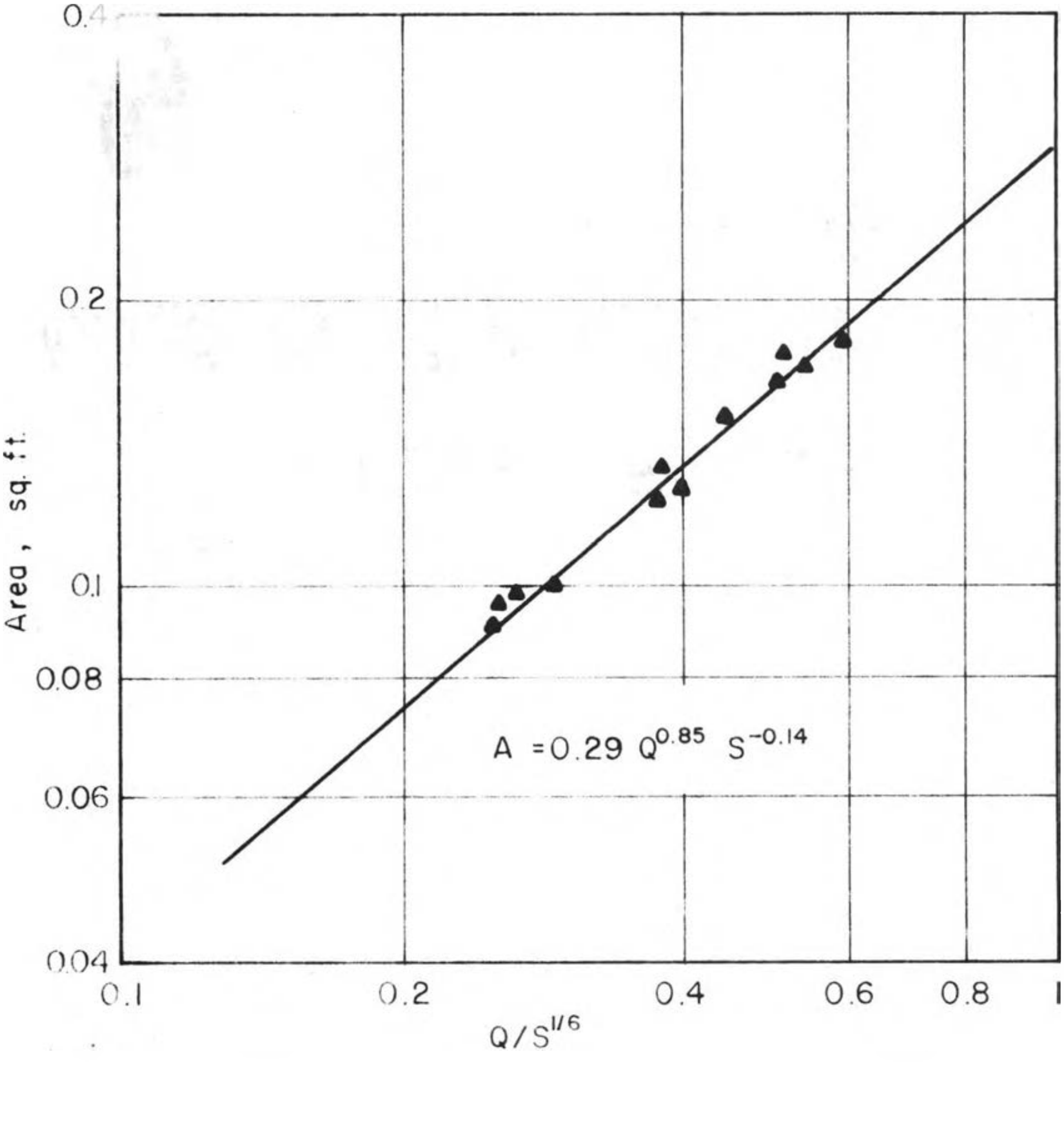

Figure 52. Variation of cross sectional area with discharge and slope in straight channels

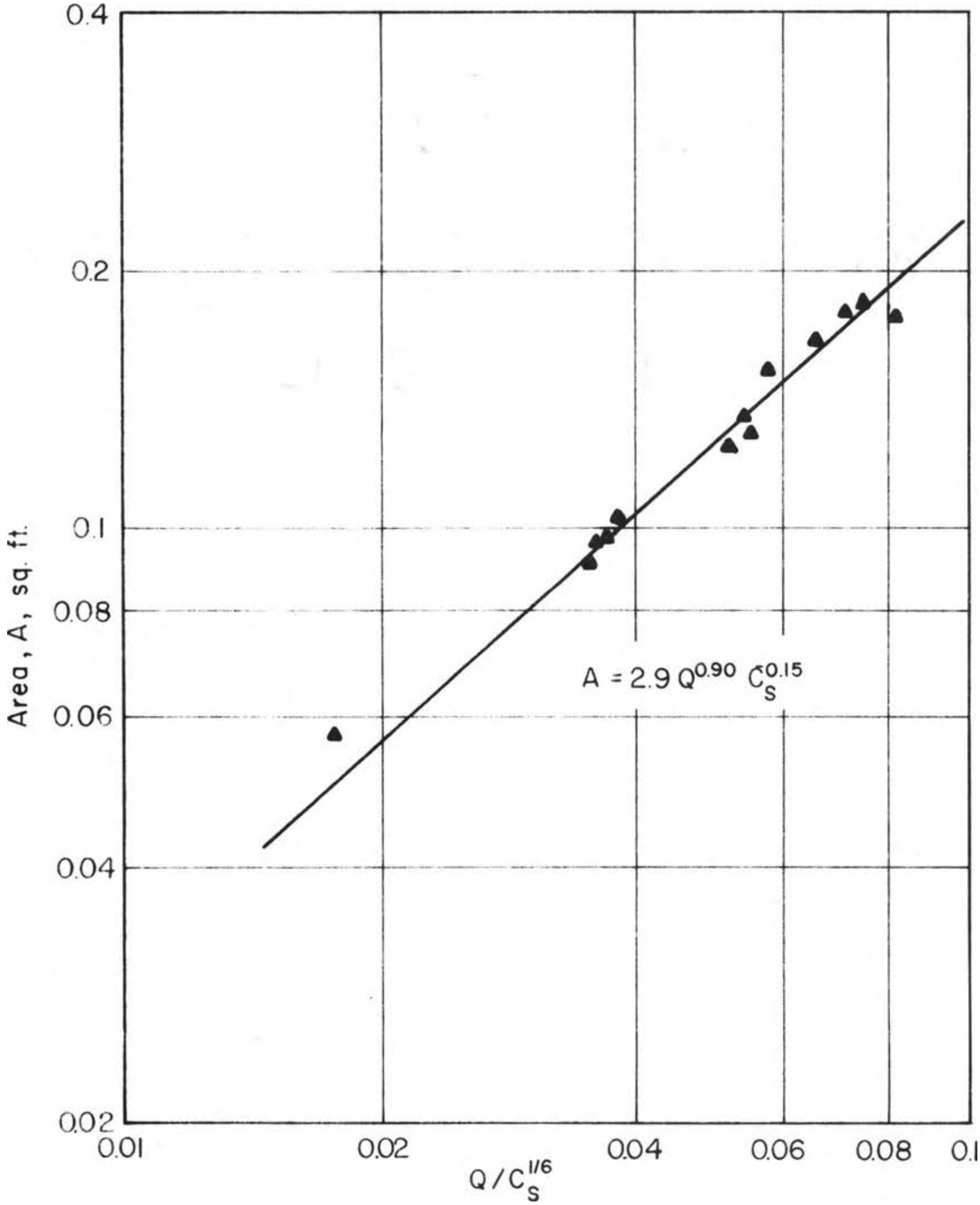

Figure 53. Variation of cross sectional area with discharge and bedload concentration in straight channels

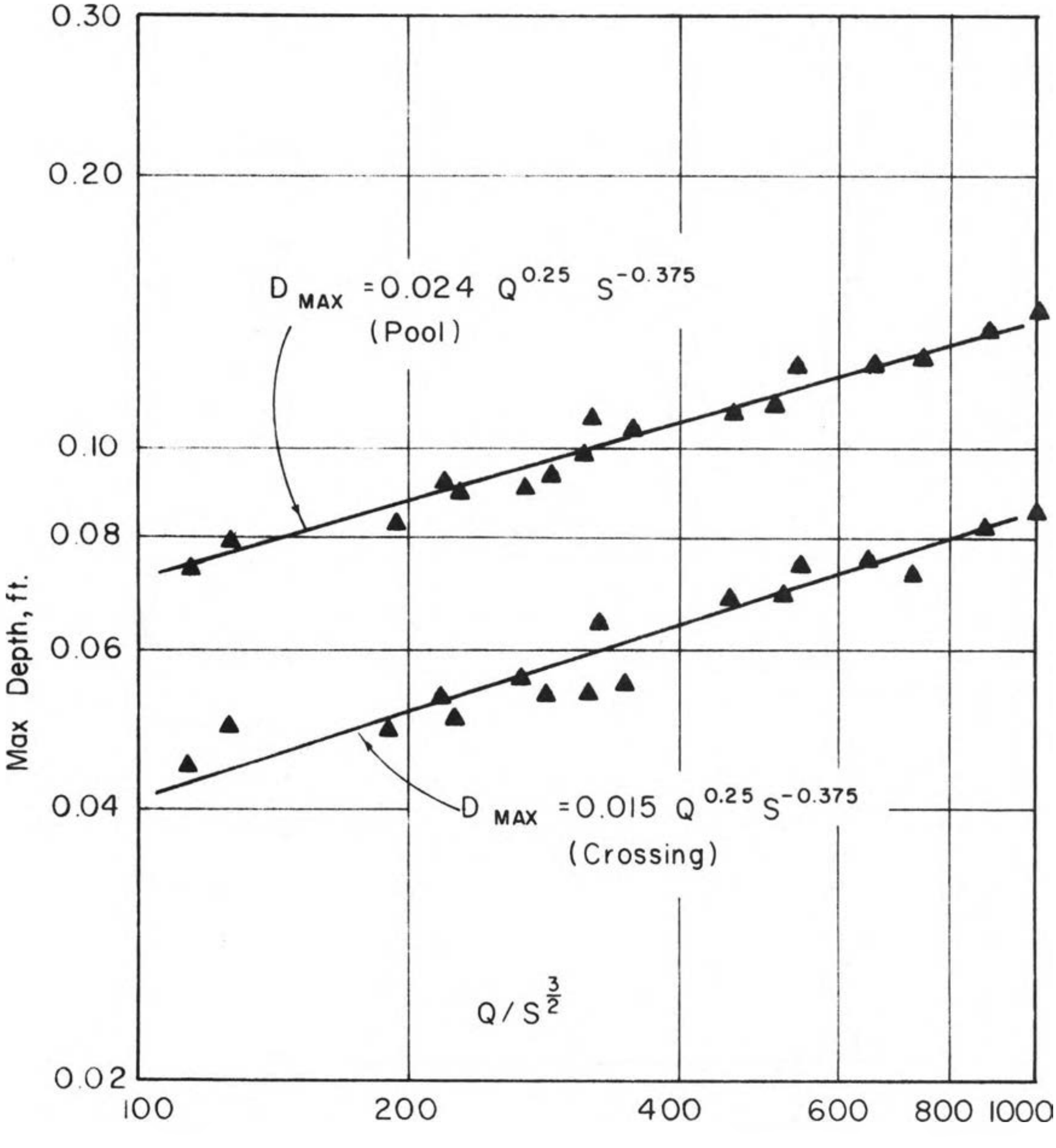

Figure 54. Relationship among maximum depths in pools and crossings, discharge, and slope for meandering thalweg channels

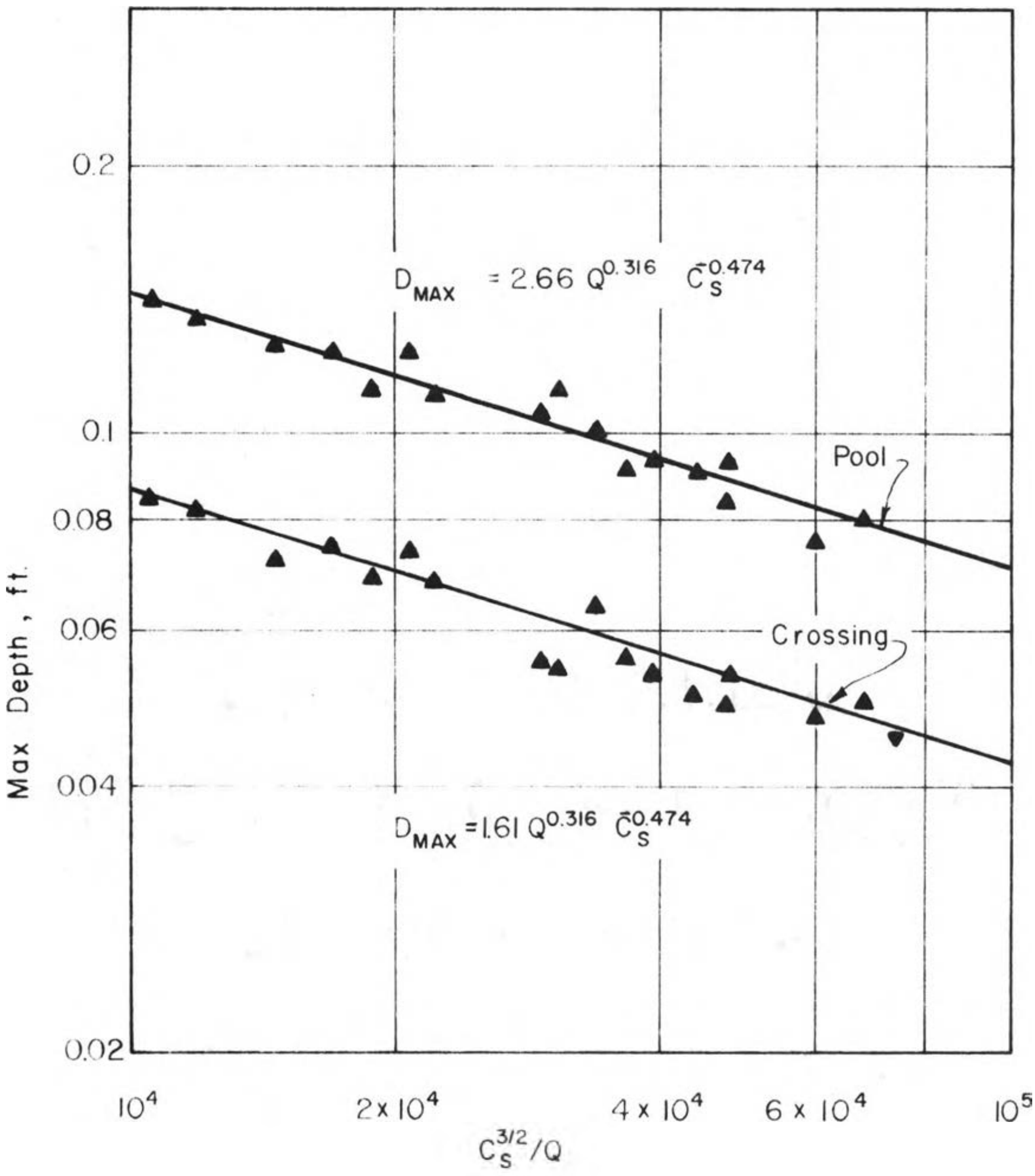

Figure 55. Relationship among maximum depths in pools and crossings, discharge, and bedload concentration in meandering thalweg channels

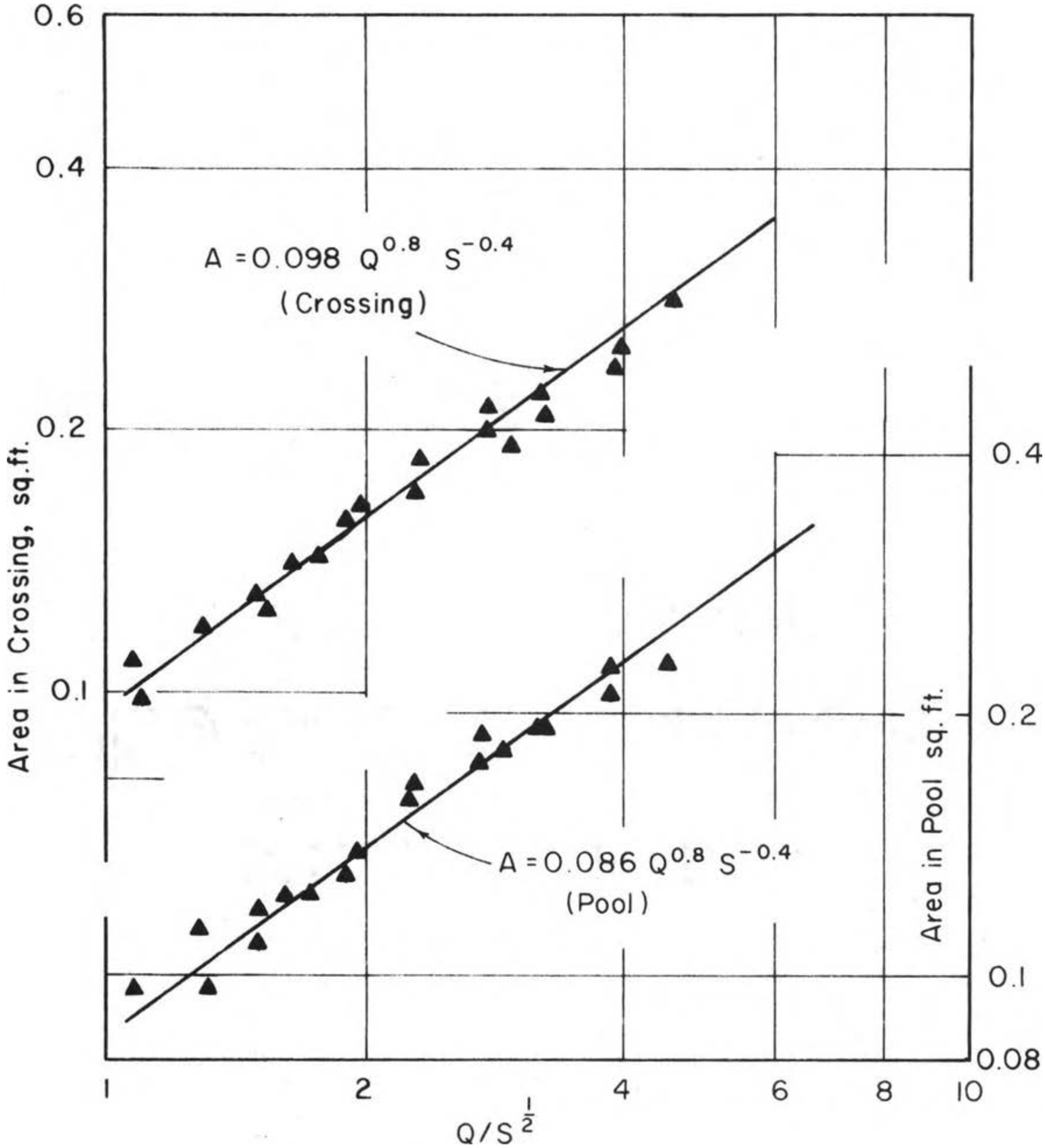

Figure 56. Relationship among areas in pools and crossings, discharge, and slope in meandering thalweg channels

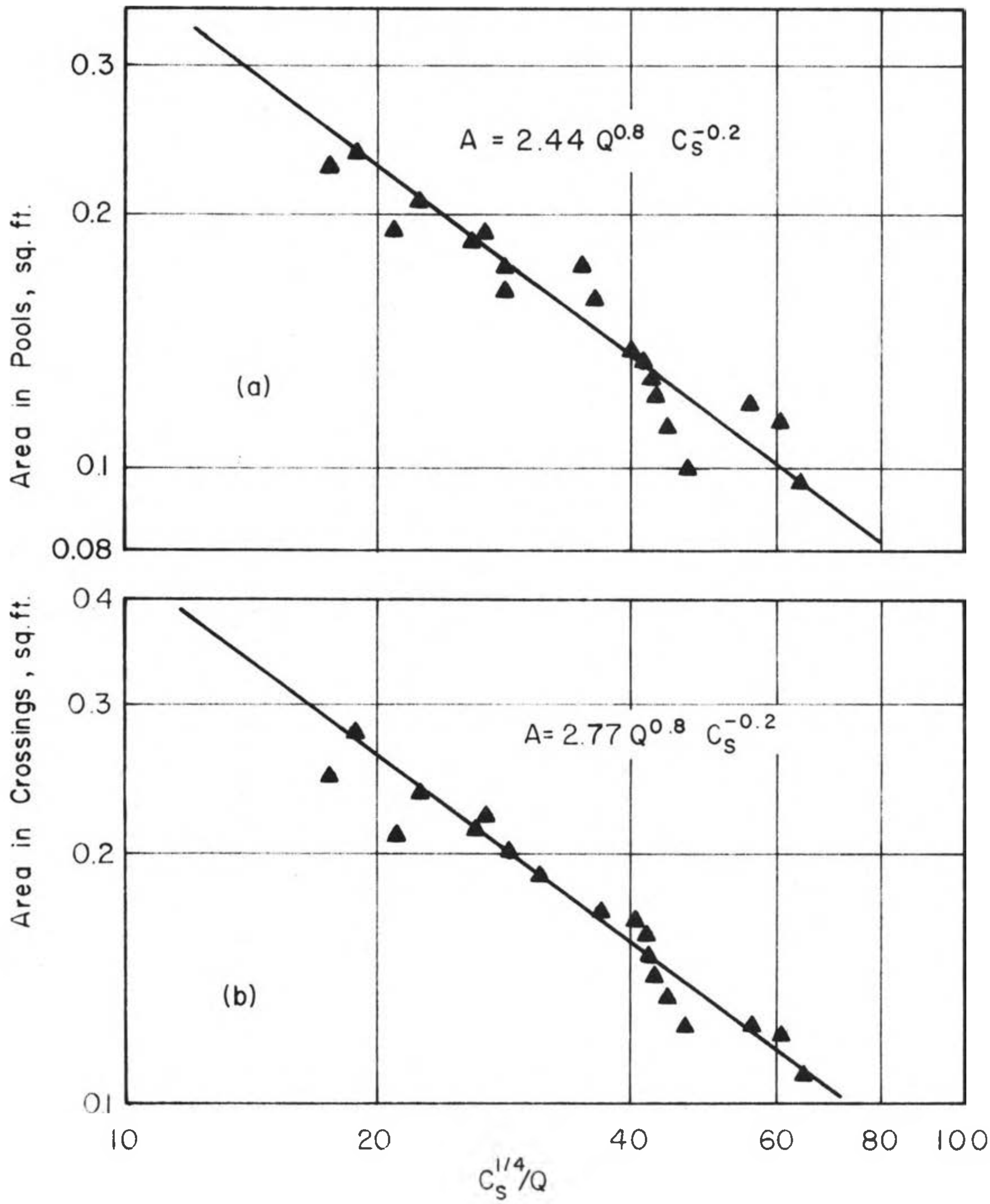

Figure 57. Relations among areas in (a) pools, and (b) crossings, discharge, and bedload concentration for meandering thalweg channels

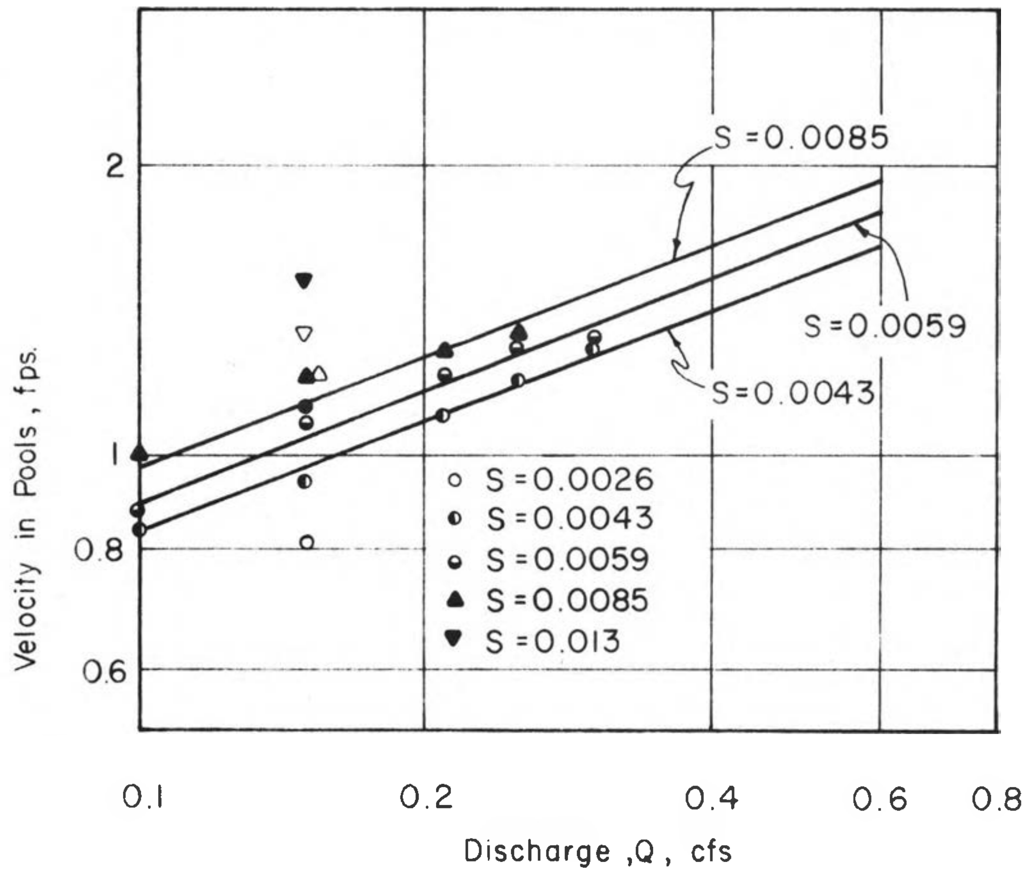

Figure 58. Variation of velocity in pools with discharge and slope in meandering thalweg channels

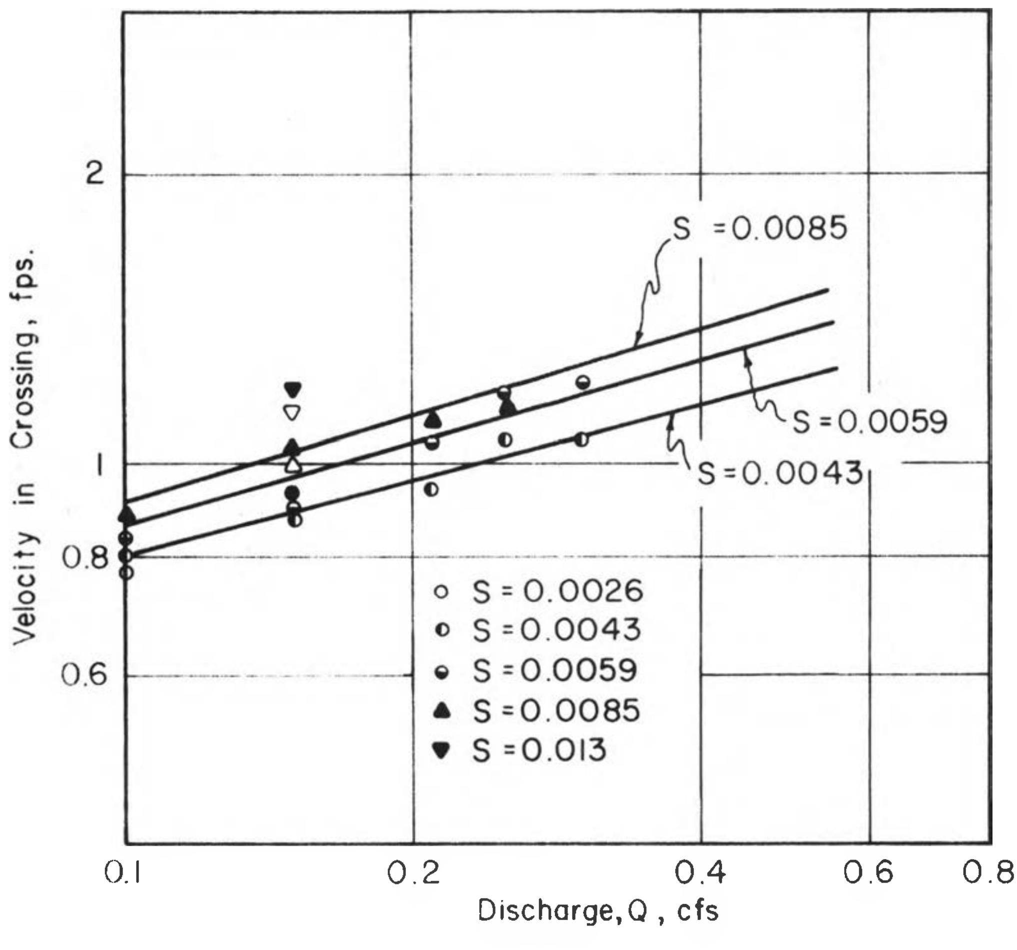

Figure 59. Variation of velocity in crossings with discharge and slope in meandering thalweg channels

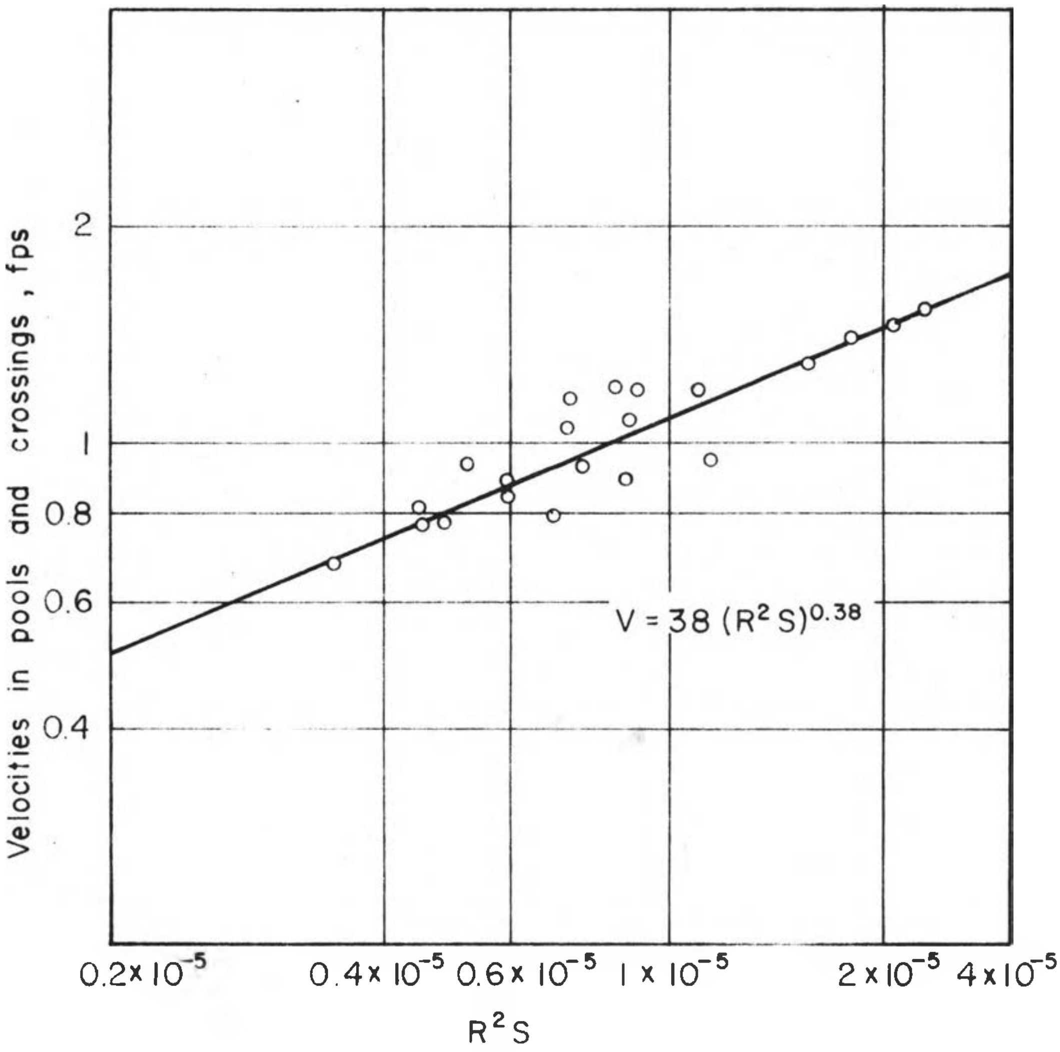

Figure 60. Relations among velocity in pools and crossings, hydraulic radius, and slope in meandering thalweg channels

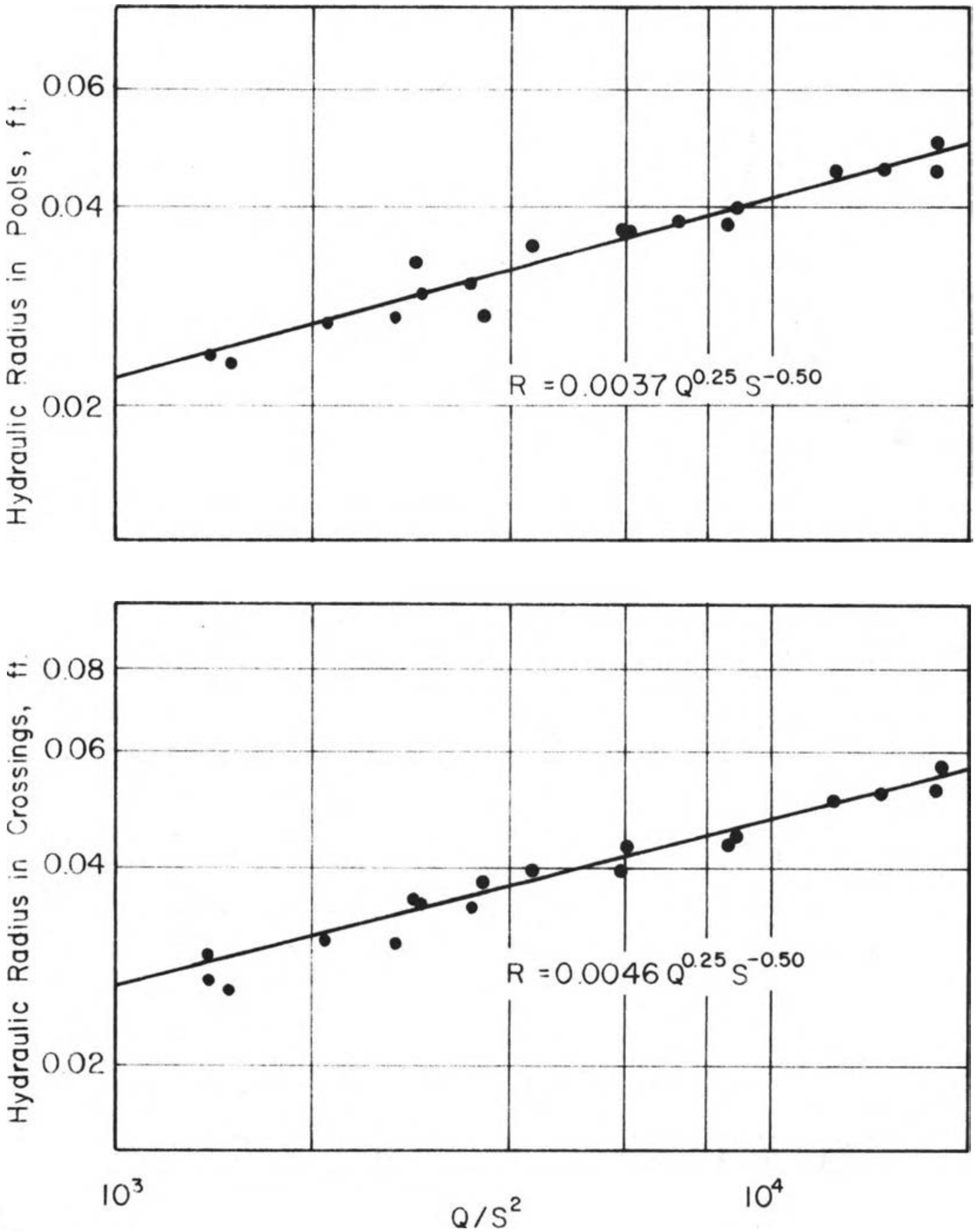

Figure 61. Relations among hydraulic radius in pools and crossings, discharge and slope for meandering thalweg channels

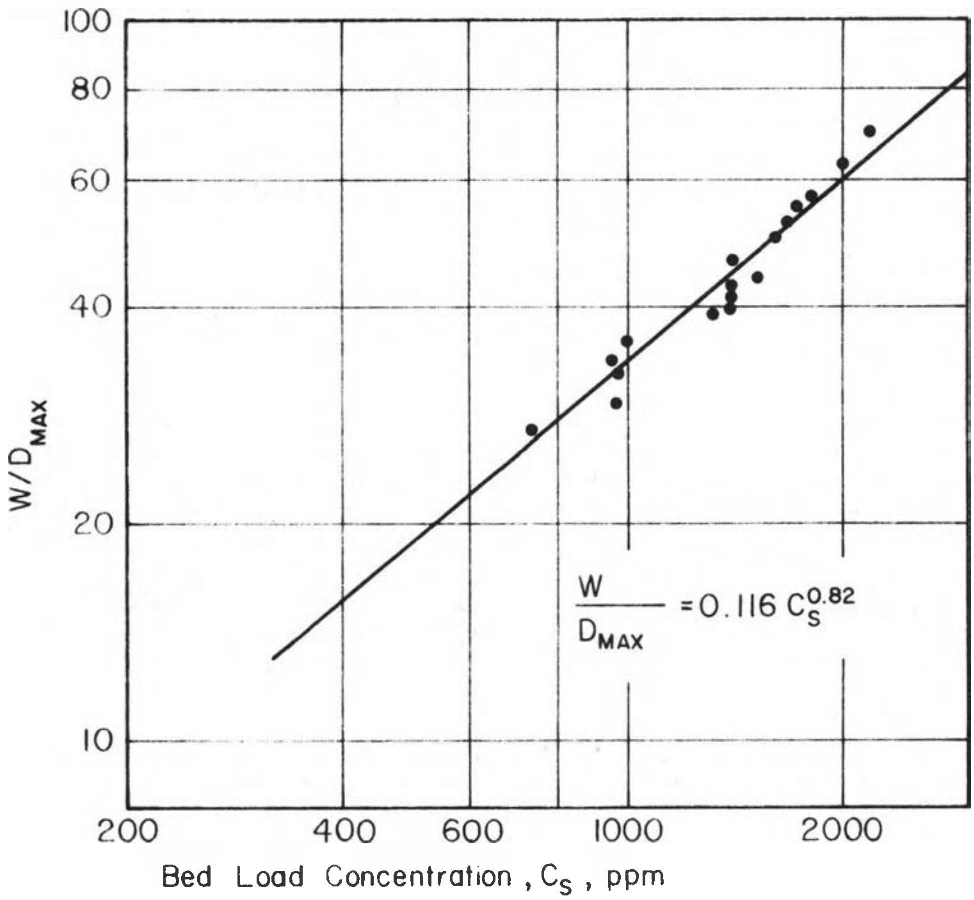

Figure 62. Relationship between $\frac{W}{D_{max}}$ and bedload concentration in meandering thalweg channels

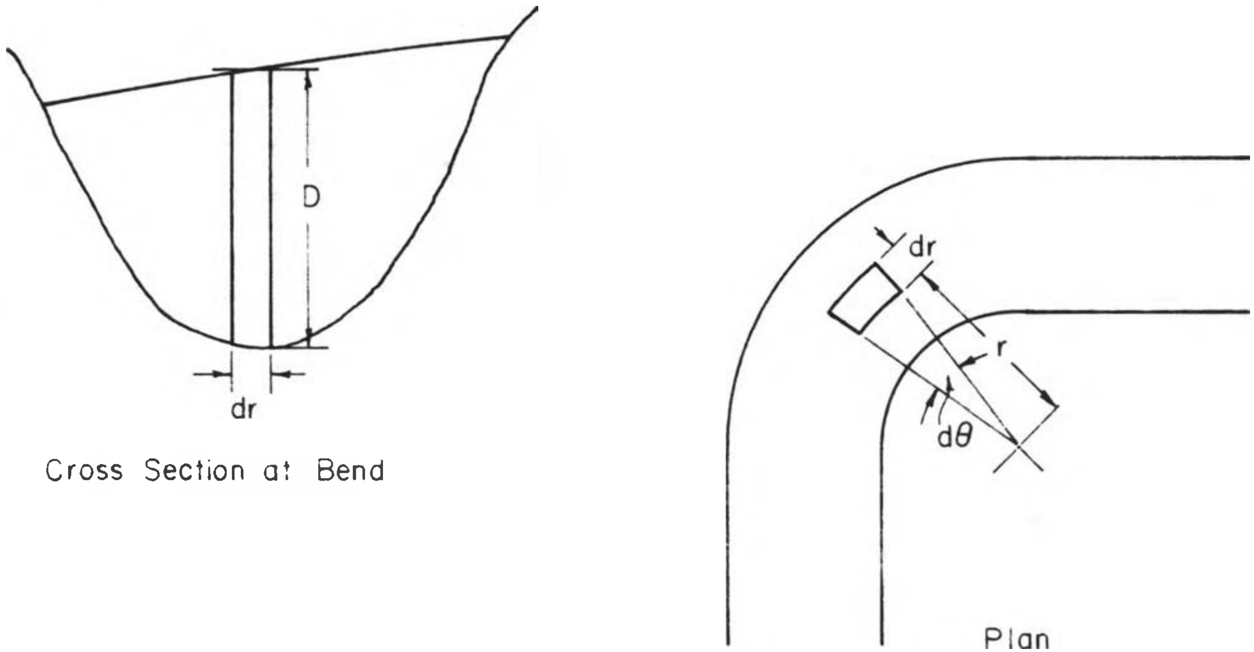

Figure 63. Transverse inclination of water surface at bends of open channels

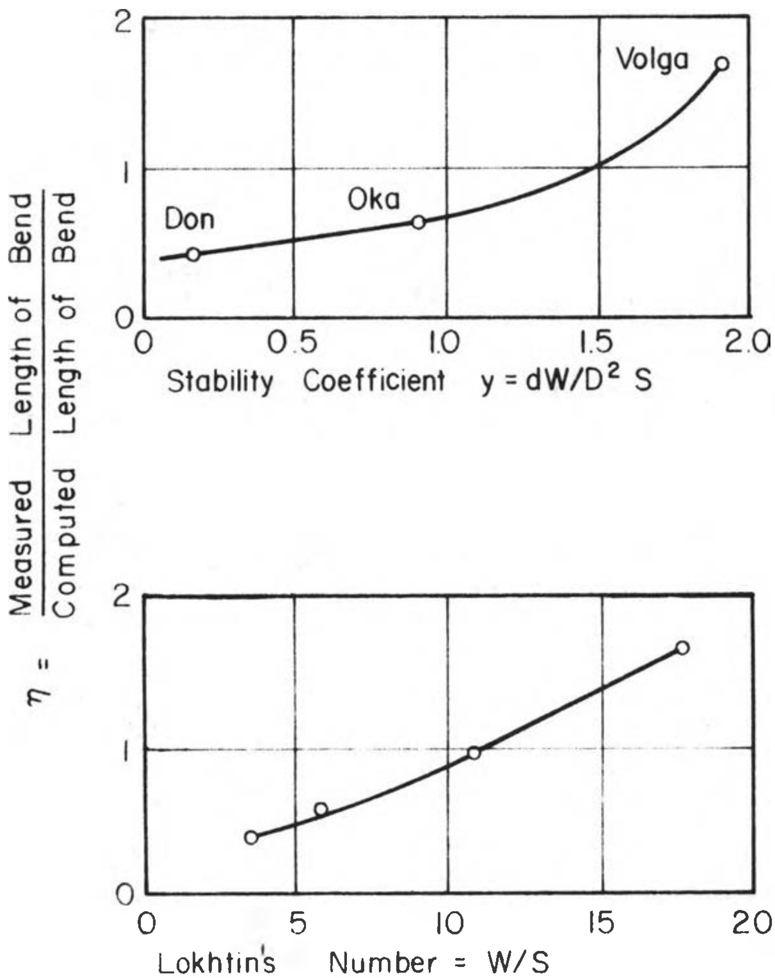

Figure 64. Relation of coefficient of η to the stability coefficient and to Lokhtins number (after Rzhanitsyn, 1960)

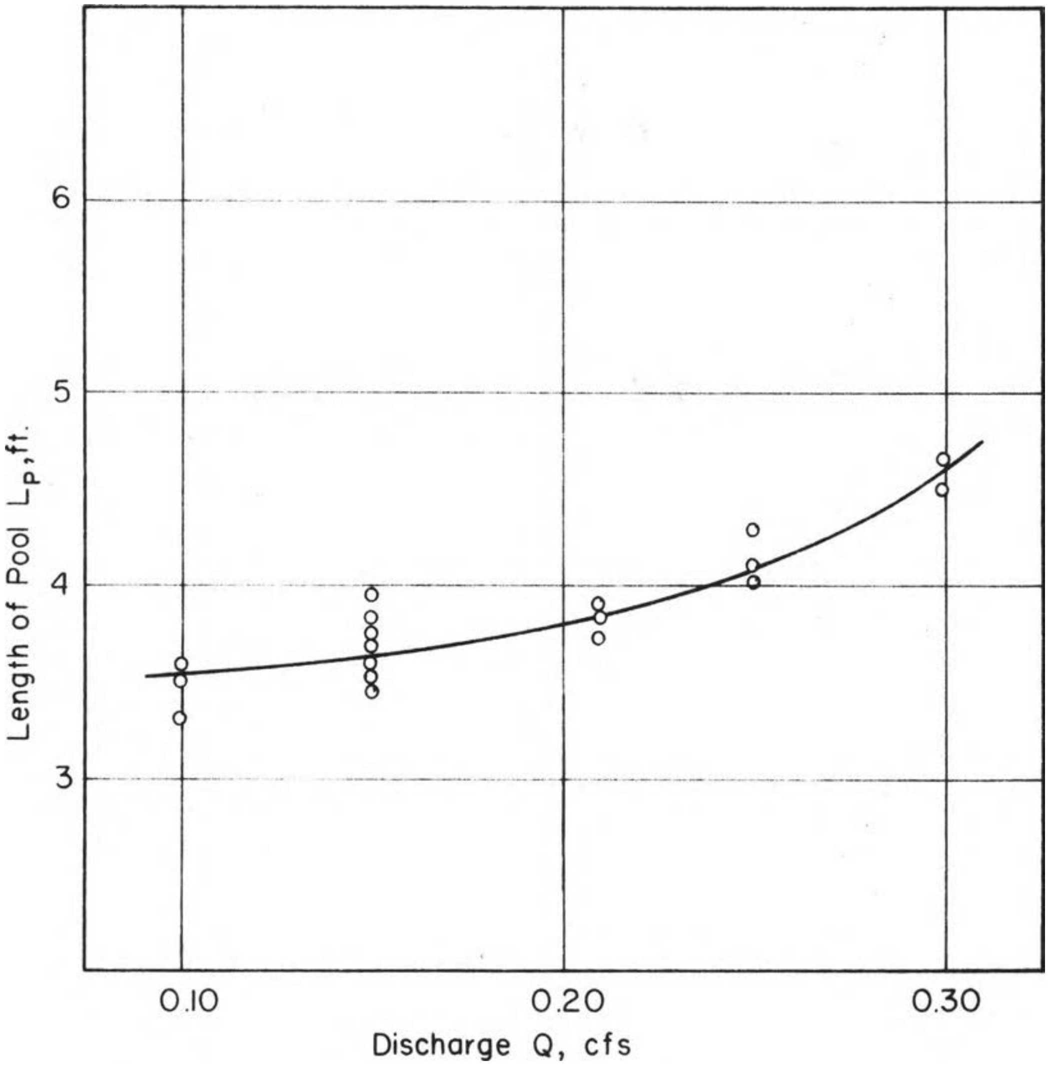

Figure 65. Length of pool versus discharge in meandering thalweg channels

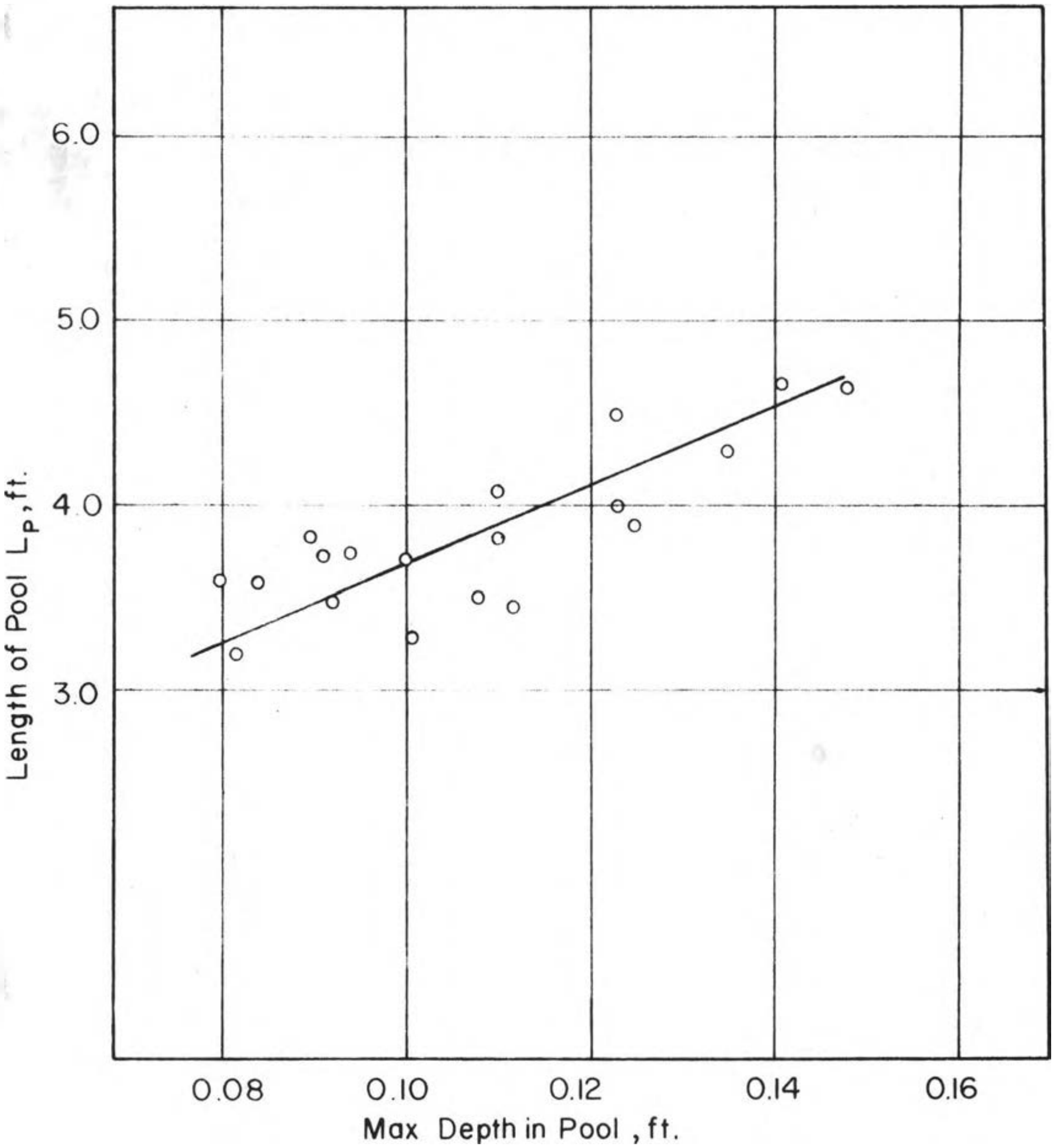

Figure 66. Length of pools versus maximum depths in pools in meandering thalweg channels

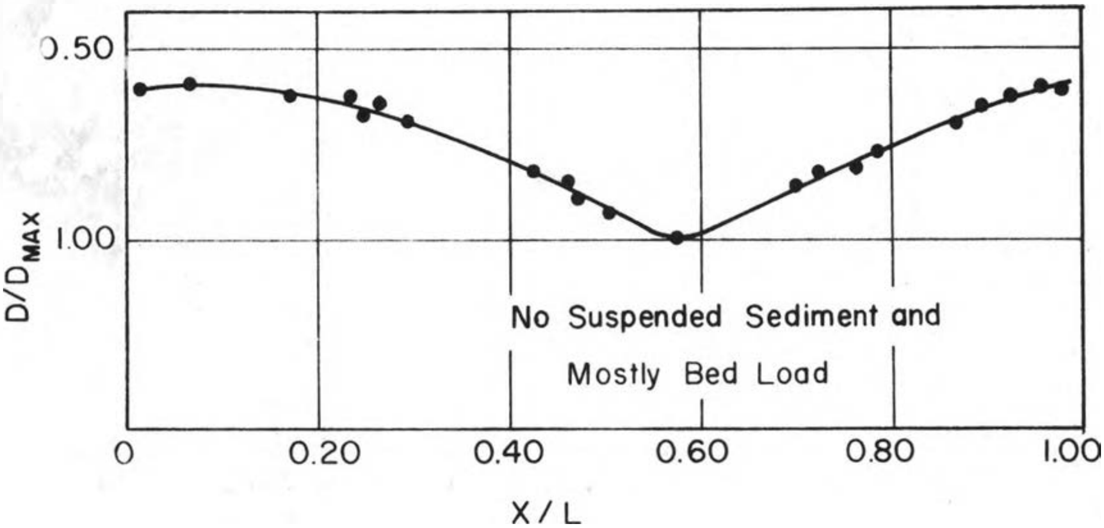

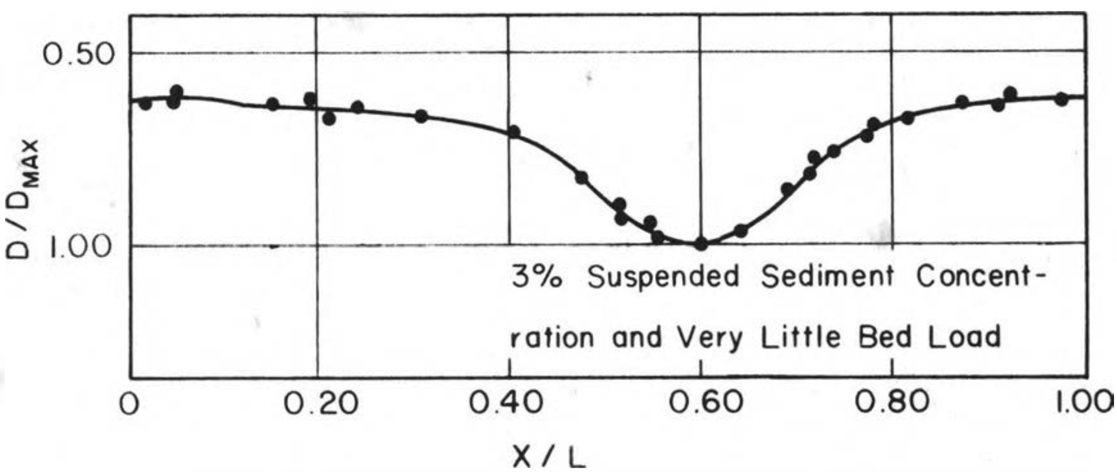

D = Depth at a Distance X From Start of Bend

D_{MAX} = Max Depth in Pool

L = Length of Bend

Figure 67. Nondimensional longitudinal profile of channel bed at bends

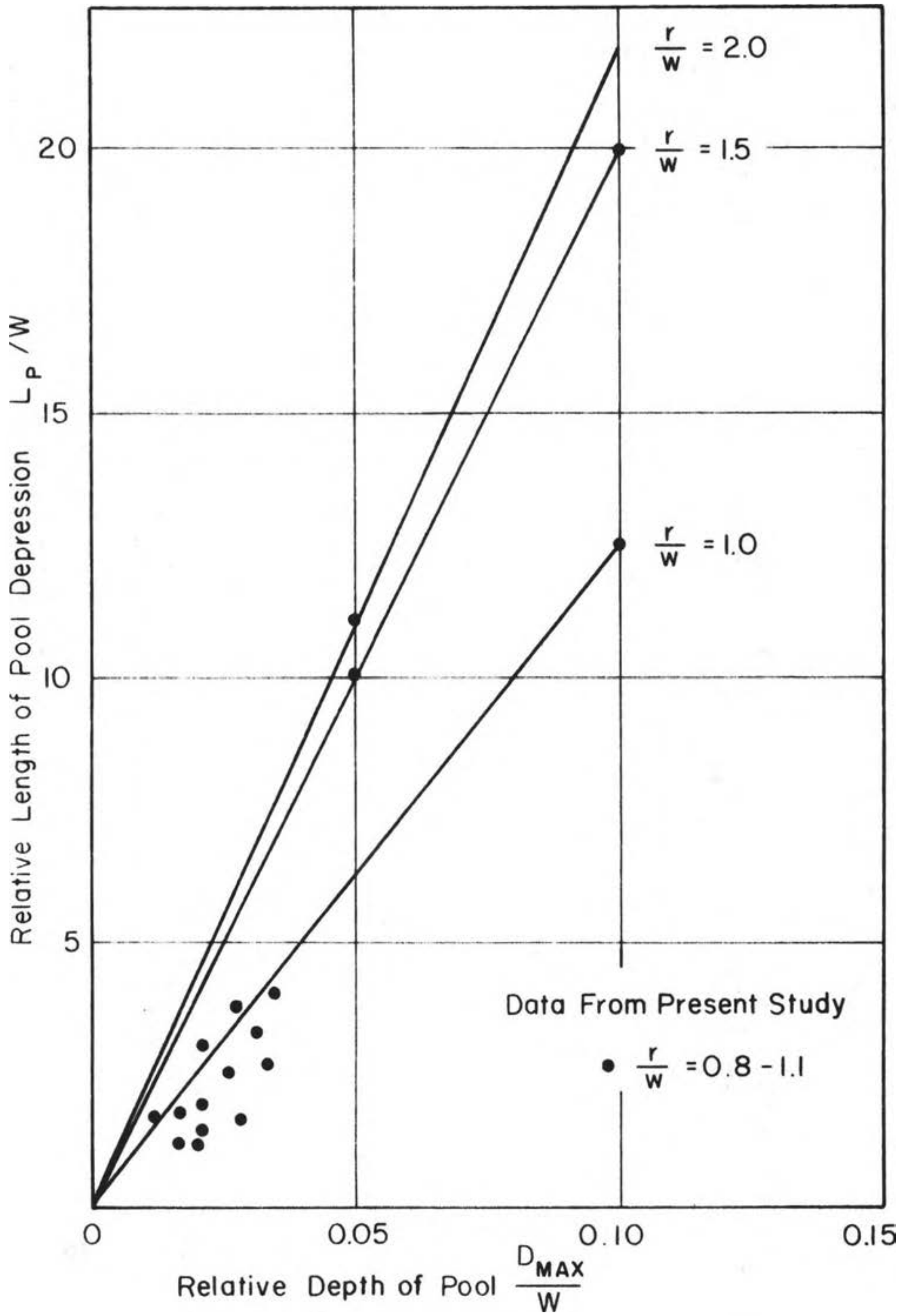

Figure 68. Relative depth of pool versus relative length of pool depression (after Rzhanitsyn, 1960)

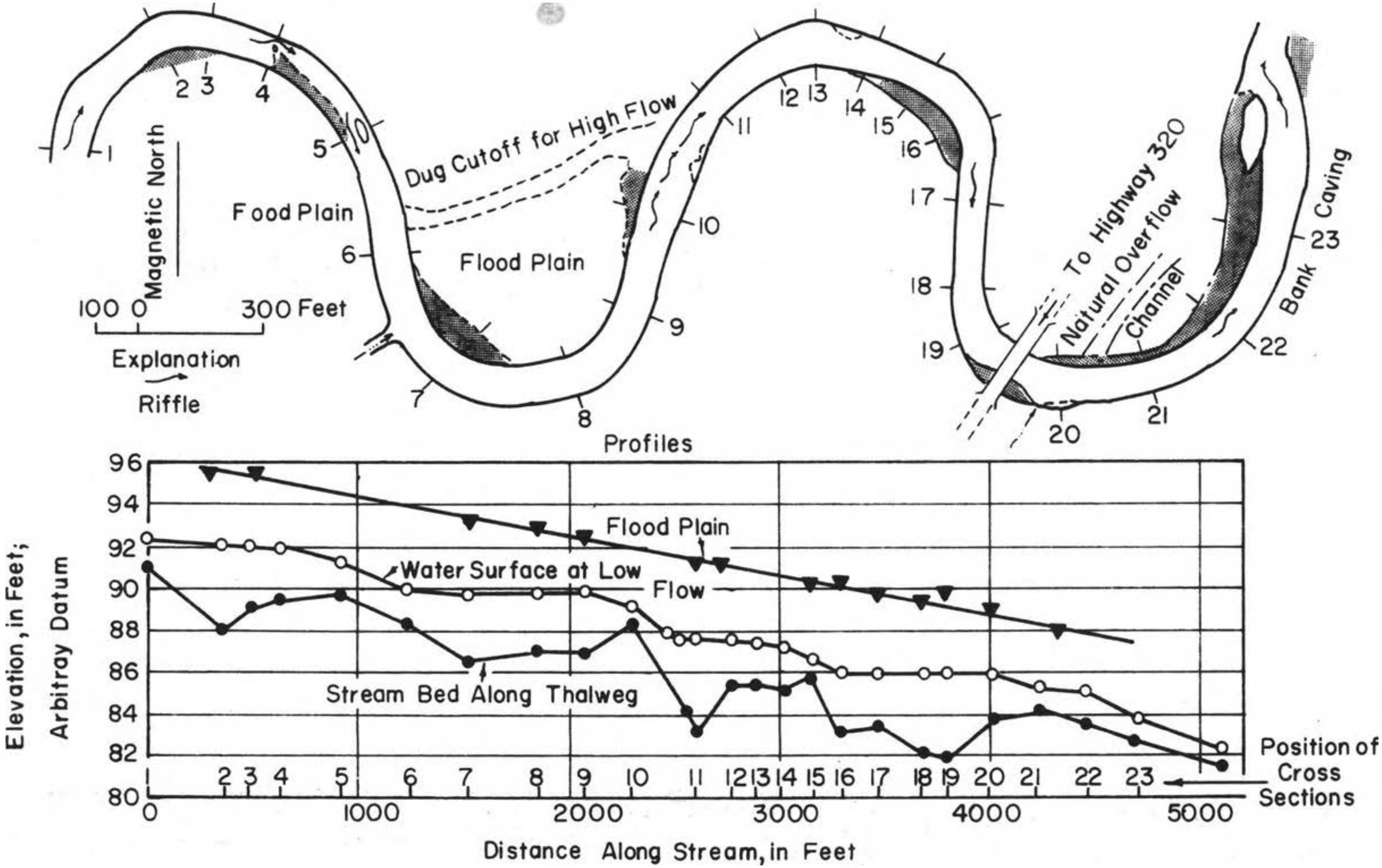

Figure 69. Plan and profile of a meandering reach of the Popo Agie River near Hudson, Wyoming (after Leopold and Wolman, 1957)

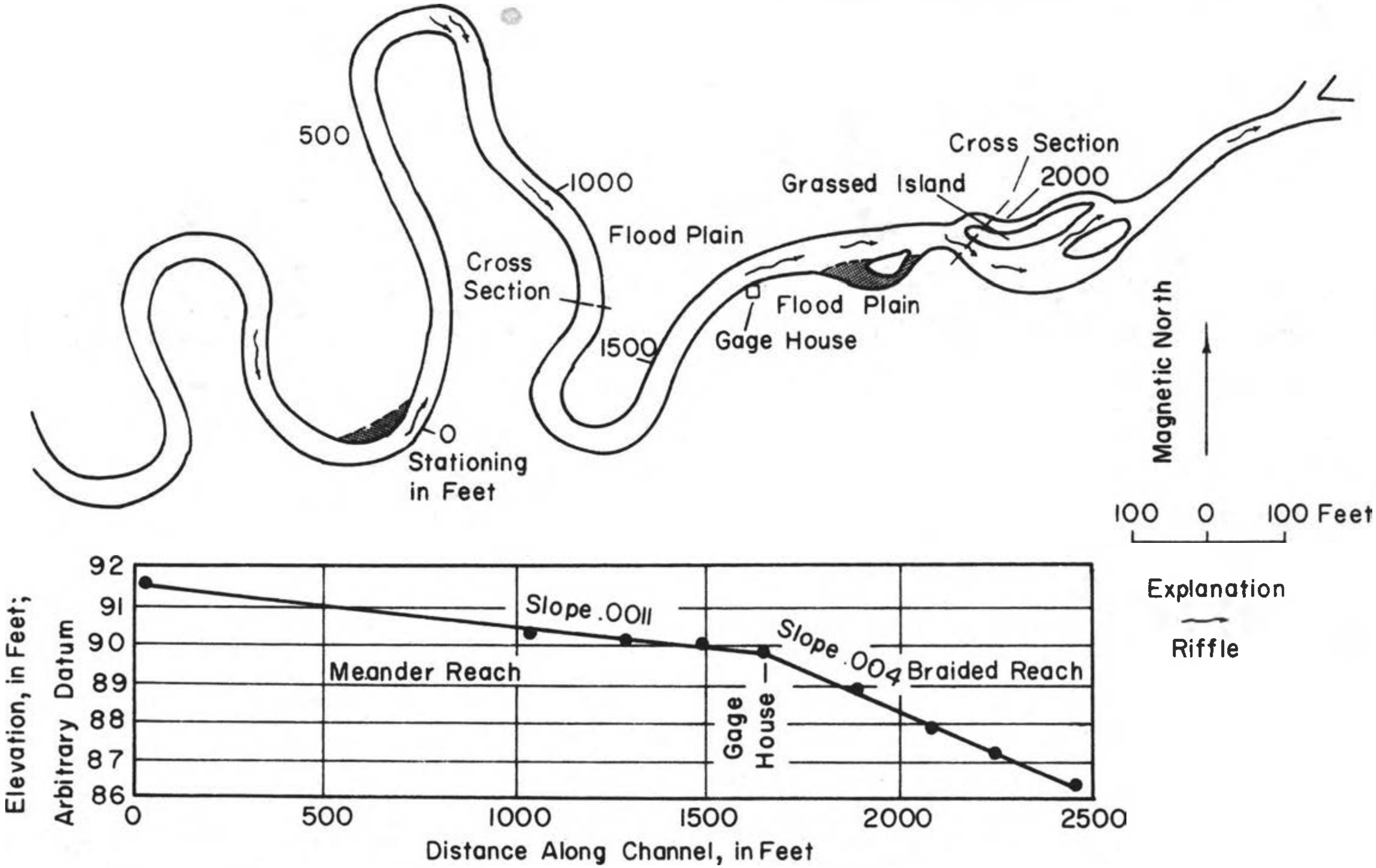

Figure 70. Plan and profile of Cottonwood Creek near Daniel, Wyoming. In this reach the river changes its pattern from meander to braid (after Leopold and Wolman, 1957).

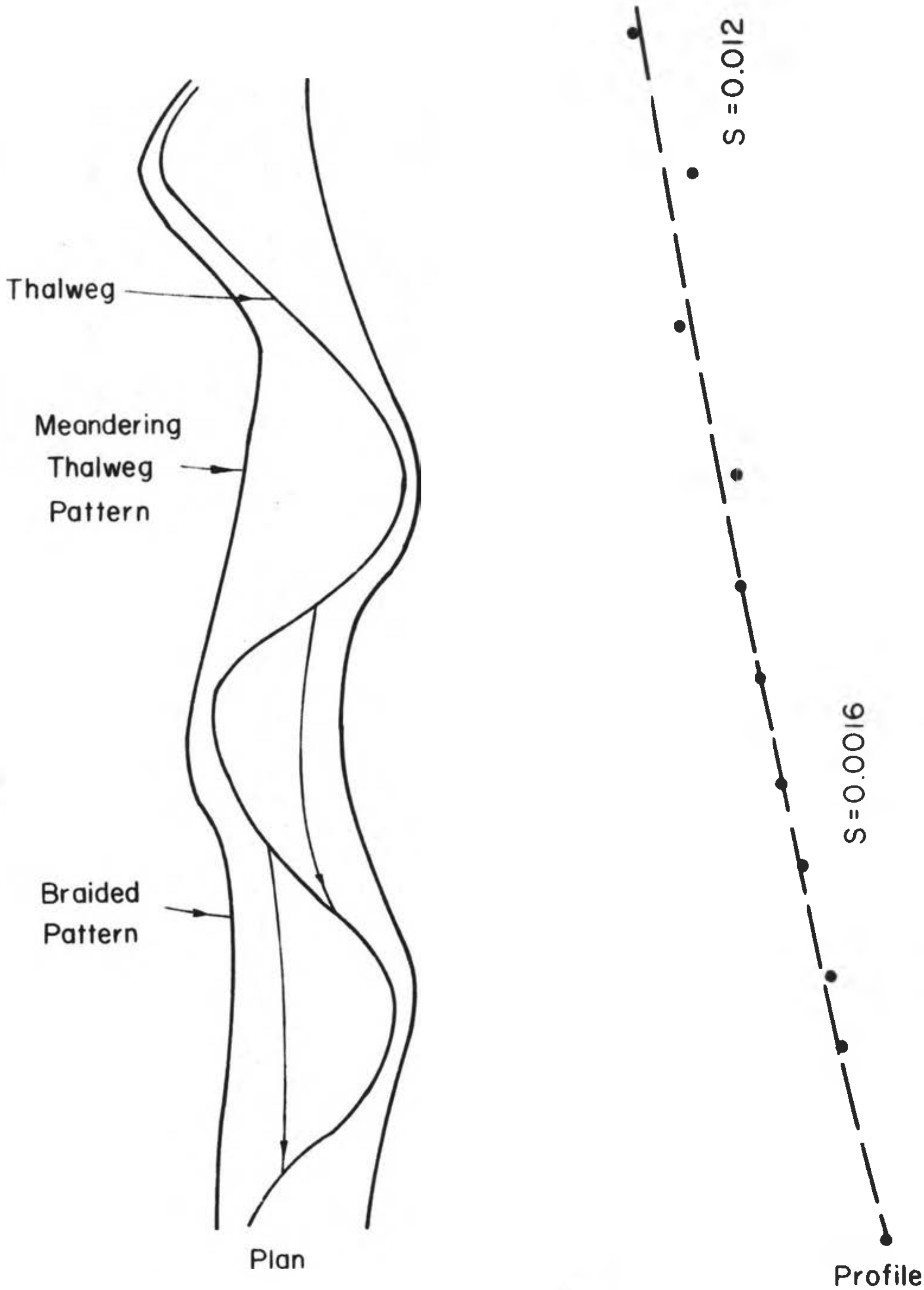

Figure 71. Plan and profile of laboratory stream showing combination of meandering thalweg and braided channel patterns

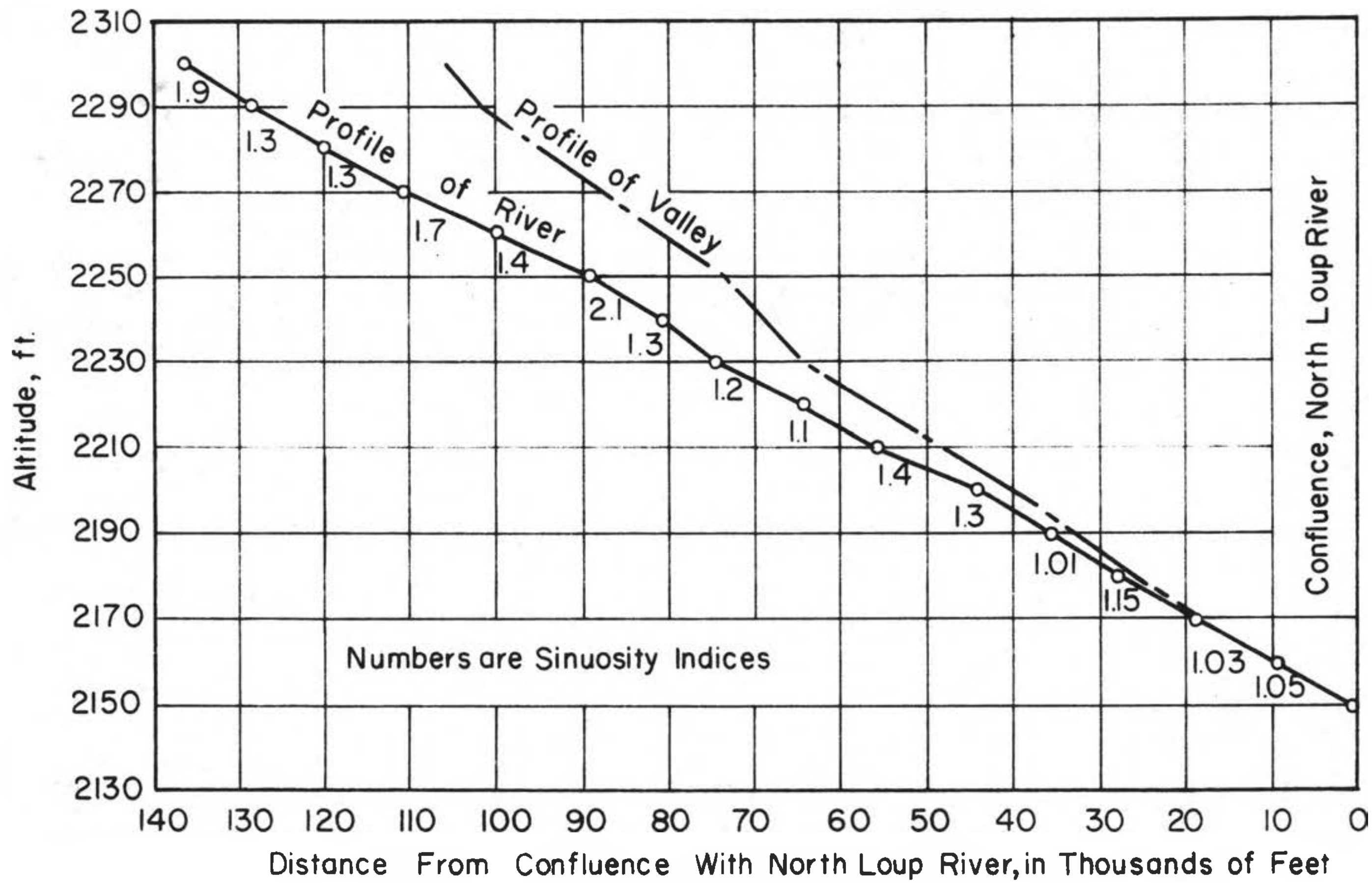

Figure 72. Longitudinal river profile and valley profile, Calamus River, Nebraska (after Brice, 1964)

APPENDIX B

Data

1. STRAIGHT ENTRANCE

Table 3.

Slope $S = 0.0015$

River Channel Pattern: Straight

Discharge Q, cfs	0.10	0.15	0.20
Max Depth D_{max}, ft	0.090	0.098	0.113
Channel Width W, ft	1.50	1.70	1.95
Area, A, sft	0.102	0.151	0.182
Velocity V, fps	0.98	0.99	1.10
Wetted Perimeter, ft	1.77	2.00	2.32
Hydraulic Radius R, ft	0.058	0.076	0.078
Bedload Discharge Q_s, gm/min	52	87	122
Bedload Concentration C_s, ppm	302	316	356
Chezy C, $ft^{1/2}$/sec	80	77	84
W/D_{max}	16.7	17.3	17.2
Shear $\tau_o = \gamma RS$, pound/sft	0.0054	0.0070	0.0073

Table 4.

Slope $S = 0.0028$

River Channel Pattern: Straight

Discharge Q, cfs	0.10	0.15	0.20
Max Depth D_{max}, ft	0.077	0.080	0.108
Channel Width W, ft	1.75	2.13	2.22
Area A, sft	0.098	0.129	0.171
Velocity V, fps	1.02	1.16	1.17
Wetted Perimeter P, ft	1.85	2.30	2.41
Hydraulic Radius R, ft	0.053	0.056	0.071
Bedload Discharge Q_s, gm/min	67	107	140
Bedload Concentration C_s, ppm	392	417	410
Chezy $C = V/R^{1/2}S^{1/2}$, $ft^{1/2}/sec$	84	78	83
$\frac{W}{D_{max}}$	22.7	26.6	24.4
Shear $\tau_o = \gamma RS$, pounds/sft	0.0093	0.0098	0.0120

Table 5.

Slope S = 0.0038

River Channel Pattern: Straight

Discharge Q, cfs	0.10	0.15	0.20
Max Depth D_{max}, ft	0.066	0.084	0.085
Channel Width W, ft	1.85	2.15	2.30
Area A, sft	0.098	0.135	0.179
Velocity V, fps	1.02	1.11	1.12
Wetted Perimeter P, ft	1.90	2.40	2.57
Hydraulic Radius R, ft	0.050	0.056	0.070
Bedload Discharge Q_s, gm/min	79	128	172
Bedload Concentration C_s, ppm	462	500	502
Chezy $C = V/R^{1/2}S^{1/2}$, $ft^{1/2}/sec$	74	76	69
W/D_{max}	28.10	25.6	27.1
Shear $\tau_o = \gamma RS$, pounds/sft	0.0120	0.013	0.012

Table 6

Slope $S = 0.0040$

River Channel Pattern: Straight

Discharge Q, cfs	0.10	0.15	0.20
Max Depth D_{max}, ft	0.063	0.065	0.073
Channel Width W, ft	1.85	2.18	2.35
Area A, sft	0.091	0.125	0.166
Velocity V, fps	1.10	1.20	1.20
Wetted Perimeter P, ft	2.00	2.40	2.60
Hydraulic Radius R, ft	0.046	0.052	0.063
Bedload Discharge Q_s, gm/min	93	152	202
Bedload Concentration C_s, ppm	543	592	590
Chezy $C = V/R^{1/2}S^{1/2}$, $ft^{1/2}$/sec	81	83	76
W/D_{max}	29.40	33.50	32.20
Shear $\tau_o = \gamma RS$, pounds/sft	0.011	0.013	0.015

II. ENTRANCE AT AN ANGLE

Table 7.

River Channel Pattern: Straight

Slope S	0.0010	0.0017	0.0020
Discharge Q, cfs	0.15	0.15	0.15
Channel Width W, ft	1.16	2.15	2.20
Maximum Depth D_{max}, ft	0.170	0.120	0.112
Area A, sft	0.192	0.187	0.187
Velocity V, fps	0.780	0.800	0.800
Wetted Perimeter P, ft	1.36	2.34	2.50
Hydraulic Radius R, ft	0.141	0.080	0.074
Bedload Discharge Q_s, gm/min	119	134	147
Bedload Concentration C_s, ppm	464	523	573
Chezy $C = V/R^{1/2}S^{1/2}$, $ft^{1/2}$/sec	70	67	67
$\frac{W}{D_{max}}$	6.8	17.9	19.7
Shear $\tau_o = \gamma RS$, pounds/sft	0.0081	0.0090	0.0093
Froude Number $F = V/g^{1/2}D_{max}^{1/2}$	0.33	0.40	0.42
Stream Power $= \gamma QS$, $\frac{\text{ft pounds}}{\text{sec ft}}$	0.0095	0.0159	0.0187

Table 8.

Slope S = 0.0043

Channel Pattern: Meandering Thalweg

Discharge, cfs	0.10	0.15	0.21	0.25	0.30
Radius of Bend, ft	3.60	4.20	4.60	4.95	5.20
Channel Width, ft	3.10	3.80	4.20	4.50	5.10
Max Depth in Pool, ft	0.105	0.112	0.125	0.135	0.141
Max Depth in Crossing, ft	0.055	0.066	0.072	0.082	0.085
Area in Pool, sft	0.119	0.160	0.191	0.208	0.231
Area in Crossing, sft	0.125	0.170	0.221	0.236	0.283
Velocity in Pool, fps	0.84	0.94	1.10	1.20	1.30
Velocity in Crossing, fps	0.80	0.88	0.95	1.06	1.06
Wetted Perimeter in Pool, ft	3.23	3.91	4.37	4.60	5.23
Wetted Perimeter in Crossing, ft	3.13	3.78	4.35	4.53	5.40
Hydraulic Radius in Pool, ft	0.037	0.041	0.0438	0.0454	0.0443
Hydraulic Radius in Crossing	0.040	0.045	0.051	0.0520	0.052
Thalweg Meander Wave Length, ft	16.60	19.40	20.60	22.00	23.00
Thalweg Meander Width, ft	4.50	5.00	6.60	7.50	7.70
Bedload Discharge, gm/min	164	240	354	416	510
Bedload Concentration C_s, ppm	965	945	990	980	1,000
Thalweg Sinuosity	1.10	1.14	1.19	1.23	1.26
Channel Sinuosity	1.010	1.030	1.032	1.028	1.026
Chezy C, $ft^{1/2}/sec$	67	71	80	85	94
W/D_{max} in Pool	29.50	34.00	33.60	33.30	36.10
Morphometric Parameter K_o	0.70	0.73	0.58	0.54	0.42
Length of Bend (measured), ft	9.90	11.50	13.00	14.80	16.00

Table 8. (Continued)

Length of Bend (computed), ft	9.25	10.50	14.80	18.00	20.00
η	1.07	1.10	0.88	0.83	0.80
Length of Pool, ft	3.70	3.70	3.90	4.30	4.67
Shear τ_o, pounds/sft	0.0100	0.011	0.0118	0.0122	0.0119
Froude Number $F = V/g^{1/2}D_{max}^{1/2}$	0.46	0.50	0.55	0.58	0.61
Stream Power = γQS, $\frac{\text{ft pounds}}{\text{sec ft}}$	0.0269	0.0404	0.0565	0.0672	0.0806

Table 9.

Slope S = 0.0059

Channel Pattern: Meandering Thalweg

Discharge, cfs	0.10	0.15	0.21	0.25	0.30
Radius of Bend, ft	3.80	4.30	4.55	5.10	5.30
Channel Width, ft	3.60	4.00	4.60	5.20	5.70
Max Depth in Pool, ft	0.092	0.100	0.110	0.123	0.123
Max Depth in Crossing, ft	0.053	0.064	0.068	0.074	0.075
Area in Pool, sft	0.114	0.139	0.174	0.192	0.229
Area in Crossing, sft	0.121	0.067	0.200	0.210	0.248
Velocity in Pool, fps	0.88	1.08	1.21	1.30	1.31
Velocity in Crossing, fps	0.83	0.90	1.05	1.19	1.21
Wetted Perimeter in Pool, ft	3.72	4.05	4.73	5.33	5.81
Wetted Perimeter Crossing, ft	3.40	4.15	4.65	5.00	5.65
Hydraulic Radius in Pool, ft	0.0307	0.0344	0.0368	0.0360	0.0394
Hydraulic Radius Crossing, ft	0.036	0.040	0.0430	0.042	0.044
Thalweg Meander Wave Length, ft	17.60	19.80	21.20	22.60	24.60
Thalweg Meander Width, ft	5.60	5.90	7.40	8.00	8.20
Bedload Discharge, gm/min	227	353	468	594	706
Bedload Concentration, ppm	1320	1370	1300	1390	1380
Thalweg Sinuosity	1.120	1.190	1.265	1.280	1.340
Channel Sinuosity	1.020	1.027	1.032	1.030	1.030
Chezy C, $ft^{1/2}/sec$	66	76	82	90	86
W/D_{max} in Pool	39.2	40.0	41.3	42.2	46.5
Morphometric Parameter K_o	0.92	0.75	0.61	0.52	0.57
Length of Bend (measured), ft	10.80	12.70	14.20	16.20	17.20

Table 9. (Continued)

Length of Bend (Computed), ft	7.00	10.2	11.2	14.9	15.6
η	1.55	1.25	1.27	1.09	1.10
Length of Pool, ft	3.50	3.71	3.82	4.00	4.50
Shear τ_o, pounds/sft	0.0113	0.0127	0.0137	0.0140	0.0143
Froude Number $F = V/g^{1/2}D_{max}^{1/2}$	0.51	0.60	0.64	0.65	0.66
Stream Power = γQS, $\frac{\text{ft pounds}}{\text{sec ft}}$	0.0369	0.0554	0.0775	0.0922	0.110

Table 10.

Slope S = 0.0085

River Channel Pattern: Meandering Thalweg

Discharge, cfs	0.10	0.15	0.21	0.25
Radius of Bend, ft	3.97	4.28	5.00	5.20
Channel Width, ft	4.20	4.70	5.20	5.20
Max Depth in Pool, ft	0.080	0.084	0.091	0.110
Max Depth in Crossing, ft	0.050	0.049	0.056	0.054
Area in Pool, sft	0.0981	0.123	0.164	0.192
Area in Crossing, sft	0.111	0.143	0.189	0.217
Velocity in Pool, fps	1.02	1.22	1.28	1.30
Velocity in Crossing, fps	0.90	1.05	1.11	1.15
Wetted Perimeter in Pool, ft	4.40	4.70	5.20	5.23
Wetted Perimeter in Crossing, ft	4.05	4.62	5.25	5.40
Hydraulic Radius in Pool, ft	0.0223	0.0262	0.0316	0.0367
Hydraulic Radius in Crossing, ft	0.0275	0.0310	0.0360	0.0355
Thalweg Meander Wave Length, ft	19.20	21.00	22.60	24.60
Thalweg Meander Width, ft	6.60	7.40	8.00	8.20
Bedload Discharge, gm/min	284	430	620	765
Bedload Concentration, ppm	1670	1710	1780	1790
Thalweg Sinuosity	1.20	1.24	1.29	1.31
Channel Sinuosity	1.022	1.035	1.037	1.032
Chezy C, $ft^{1/2}/sec$	75	70	78	74
W/D_{max} in Pool	52.50	56.00	57.10	45.00
Morphometric Parameter K_o	0.88	1.10	1.00	0.90
Length of Bend (measured), ft	12.90	15.20	17.00	17.90

Table 10. (Continued)

Length of Bend (computed), ft	6.30	7.8	8.7	14.7
η	2.05	1.95	1.95	1.21
Length of Pool, ft	3.60	3.60	3.75	4.10
Shear τ_o, pounds/sft	0.0127	0.0143	0.0160	0.0170
Froude Number $F = V/g^{1/2}D_{max}^{1/2}$	0.64	0.75	0.76	0.69
Stream Power = $\gamma QS \frac{\text{ft pounds}}{\text{sec ft}}$	0.053	0.0796	0.111	0.133

Table 11.

River Channel Pattern: Meandering Thalweg

Slope	0.0026	0.0064	0.0075	0.0100	0.013
Discharge, cfs	0.15	0.15	0.15	0.15	0.15
Radius of Bend, ft	4.10	4.50	4.70	4.49	4.63
Channel Width, ft	3.10	4.10	4.50	4.70	4.90
Max Depth in Pool, ft	0.108	0.094	0.090	0.074	0.070
Max Depth in Crossing, ft	0.058	0.053	0.050	0.048	0.045
Area in Pool, sft	0.183	0.133	0.125	0.111	0.098
Area in Crossing, sft	0.193	0.163	0.148	0.132	0.125
Velocity in Pool, fps	0.82	1.13	1.20	1.35	1.53
Velocity in Crossing, fps	0.78	0.92	1.01	1.14	1.20
Wetted Perimeter in Pool, ft	3.30	4.19	4.62	4.81	5.15
Wetted Perimeter in Crossing, ft	3.27	4.23	4.70	5.00	5.33
Hydraulic Radius in Pool, ft	0.055	0.032	0.027	0.023	0.0190
Hydraulic Radius in Crossing, ft	0.059	0.038	0.031	0.026	0.023
Thalweg Meander Wave Length, ft	18.00	20.30	20.75	22.20	22.70
Thalweg Meander Width, ft	4.30	7.30	7.55	7.70	7.83
Bedload Discharge, gm/min	190	388	415	512	563
Bedload Concentration, ppm	740	1510	1620	2000	2180
Thalweg Sinuosity	1.07	1.19	1.23	1.25	1.25
Chanel Sinuosity	1.01	1.03	1.033	1.034	1.032
Chezy C, $ft^{1/2}/sec$	67	79	84	99	97
$\frac{W}{D_{max}}$ in Pool	28.80	43.60	50.00	63.60	70.00
Morphometric Parameter K_o	0.63	0.73	0.75	0.68	0.91
Length of Bend (Measured), ft	8.00	13.20	14.20	16.10	17.20

Table 11. (Continued)

Length of Bend (Computed), ft	9.20	10.70	10.70	10.20	15.20
η	0.87	1.23	1.32	1.60	1.13
Length of Pool, ft	3.50	3.75	3.82	3.87	3.92
Shear $\tau_o = \gamma RS$, pounds/sft	0.0095	0.0127	0.0127	0.0132	0.016
Froude Number $F = V/g^{1/2}D_{max}^{1/2}$	0.44	0.65	0.71	0.88	1.02
Stream Power = $\gamma QS \frac{\text{ft pounds}}{\text{sec ft}}$	0.0244	0.0600	0.0705	0.094	0.122

Table 12.

Slope S = 0.015

River Channel Pattern: Combination of Meandering Thalweg and Braided

Discharge Q, cfs	0.15
Channel Width W, ft	5.10
Max Depth D_{max}, ft	0.060
Area A, sft	0.0883
Velocity V, fps	1.70
Wetted Perimeter P, ft	4.90
Hydraulic Radius R, ft	0.0180
Bedload Discharge Q_s, gm/min	738
Bedload Concentration C_s, ppm	2880
Chezy $C = V/R^{1/2}S^{1/2}$, $ft^{1/2}/sec$	103
W/D_{max}	85
Shear $\tau_o = \gamma RS$, pounds/sft	0.0170
Froude Number $F = V/g^{1/2}D_{max}^{1/2}$	1.22
Stream Power = $\gamma QS \frac{\text{ft pounds}}{\text{sec ft}}$	0.140

Table 13.

River Channel Pattern: Braided

Slope, S	0.016	0.018	0.020
Discharge Q, cfs	0.15	0.15	0.15
Channel Width W, ft	5.30	5.47	5.63
Max Depth D_{max}, ft	0.057	0.057	0.054
Area A, sft	0.0777	0.0704	0.0625
Velocity V, fps	1.93	2.14	2.40
Wetted Perimeter P, ft	4.30	4.00	3.90
Hydraulic Radius R, ft	0.0182	0.0178	0.016
Bedload Discharge Q_s, gm/min	825	926	1003
Bedload Concentration C_s, ppm	3110	3605	3900
Chezy $C = V/R^{1/2}S^{1/2}$, $ft^{1/2}/sec$	114	120	134
$\frac{W}{D_{max}}$	93	96	104
Shear $\tau_o = \gamma RS$, pounds/sft	0.018	0.020	0.021
Froude Number $F = V/g^{1/2}D_{max}^{1/2}$	1.43	1.58	1.82
Stream Power = $\gamma Q_s \frac{\text{ft pounds}}{\text{sec ft}}$	0.150	0.169	0.193

III. SUSPENDED SEDIMENT TESTS

Table 14.

River Channel Pattern: Meandering

Slope	0.0026	0.0064	0.0075	0.0085
Discharge, cfs	0.15	0.15	0.15	0.15
Radius of Bend, ft	4.26	4.50	4.70	4.60
Channel Width, ft	1.40	1.84	2.00	2.20
Max Depth in Pool, ft	0.15	0.145	0.156	0.162
Max Depth in Crossing, ft	0.080	0.0802	0.074	0.088
Area in Pool, sft	0.155	0.118	0.11	0.094
Area in Crossing, sft	0.160	0.133	0.131	0.1155
Velocity in Pool, fps	0.97	1.27	1.37	1.60
Velocity in Crossing, fps	0.94	1.13	1.14	1.30
Wetted Perimeter in Pool, ft	1.58	2.15	2.25	2.34
Wetted Perimeter Crossing, ft	1.52	2.27	2.35	2.40
Hydraulic Radius in Pool, ft	0.098	0.055	0.049	0.040
Hydraulic Radius in Crossing, ft	0.105	0.0587	0.0558	0.0482
Meander Wave Length, ft	18.40	20.70	20.95	21.00
Meander Width, ft	4.70	7.75	7.79	7.50
Bedload Discharge, gm/min	26	58	76	85
Bedload Concentration, ppm	102	227	297	333
Suspended Sediment Conc., ppm	30,000	30,000	30,000	30,000
Sinuosity	1.075	1.24	1.260	1.260
Chezy C, $ft^{1/2}$/sec	98	98	97	87
W/D_{max} in Pool	7.6	12.7	12.8	13.6

Table 14. (Continued)

Morphometric Parameter K_o	1.50	1.67	1.35	0.82
Length of Bend (Measured), ft	8.2	13.5	14.27	16.30
Length of Bend (Computed), ft	43.0	42.5	40.0	41.5
η	0.19	0.32	0.36	0.4[illegible]
Shear τ_o, pounds/sft	0.0159	0.0220	0.0229	0.0212

458696

Julie M. Dunning
315 East Trilby Road, Lot G
Fort Collins, Colorado